Annual Report (2019)

No.31
The NOVARTIS Foundation (Japan)
for the Promotion of Science

令和元年度

財団年報 第31号

公益財団法人 ノバルティス科学振興財団

Contents

Introduction

Akimichi Kaneko, MD, PhD
Chairman of the Board of Trustees

We have compiled here the research accomplishments of the grantees of the NOVARTIS Foundation (Japan) for the Promotion of Science in FY2017. The Foundation was originally established on September 4, 1987 with the generous donation of JPY 1 billion from Ciba-Geigy AG, Switzerland, for the purpose of "contributing to academic development and thus improving public health and welfare of the people by subsidizing to promote creative research and international exchange in the fields of biological and life sciences and related chemistry". Since then, the Foundation has granted nearly JPY 2 billion to approximately 1,764 research cases in 32 years. Research funds provided by the Foundation may be only a part of the cost of the entire research, however, we have continued to subsidize in belief that we could contribute to the development of excellent research. Joy of grantees could be felt in the acknowledgment of the papers received by the Secretariat, and we are pleased with our humble contribution.

The Foundation supports creative research in the fields of biological and life sciences, related chemistry and information science. Numerous entries submitted are examined by specialized researchers in a strict, fair and impartial manner. While we value originality as selection criteria, considerations are given to those start-up laboratories in urgent needs of research funds, as well as age and women researchers. In each case, we believe that excellent research is selected. In fact, we are informed that the quality of the research funded by the Foundation is highly esteemed by researchers in Japan, proving our purposes have not been wrong. We hope that these researches will lead the development of life sciences, and eventually to the development of new drugs and therapies.

As usual every year, the timing we are preparing this annual report is the timing of release for Nobel Prize in Physiology or Medicine. Last year 2018, Prof. Tasuku Honjo at Kyoto University was awarded the Prize. I have a big dream that some of younger researchers follow him, and I hope that our Foundation helps them. With such a dream we are continuing our research funding services.

This Annual Report summarizes the excellent research outcomes. It is an outstanding achievement accomplished within a limited period of one year. We are deeply grateful to everyone who supported the activities of the Foundation, including the selection committee members who have selected these excellent researches.

はじめに

代表理事　金子　章道

ここに第31回 ノバルティス科学振興財団の研究助成金を受けられた方々の研究報告（2018年４月～ 2019年３月の研究）を収録いたしました。（研究奨励金 41件、研究集会 5件）

当財団は1987年9月4日、スイス、チバガイギー社からの10億円のご寄附をもとに、「生物・生命科学および関連する化学の領域において、創造的な研究ならびに国際交流への助成を行うことにより、学術の振興を図り国民の健康と福祉の向上に寄与する」ことを目的に設立されました。爾来32年間に1,764件、金額にしておよそ20.5億円の助成を行ってまいりました。

当財団が提供する研究費は、研究全体に要する費用の一部かも知れませんが、優れた研究の発展に少しでも寄与できればと考え、助成して参りました。事務局に寄せられた論文等の謝辞からも受賞者の喜びが伝わり、多少なりとも貢献できているものと嬉しく思っております。

当財団は、生物・生命科学、関連する化学および情報科学の領域における創造的な研究を助成しております。数多く寄せられた応募を専門の研究者が厳正に公正かつ公平に審査しております。選考基準と致しまして独創性を重視しておりますが、研究室を新たに立ち上げ研究資金に逼迫しているケースや年齢、女性研究者にも配慮しており、いずれも優れた研究が選択されたものと考えております。事実、当財団で助成を受けた研究の質が高いと国内の研究者の間で評価されていることを聞くにつけ、我々の目指すところは間違っていないことを確信する次第であります。このような研究が生命科学の発展、ひいては新しい治療薬の開発や治療法の開発に発展することを期待しております。

この巻頭言を準備している頃、毎年ノーベル生理学・医学賞の発表時期を迎えます。昨年は京都大学の本庶佑先生がノーベル賞を受けられました。我が国から次々と受賞者が選ばれますことを祈り、また、これらの受賞者に続く若い研究者を輩出するお手伝いができればと大それた願いを持ちつつ財団の助成事業を続けている次第です。

この年報にはこのような優れた研究の成果をまとめております。１年間という限られた時間の中で達成された立派な業績であります。なお、これらの優れた研究を選考していただいた選考委員の皆様をはじめ、財団の活動を支えて下さっている関係者の皆様に深く感謝いたします。

II.

Reports from the Recipients of Novartis Research Grants

Epigenetic and metabolic changes on transdifferentiation of white adipocytes

Tekeshi Inagaki
Inagaki@gunma-u.ac.jp
Institute for Molecular and Cellular Regulation Gunma University

Summary Abstract

It is considered that the quantitative changes in the levels of intracellular metabolites are recorded as forms of epigenetics which will contribute for developing the life-style related diseases including obesity and diabetes. In this project, we sought to measure intra-cellular concentrations of Fe(II) and α-ketoglutarate which are indispensable metabolites for activating JmjC domain-containing histone demethylases and other epigenetic enzymes. Additionally, we tried to establish a system to determine cellular histone modifications comprehensively. By establishing and performing these systems, we elucidated the changes in metabolites and histone marks during adipocyte differentiation.
Key Words：Histone demethylase, Metabolite, Adipocyte, Epigenetics

Introduction

We recently presented a two-step working mechanism in which histone demethylase JMJD1A is recruited to the target genomic regions by being phosphorylated at S265 (Step 1) and thus demethylases methylated histones which locate in the vicinity regions of its biding (Step 2) [1,2]. Because Fe(II) and α-ketoglutarate (αKG) are indispensable metabolites for activating JmjC domain-containing histone demethylases including JMJD1A[3,4,5], we speculate that the transition from Step 1 to Step 2 would be mediated by the concentration of these metabolites. Therefore, we sought to establish the novel systems to determine the cellular concentrations of Fe(II) and αKG as well as various histone modifications.

Results

In this project, we have performed experiments for establishing probes to detect the intra-cellular concentrations of Fe(II) and αKG which are indispensable metabolites for activating epigenetic enzymes including JmjC domain-containing histone demethylases[3,4,5]. We additionally sought to establish a comprehensive analysis protocol of histone modifications.

The sensing system of nuclear αKG was established based on a fluorescence resonance energy transfer (FRET) system. We inserted the functional αKG-binding domain of the nitrogenase transcriptional regulator protein NifA between the yellow fluorescent protein (YFP) and the cyan fluorescent protein (CFP) as a FRET probe. The established plasmids were transduced into the preadipocytes by transient transfection or retrovirus infection. Transient transfection of the FRET prove enables us to observe intra-cellular concentration of αKG, while retrovirus infected cells showed reduced fluorescent level. Although the exact reason for the reduction of fluorescent level was not clear, it is considered that a recombination between CFP coding sequence and YFP coding sequence occurred during the reverse transcription step in retrovirus. Therefore, we employed PiggyBac transposon-mediated system for establishing the preadipocytes which stable express the

FRET probe during their differentiation. On the other hand, the concentration of intracellular Fe(II) was measured using its specific chemical probe SiRhonox which was kindly provided by the group of Dr. Hideko Nagasawa and Dr. Tasuku Hirayama. Using these measuring probes, we revealed that the cellular concentration of both Fe(II) and αKG changes during adipocyte differentiation. In addition, the cellular iron concentration affected the levels of adipocyte differentiation with mediating histone methylation levels. Thus, these data presented an important link between the adipocyte differentiation and the epigenetic demethylation enzymes which require both Fe(II) and αKG for its activity.

We also sought to establish a protocol to determine the intra-cellular histone modifications comprehensively. Although chromatin immunoprecipitation (ChIP) is widely used for examining changes in histone modifications during cell differentiation, ChIP is not appropriate method for examining comprehensive histone modifications. Because the specific antibody against a certain histone modification is required for each ChIP analysis, ChIP requires as many numbers of antibodies as the number of histone modifications we target. Therefore, we established a novel method to determine intra-cellular histone modifications comprehensively using a mass spectrometer. First, we have purified histones from pre- and post-differentiated adipocytes and the purified histones were alkylated at lysine residues and digested by trypsin to cut at arginine residues. Next, the fragments of histone tails were applied to mass spectrometry and the obtained data were analyzed by the MASCOT search engine, Progenesis software, and a statistical software. This novel protocol enables to present novel combinations of histone modifications on a single histone tail. As a consequence of the primary analysis, we found that the several combinations of histone modification marks in preadipocytes were resolved following adipocyte differentiation, which indicates their potential role to regulate adipogenic gene expression. Although this protocol for analyzing multiple histone modifications using mass spectrometer is a powerful tool to elucidate histone modifications comprehensively, an additional minor modification was required. Because the pretreatment step of histone tail with propionic acid in our protocol made a pair of multiple modifications indistinguishable. To avoid this problem, we employed an isotope labeling. By performing the modified mass spectrometric analysis of histone modifications using an isotope labeling, we successfully determined novel combinations of posttranslational modifications which occur on a histone tail.

Discussion & Conclusion

In this project, we have established the systems to determine intra-cellular concentrations of Fe(II) and α-ketoglutarate which are indispensable metabolites for activating multiple epigenetic enzymes. We also succeeded to establish a system to determine cellular histone modifications comprehensively. Establishment of the protocols required multiple modifications such as employing PiggyBac system for stably expressing the FRET probe in preadipocyte and using an isotope labeling for enabling determine indistinguishable modifications. By performing the established protocol, we elucidated a link between adipocyte differentiation and epigenetic demethylation enzymes which require both Fe(II) and αKG for its activity. In addition, we determined novel combinations of histone modifications which changes during adipocyte differentiation. Collectively, these data indicate that the concentrations of intra-cellular metabolites mediate epigenetic memory by mediating histone modifications, while further investigations would be required to reach such a consequence.

References

1) Abe, Y, Fujiwara, Y, Takahashi, H, Matsumura, Y, Sawada, T, Jiang, S, Nakaki, R, Uchida, A, Nagao, N, Naito, M, Kajimura, S, Kimura, H, Osborne, TF, Aburatani, H, Kodama, T, Inagaki, T, Sakai, J. Histone demethylase JMJD1A coordinates acute and chronic adaptation to cold stress via thermogenic phospho-switch. Nat Commun, 9: 1566, 2018
2) Abe, Y, Rozqie, R, Matsumura, Y, Kawamura, T, Nakaki, R, Tsurutani, Y, Tanimura-Inagaki, K, Shiono, A, Magoori, K, Nakamura, K, Ogi, S, Kajimura, S, Kimura, H, Tanaka, T, Fukami, K, Osborne, TF, Kodama, T, Aburatani, H, Inagaki, T, Sakai, J. JMJD1A is a signal-sensing scaffold that regulates acute chromatin dynamics via SWI/SNF association for thermogenesis. Nat Commun, 6: 7052, 2015
3) Inagaki, T, Sakai, J, Kajimura, S. Transcriptional and epigenetic control of brown and beige adipose cell fate and function. Nat Rev Mol Cell Biol, 17: 480-495, 2016
4) Inagaki, T. Histone demethylases regulate adipocyte thermogenesis. Diabetol Int, 9: 215-223, 2018
5) Tanimura, K, Suzuki, T, Vargas, D, Shibata, H, Inagaki, T. Epigenetic regulation of beige adipocyte fate by histone methylation. Endocr J, 66: 115-125, 2019

一般の皆様へ

肥満症や糖尿病といった生活習慣病は、遺伝要因と環境要因によって発症する。しかしながら、生体がさらされてきた外部環境がどのように細胞に記憶されているかの分子機構は不明な点が多い。エピゲノムはゲノム配列によらない遺伝子発現の制御機構であり、可塑性が高いシステムであるため、外部環境を記憶するシステムとして優れていると考えられている。今回、エピゲノム酵素の働きの制御に関わる細胞中の代謝物濃度を測定する方法を立ち上げ、さらにヒストン修飾というエピゲノムマークを網羅的に解析する手法を立ち上げることで、代謝環境のエピゲノム記憶を制御する機構に迫った。その結果、肥満症と関連が深い脂肪細胞分化の過程で、代謝物濃度とエピゲノムの変化が見いだされた。

Development of super resolution chemical imaging microscopy

Yasufumi Takahashi
yasufumi@se.kanazawa-u.ac.jp
Kanazawa University

Summary Abstract

We have developed scanning probe microscopy based chemical imaging tool for visualizing the chemical concentration profile around the cell.

Key Words：Scanning probe microscopy, super resolution microscopy, live cell imaging

Introduction

Scanning ion conductance microscopy (SICM) uses a less than 50 nm radius nanopipette for detecting ion current and is an effective tool for non-contact live cell nanoscale topography imaging, local chemical delivery, and cytosol collection. We have developed miniaturized electrochemical sensor and mounted the sensor on SICM probe to achieve 3D chemical concentration profile imaging.

Results

The permeation properties of cell membranes play a crucial role in intracellular and cell-surface biochemical reactions. Scanning electrochemical microscopy (SECM) uses ultramicroelectrode for detecting faradaic current and is a potentially effective tool for evaluating membrane permeability; however, conventional SECM does not have sufficient spatial resolution to image inhomogeneous membrane permeability on a single cell surface. The curvature of a cell surface is an important factor for accurately evaluating permeability, and most previous SECM studies evaluated permeability based on numerical simulation wherein the cell membrane was assumed to be flat. Various micro/nanostructures, such as surface microvilli, are present on actual cell surfaces, and therefore, one should not ignore such structures in numerical simulation when evaluating local cell permeability. SECM-SICM hybrid probe system can provide a 3D electrochemical image at nanometer resolution, providing real features of the local membrane permeability and the ion concentration distribution. To demonstrate a local membrane permeability measurement, we used the system for high-resolution imaging of 3T3-L1 fixed cells, which have large lipid droplets. In the measurements, we defined the setpoint for stopping probe approach in hopping mode at a 6.0% decrease from bulk ion current to bring the electrode very close to the

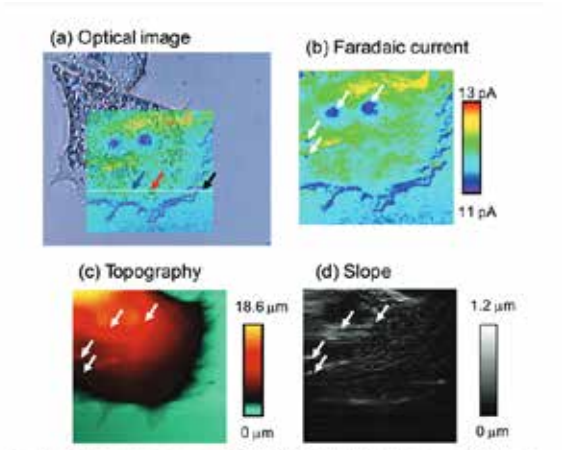

Fig.1 (a) Optical image and SECM–SICM, (b) faradaic current, (c) topography, and (d) slope images of adipocyte in 0.5 mM $FcCH_2OH$ + PBS. The SECM electrode radius is 117 nm with RG = 1.1. The SECM and SICM electrodes were held at 500 and 200 mV vs. Ag/AgCl, respectively. Hopping amplitude was 3.0 μm. The surface area of the captured images was 80 μm × 80 μm.

substrate. Fig. 1 shows the SECM–SICM images of 3T3-L1 in PBS containing 0.5 mM $FcCH_2OH$. The SECM image is based on the oxidation of $FcCH_2OH$, a hydrophobic mediator which can cross the cell membrane. The SICM images represent the topography, whereas the SECM images measure the flux of $FcCH_2OH$. Therefore, the SECM provides information about the local membrane permeability of $FcCH_2OH$ and thus the local structure of the cell.

Discussion & Conclusion

We performed 3D electrochemical and ion current imaging for measuring cell-membrane permeability and ionic strength using SECM–SICM. The pyrolytic carbon SECM–SICM probe is effective for such experiments because the small electrode size and RG bring the electrode close to the sample surface, without contact. In adipocyte imaging, 3Delectrochemical imaging visualizes inhomogeneous permeability. Even with a fixed cell, we could observe the ionic strength difference on the cell surface. Hopping-mode SECM–SICM breaks the limit of microscale spatial resolution of SECM and opens up new possibilities for special chemical and ion strength profile imaging. This method will allow for the visualization of inhomogeneous chemical distribution and permeability on single cells, such as neurotransmitter concentration profiles or respiration activity.

References

Zhou, Y. S.; Saito, M.; Miyamoto, T.; Novak, P.; Shevchuk, A. I.; Korchev, Y. E.; Fukuma, T.; Takahashi, Y., Nanoscale Imaging of Primary Cilia with Scanning Ion Conductance Microscopy. *Anal Chem* 2018, *90* (4), 2891-2895.

Matsumae, Y.; Takahashi, Y.; Shiku, H.; Matsue, T., Quantitative Real-Time Monitoring of Antibody-Induced Internalization of Epidermal Growth Factor Receptor on Single Living Mammalian Cells Using Scanning Electrochemical Microscopy. *Chemelectrochem* 2018, *5* (20), 3096-3101.

Takahashi, Y.; Kumatani, A.; Shiku, H.; Matsue, T., Scanning Probe Microscopy for Nanoscale Electrochemical Imaging. *Anal Chem* 2017, *89* (1), 342-357.

Takahashi, Y.; Ida, H.; Matsumae, Y.; Komaki, H.; Zhou, Y. S.; Kumatani, A.; Kanzaki, M.; Shiku, H.; Matsue, T., 3D electrochemical and ion current imaging using scanning electrochemical-scanning ion conductance microscopy. *Phys Chem Chem Phys* 2017, *19* (39), 26728-26733.

一般の皆様へ

細胞―細胞間のコミュニケーションや細胞の代謝により、細胞近傍の化学物質の濃度プロファイルは時々刻々と変化している。そのため、この細胞表面の化学物質の濃度プロファイルを捉えることは、非常に重要である。しかし、一般的に利用されている化学物質のセンシング技術は、位置情報と時間情報が失われた状態で計測が行われている。その一つの理由として、化学センサーの感度と、非常に柔らかい細胞近傍にセンサーを配置することが困難なためである。そこで、走査型プローブ顕微鏡のプローブとして、微小な電極やナノピペットに化学修飾を施したケミカルセンサーを用いることで、細胞近傍の化学物質の濃度プロファイルを形状方法とともに３次元的に取得した。

Elucidation of molecular bauplan to determine the positioning of the posterior body structure along the anteroposterior axis

Takayuki Suzuki
suzuki.takayuki@j.mbox.nagoya-u.ac.jp
Nagoya University

Summary Abstract

In this study, we examined the molecular mechanism how posterior body structure is formed based on the initiation timing of *GDF11* to identity molecular bauplan establishing our body structure. We identified common enhancer sequence of *GDF11* which is involved in the determination of the position of the posterior body.

Key Words：Tetrapods, morphological diversity, vertebral formula, gene expression, heterochrony

Introduction

Tetrapods including human has vertebral bones at the center of our body. Our organs develop along the antero-posterior axis based on the vertebral formula. Recently, we found that one of the TGF-β signaling molecules, GDF11, expressing at the posterior side of the developing presomitic mesoderm, PSM, coordinates the position of the hindlimb to the sacral vertebrae. Interestingly, initiation timing of *GDF11* differs among tetrapod embryos, frog, chick, mouse, gecko, and snake. These results strongly support the idea that specifies-specific hindlimb/sacral vertebra position was brought about by unique initiation timing of *GDF11*. In *GDF11* knockout mice, hindlimb position together with sacral vertebra and other organs located at posterior body structure was shifted posteriorly. Therefore, in this study, we examined the molecular mechanism how posterior body structure is formed based on the initiation timing of *GDF11* to identity molecular bauplan establishing our body structure.

Results

To identify the molecular mechanisms involving species-specific initiation timing of *GDF11*, we thought two hypotheses. One is each specie has unique enhancer sequence to induce unique initiation timing of *GDF11*. Second hypothesis is that tetrapods have common enhancer sequences to induce the expression, however, initiation timing of transcriptional factors that bind to common enhancer sequence would be different. To explore these hypotheses, first, we looked for enhancer sequence of mouse *GDF11*. We compared mouse *GDF11* locus with birds, alligator, and lizard, and found that there were only 3 short-conserved sequences between exon1 and exon2 at *GDF11* locus. Thus, non-cording sequence near *GDF11* locus was not conserved well. Next, we performed *in vivo* reporter assay to analysis whether these sequences has enhancer activity where *GDF11* is expressed. We tandemly inserted expected enhancer sequences upstream of tk-EGFP. We electroporated these reporter constructs with pCAGGS-mCherry vector as control for electroporation. We found that only 1 sequence showed enhancer activity at the posterior side of presomitic mesoderm where Gdf11 is expressed. In this region, we found putative transcriptional factor binding sites, ETS and TCF4, downstream of FGF and WNT signaling, respectively. These results indicate that FGF and WNT signaling is involved in the initiation of *GDF11* expression.

Therefore, next, we treated chick embryos with FGF signaling antagonist, PD173074, and WNT signaling antagonist XAV939. We found that *GDF11* expression was strongly down-regulated. In contrast, when we electroporated constitutive active MEK1 which is downstream target of FGF signaling, *GDF11* expression was up-regulated. As well, when chick embryos were treated with WNT agonist, Chiron, *GDF11* expression was also up-regulated. There results indicate that both FGF and WNT signaling up-regulate *GDF11* expression *in vivo*. Next, we examined whether putative transcriptional factor binding sites of EST and TCF4 are necessary for its enhancer activity. We made mutant reporter constructs that ETS or TCF4 binding sites were mutated. After electroporation of these constructs where *GDF11* is expressed, enhancer activity was strongly down-regulated in the case of only one transcriptional factor binding site was mutated. These results indicate that ETS or TCF4 binding sites on this enhancer sequence are necessary for enhancer function to induce *GDF11* expression. Next, we examined whether this enhancer sequence is involved in the determination of the positioning of the posterior body structure. We made the enhancer knockout mice by Crisper/Cas9, and found that position of the hindlimb and sacral vertebrae were shifted posteriorly by 1 vertebra level (right panel). This phenotype indicates that this enhancer sequence is involved in the position of the posterior body structure through *GDF11* expression. However, in *GDF11* knockout mice, both hindlimb and sacral vertebrae were shifted more posteriorly by 7-9 vertebral level, implying that there should be other *GDF11* enhancer sequences in the mouse. Then, we looked for other *GDF11* enhancer sequences by *in silico* analysis using SMC1-ChIAPET signals that show open chromatin. Now we are testing whether expected enhancer sequences has enhancer activity where *GDF11* is expressed. Thus, we are focusing on long-range enhancer of *GDF11* that coordinates initiation timing of *GDF11* in the mouse. We are also looking for species-specific enhancer element in the turtle and snake by ATAC-seq. We are going to compare these enhancer sequences in this year.

Discussion & Conclusion

In this study, we identified common enhancer sequence of *GDF11* which is involved in the determination of the position of the posterior body. From reporter assay, it was thought that difference of WNT and FGF signaling activity at the posterior side of the presomitic mesoderm might bring about positional difference of the positioning of the posterior body structure among tetrapods. Our results also imply the existence of other enhancer element of *GDF11*, especially as long-range enhancer. In conclusion, to establish common body structures as bauplan, both common enhancer sequence and species-specific enhancer sequence would be necessary to induce species-specific initiation timing of *GDF11*. In tetrapods, common posterior structure of our body is developed downstream of *GDF11* which initiates species-specific timing during developmental stages.

一般の皆様へ

私たち人を含む脊椎動物は体の中心に背骨を持っており、頭から頸椎、胸椎、腰椎、仙椎、尾椎に分けられる。興味深い事に、私たちの体の下半身には、仙椎の位置に後ろ足や生殖器、腎臓などの臓器があり、これらの器官の場所はどの動物においても同じである。今回我々は、このような下半身の位置がそれぞれの動物で異なりながらも、何故下半身に位置する器官の位置関係が保存されているのか、そのメカニズムを明らかにすることを試みた。その結果、*GDF11*という１つの遺伝子が働くタイミングを生み出す機構がそれぞれの動物で異なることが、ヘビのような特異な体の形を生み出していることが明らかとなった。

Neural circuits that regulate glucose metabolism between hypothalamus and peripheral organs.

Kunio Kondoh
kkondoh@nips.ac.jp
National Institute for Physiological Sciences

Summary Abstract

The purpose of this funded study is to elucidate neural circuits that transmit leptin signals from the hypothalamus to peripheral tissues. I infected neurons in the skeletal muscle and brown adipose tissues, major peripheral regulators of glucose uptake, with pseudorabies viruses that can travel across synapses retrogradely. I found virus-infected neurons in the hindbrain and the hypothalamic areas, suggesting that these areas play an important role in transmitting signals from brains to peripheral tissues involved in glucose uptake.
Key Words：Hypothalamus, Glucose metabolism, Skeletal muscle, Brown adipose tissue

Introduction

Glucose is a major energy source in the body, and the brain maintains glucose levels in the body at a proper level. Leptin, which is secreted from white fat, acts on the hypothalamus of the brain to promote muscle and fat glucose uptake and plays an important role in lowering blood glucose levels[1]. Neurons in the hypothalamus then control glucose levels in the body by regulating glucose utilization in peripheral tissues including skeletal muscle and brown adipose tissues as well as glucose production in the liver[2]. However, the neural circuits that transmit leptin signals from the hypothalamus to peripheral tissues are poorly understood.

Results

In this study, to investigate mechanisms by which leptin regulates glucose metabolism, I analyzed the anatomical organization of neural circuits that transmit signals from the hypothalamus to skeletal muscle (soleus) or brown adipose tissues (BAT).

The Bartha strain pseudorabies virus (PRV) is a neurotropic virus that can infect neurons, replicate, and retrogradely travel to upstream neurons through synaptic connections[3] (Figure 1). Using PRV, it is possible to comprehensively identify upstream neurons that transmit signals to specific neurons. In addition, by analyzing virus-infected cells every day after virus injection, one can estimate the number of synaptic connections between each neuron and primarily infected neurons[4]. To investigate neural circuits that transmit leptin signals from the hypothalamus to peripheral tissues, I infected soleus and BAT with PRVs that express green and

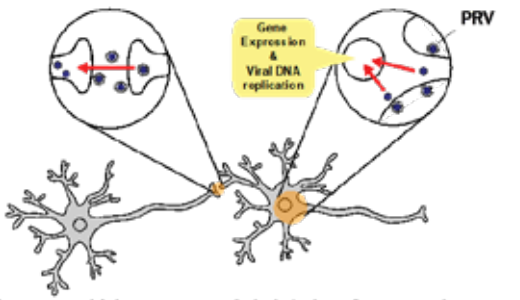

Figure 1 Bartha strain Pseudorabies Viruses (PRVs) for tracing neural circuits

red fluorescent proteins, respectively (Figure 2).

I observed PRV infected neurons in different brain areas on different days after virus injection. Interestingly, I also observed many infected neurons that express both green and red fluorescent proteins, suggesting that these neurons send signals to both soleus and BAT. Since the only function that is shared by soleus and BAT is energy expenditure including glucose uptake, it is possible that the double-labeled neurons play an important role to send glucose uptake-related signals from the brain to both soleus and BAT.

Two days after infection (possibly two synapses upstream of soleus and BAT), virus infected neurons were observed only in the spinal cord. In the spinal cord, the infected neurons were accumulated in the intermediolateral nucleus (IML), where neurons that consist of the autonomic nervous systems are located. This result is consistent with previous findings suggesting that sympathetic nervous systems are involved in the hypothalamic regulation of glucose uptake in skeletal muscle and BAT.

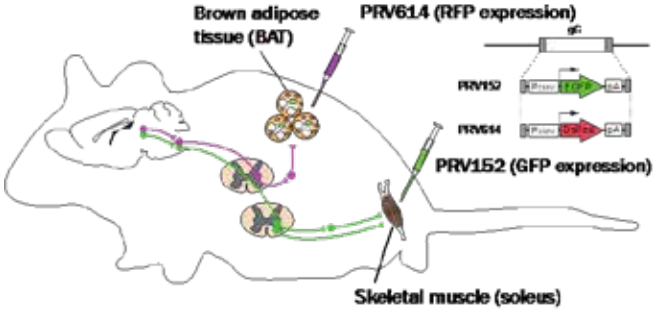

Figure 2 Analysis of Neural circuits from the brain to BAT/skeletal muscles by using PRVs

Three days after infection (possibly three synapses upstream of soleus and BAT), virus infected neurons were observed in several central brain areas. These brain areas included several areas in the medulla oblongata, and one area in the hypothalamus, the paraventricular nucleus of the hypothalamus (PVH). Since I did not observe any infected neurons in the brain two days after virus injection, the neurons infected three days after infection could send direct inputs to neurons in the IML. Therefore, these results suggest that the medulla oblongata and PVH is the two downstream brain area that integrates signals in the central brain.

Four days after infection, virus infected neurons were found in several hypothalamic brain areas that are known to express leptin receptors and receive leptin signaling. They include the ventromedial nucleus (VMH) and the arcuate nucleus (ARC). Therefore, the leptin signals may be received in the VMH and/or ARC and be transmitted to soleus and BAT through brain areas infected with PRVs three days after infection. These results, taken together, suggest the possible organization of neural circuits from hypothalamus to soleus and BAT that regulate glucose uptake. Leptin signals that are received in the ARC or VMH may be transmitted first to PVH and/or medulla oblongata, secondly to the IML in the spinal cord, and then to sympathetic nerves in the soleus and BAT.

Discussion & Conclusion

The results from this study revealed the anatomical organization of neural circuits from the hypothalamus to two peripheral tissues, skeletal muscle (soleus) and BAT, major regulators of glucose uptake in the body. The results suggest that leptin sends signals to peripheral tissues through two brain areas, PVH and medulla oblongata. In addition, I found many neurons in many brain areas that are upstream of both skeletal muscle and BAT. Since glucose uptake is a shared function between skeletal muscle and BAT, it is possible that the neural pathway that regulates both skeletal muscle and BAT regulate glucose uptake by leptin. The next step is whether leptin actually activates brain areas identified in this study.

References

1) Minokoshi Y, Haque MS, Shimazu T. Microinjection of leptin into the ventromedial hypothalamus increases glucose uptake in peripheral tissues in rats. Diabetes (1999) 48, 287–291
2) Toda C, Shiuchi T, Lee S, Yamato-Esaki M, Fujino Y, Suzuki A, Okamoto S, Minokoshi Y. Distinct effects of leptin and a melanocortin receptor agonist injected into medial hypothalamic nuclei on glucose uptake in peripheral tissues. Diabetes (2009) 58, 2757–2765
3) Li J, Liu T, Dong Y, Kondoh K, Lu Z. Trans-synaptic Neural Circuit-Tracing with Neurotropic Viruses. Neurosci Bull. (2019) [Epub ahead of print]
4) Kondoh K, Lu Z, Ye X, Olson DP, Lowell BB, Buck LB. A specific area of olfactory cortex involved in stress hormone responses to predator odours. Nature (2016) 532, 103-106.

一般の皆様へ

脳の視床下部は体内の血糖値を一定の値に保つために重要な働きをしています。そのために視床下部は、白色脂肪から分泌されるレプチンなどの様々な体内・体外のシグナルを受け取り、末梢組織の糖の産生・消費をコントロールしています。今回私は、視床下部から糖の消費を担う２つの末梢組織（骨格筋・褐色脂肪）へシグナルが送られる際に使われる神経回路網の構造を明らかにしました。今回明らかになった神経回路の機能を解明することで、将来的に糖尿病や肥満の治療法の開発につなげていきたいと考えています。

Exploratory analysis to evaluate mutation spectrum of circulating tumor DNA from metastatic breast cancer treated with aromatase inhibitors

Siew-Kee LOW
siewkee.low@jfcr.or.jp
Cancer Precision Medicine Center, Japanese Foundation for Cancer Research

Summary Abstract

Liquid biopsy, particularly circulating tumor DNA (ctDNA), detected from plasma could be used to monitor breast cancer patients who develop resistance to aromatase inhibitors (AI) therapy. In this study, we used ultra-deep targeted next generation sequencing (NGS) to detect mutations from ctDNA. We detected mutations in *TP53, PIK3CA, KRAS, FGFR3,* and *ESR1*, frequently mutated genes in breast cancer patients on aromatase inhibitors. Our results suggest that ctDNA has potential to be applied for monitoring of resistance to AI therapy.
Key Words : Liquid biopsy, circulating tumor DNA, next generation sequencing, drug resistance, aromatase inhibitor.

Introduction

Aromatase inhibitors (AI), which block the peripheral conversion of androgen to estrogen, are frequently used as treatment for postmenopausal ER-positive breast cancer patients. *ESR1* mutations are rarely detectable in the primary breast tumor, but are found at significant frequency (25-30%) after secondary to AI exposure and develop endocrine resistance. Detection of ESR1 mutations in liquid biopsy from metastatic breast cancer, whom tissue biopsies are hard to access, might provide earliest indication of AI drug resistance.

Results

This exploratory study aims to evaluate mutation detected from liquid biopsy of metastatic breast cancer by using next generation sequencing (NGS) technology.

A total of 14ml of blood samples from 26 metastatic breast cancer patients were collected. After centrifugation, cell-free DNA/RNA (cfDNA/RNA) were extracted from the plasma using magnetic-based total nucleic acid extraction method. The concentration of the cfDNA/RNA ranged from 4.81 to 83.52 ng/ml of plasma, with average and median of 20.18 and 10.55ng/ml, respectively. The size of the cfDNA/RNA ranged from 105-197bp.

To perform NGS, Oncomine Pan-Cancer Cell-free assay that include 52 genes that covered >900 mutation hotspots and indels, 12 copy number variations (CNV) and 96 fusions, was used. We selected this panel as it targets many known mutation hotspots across different types of cancer. This might improve ctDNA mutation detection in this sample population. In addition, the Oncomine Pan-Cancer assay are amplicon-based panels, in which molecular coverage of amplicons is expected

to be more uniform across all targeted regions. This amplicon-based NGS technology has also integrated molecular barcode system that are known to reduce PCR error and could accurately detects low-frequency variants from 15-20 ng of input cfDNA/RNA. In brief, the samples were amplified to generate libraries for targeted sequencing. The libraries of the samples will be pooled for templating on the Ion Chef System and subsequently sequenced using the Ion S5 Prime System. Variant calling was performed by using Ion Reporter 5.10 system. The median overall and molecular depth was 48,172 and 4,284, respectively. As a result, out of 26 samples, mutations were detected in 20 patients, with detection rate of 77%. A total of 44 mutations with mutant allele frequency ranged from 0.066-14.91%. The distribution of the mutations is summarized in the pie-chart below (Figure 1). The most frequently mutated genes are *TP53, PIK3CA, KRAS, FGFR3*, and *ESR1*. The mutations detected were dominated by *TP53* and *PIK3CA* mutations. Mutations in both genes amount to 73% of all mutations detected. Among the 44 mutations, 42 are missense mutations and 2 are frameshift deletion. Two CNVs, *FGFR1* (2.85 copies) and *MET* (2.73 copies) were also detected.

Close to half of the patients (11/26 - 42%) carried multiple mutations. Presence of multiple mutations suggest the possibility of heterogenous clones being detected. In one patient, we detected 6 mutations (2 *TP53*, 2 *PIK3CA*, 1 *ESR1* and 1 *KRAS*). This suggests possible polyclonal mutations being detected.

Previous study indicated that patients with *ESR1* mutations detected in the plasma had a markedly shorter progression-free survival when treated with AIs (Schiavon G et al., 2015). Two mutations, p.E380Q and p.Y537S, on *ESR1* gene were detected from cfDNA/RNA. Both of these mutations are located on the ligand binding domain of *ESR1*. The detection rate of *ESR1* mutations is about 8% (2/26), which is lower compare to previously reported 25-30% owing to the small sample size and these patients are yet develop progression disease after AI treatment. Hence, monitoring of these patients with repetitive sampling is greatly essential to detect drug resistance of AI.

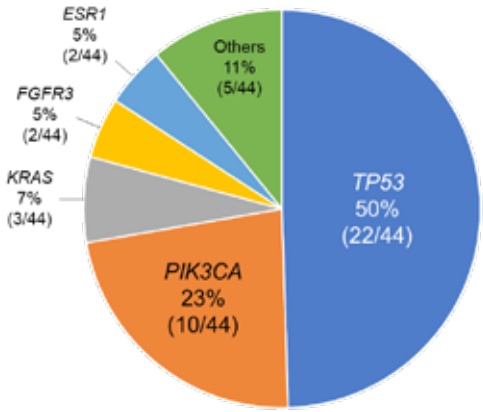

Figure 1: Mutation distribution of 26 metastatic breast cancer who received aromatase inhibitor treatment.

Discussion & Conclusion

The exploratory study is to evaluate the usefulness of liquid biopsy (blood) as an alternative biomarker to detect drug resistance in metastatic breast cancer patients who received aromatase inhibitor as first-line treatment. In addition, mutations on other cancer related genes such as *TP53, PIK3CA, KRAS* and *FGFR3* were detected in this exploratory analysis by using NGS system. Since the mutation status in ctDNA from plasma is highly concordant with corresponding tumor tissue

and the level of ctDNA increase corresponds to the stage of cancer (Bettegowda C et al., 2014), evaluation of ctDNA could be used an alternative method to detect and monitor disease status of cancer patient when tissue samples are difficult to access. Importantly, ctDNA has superior sensitivity compared to conventional biomarkers, such as CA-153, and has a greater dynamic range that correlates with changes in tumor burden (Dawson SJ et al., 2013), hence, evaluation of ctDNA could be a complementary assessment with conventional biomarkers and imaging. The next phase of this study is to monitor these cancer patients and detect AI drug resistance at an earlier stage.

References

1. Schiavon G et al., Sci Transl Med. 7(313):313ra182, 2015
2. Bettegowda C et al., *Sci Transl Med.* 6(224):224ra24, 2014;
3. Dawson SJ et al., *N Engl J Med.* 368(13):1199-209, 2013;

一般の皆様へ

これまで、診断目的のためにがん患者から生検を得る方法として、侵襲的な針による生検が行われることが多かった。しかしながら、この侵襲的な方法は複数回実行することは難しい。また、がんは非常に不均一であり、そして腫瘍のプロファイルは経時的に変化するため、原発腫瘍からの生検は、腫瘍における特定の時点でのゲノムプロファイルのみしか反映されないことになる。一方で、リキッドバイオプシー、特に ctDNA は、血液、尿、脳脊髄液および唾液から抽出することができる。 ctDNA から得られるゲノムプロファイルは、非侵襲的で迅速かつ複数回入手することができることから、とても重宝されている。

本研究では、先進的である次世代シーケンシング技術を用い、血漿（血液サンプル）からの変異を検出することを目的とした。我々はこの研究から、血漿中に1つ以上の変異を有する20/26人の進行性乳がん患者を検出した（検出率：77%）。がんに関連する突然変異は全部で44個検出され、このうち ESR1遺伝子の突然変異は薬剤耐性と関連があることが知られている。ctDNA のモニタリングは、病状のモニタリング、薬剤耐性および臨床的再発の早期発見に有用なツールである。

Investigation of the molecular mechanism of osteoblastogenesis.

Yoshinori Matsumoto
ymatsumoto@okayama-u.ac.jp
Okayama University Graduate School of Medicine, Dentistry and Pharmaceutical Sciences

Summary Abstract

The adapter protein 3BP2 is mutated in Cherubism, an autosomal dominant inherited disorder resulting in cranial facial dysmorphia. 3BP2 binds to and activates the non-receptor tyrosine kinase ABL known from genetic studies to be essential for osteoblast function. However, the molecular mechanism linking 3BP2-ABL to bone synthesis remains unclear. Here we show that nuclear ABL stabilizes the RUNX2:proteinX master transcription factor complex driving osteoblast differentiation.
Key Words：ABL, Osteoblastogenesis, Tyrosine kinase

Introduction

3BP2 encoded by the SH3BP2 locus was originally identified as an ABL binding protein and binds directly to the ABL SH3 domain via a diproline motif. 3BP2 triggers increased ABL kinase catalytic activity required for osteoblast maturation (1). 3BP2 knockout mice are osteoporotic due to defective osteoblastogenesis (1) and phenocopy ABL-/- mice (2), which demonstrate similar osteoblast dysfunction suggesting that 3BP2 and ABL are part of a common genetic and biochemical pathway. However, the molecular mechanism by which ABL regulates bone formation remains unknown.

Results

First, we asked whether ABL links to RUNX2, which is the master transcription factor for osteoblastogenesis. Previous work, which demonstrated that RUNX2 and proteinX form a transcription factor complex required for BGLAP transcription, prompted us to query whether ABL could induce BGLAP transcription through the RUNX2-proteinX complex. We observed that a constitutively active form of ABL (P242E/P249E, ABL (PP)) but not a kinase dead version of ABL (K290M, ABL (KD)) (Barila and Superti-Furga, 1998) increased the RUNX2-proteinX complex formation. These results corresponded to increase in the BGLAP transcriptional activity of RUNX2 and proteinX in the presence of active ABL. We next queried whether ABL was a direct component of the RUNX2-proteinX complex and showed by co-precipitation that ABL bound to both RUNX2 and proteinX, either in two binary complexes or as part of a single ternary complex.

Next we asked whether the formation of the RUNX2-proteinX complex was dependent on tyrosine phosphorylation of RUNX2 by ABL. Wild-type RUNX2 but not all tyrosine to phenylalanine mutant variants (YF) was abundantly tyrosine phosphorylated when co-expressed with ABL (PP), demonstrating that RUNX2 is a substrate of ABL. We observed that the RUNX2 (YF) mutant poorly formed a complex with proteinX compared to wild-type RUNX2 and was transcriptionally inactive. These data demonstrate that phosphorylation of RUNX2 by ABL was absolutely required for the formation of the ternary active transcription factor complex.

Interestingly, we found that ABL stabilized proteinX. This may be because of inhibition of phosphorylation of proteinX which is required for its protein degradation.

Lastly, to investigate whether ABL kinase activity was required for enhancing osteoblast maturation and mineralization, we used an FKBP chimeric form of ABL whose activity is inducible by the small molecule FK1012. Expression of FKBP-ABL (WT) but not kinase dead version in Saos-2 cells showed enhanced mineralization detected by Alizarin red staining.

Discussion & Conclusion

Mesenchymal commitment towards the osteoblast lineage is essential for embryonic skeletal development. In our present study, we show that ABL is poised as a critical factor needed to “lock-in” mesenchymal specification towards the osteoblast lineage.

Further studies will be needed to clear the following questions.

1. How is the proteinX stabilized by ABL?
2. Is 3BP2 involved in this ternary complex of ABL, RUNX2 and proteinX?
3. Do proteinX knockout mice suffer from osteoporosis due to osteoblast defect?
4. Is the effect of ABL on osteoblastogenesis contingent on RUNX2 and proteinX?
5. Is the transcriptional complex of RUNX2 and proteinX is dependent on 3BP2?

This project is now ongoing to investigate these questions.

References

(1) Levaot, N., Simoncic, P.D., Dimitriou, I.D., Scotter, A., La Rose, J., Ng, A.H., Willett, T.L., Wang, C.J., Janmohamed, S., Grynpas, M., et al. (2011). 3BP2-deficient mice are osteoporotic with impaired osteoblast and osteoclast functions. The Journal of clinical investigation 121, 3244-3257.

(2) Li, B., Boast, S., de los Santos, K., Schieren, I., Quiroz, M., Teitelbaum, S.L., Tondravi, M.M., and Goff, S.P. (2000). Mice deficient in Abl are osteoporotic and have defects in osteoblast maturation. Nature genetics 24, 304-308.

一般の皆様へ

健康で豊かな長寿社会を実現させる為には、骨粗鬆症の予防、改善が急務です。50歳以上の日本人女性の３割が骨折や寝たきりの原因となる骨粗鬆症を発症する為、骨形成、骨吸収を担う骨芽細胞及び破骨細胞を制御する機序の解明は骨粗鬆症の克服に必須の研究テーマですが、未だその詳細は不明です。本研究では、骨形成を担当する骨芽細胞の新たな制御機構を明らかにしました。更なる研究を積み重ね、骨粗鬆症の治療へと応用出来るよう、今後も精進致します。

Heart Cell Molecular Atlas Project to dissect the regulatory mechanisms of circulatory homeostasis

Seitaro Nomura
senomura-cib@umin.ac.jp
The University of Tokyo

Summary Abstract

Pressure overload induces a transition from cardiac hypertrophy to heart failure, but its underlying mechanisms remain elusive. Here we reconstruct a trajectory of cardiomyocyte remodeling and clarify distinct cardiomyocyte gene programs encoding morphological and functional signatures in cardiac hypertrophy and failure, by integrating single-cardiomyocyte transcriptome with cell morphology, epigenomic state and heart function. During early hypertrophy, cardiomyocytes activate mitochondrial translation/metabolism genes, whose expression is correlated with cell size and linked to ERK1/2 and NRF1/2 transcriptional networks. Persistent overload leads to a bifurcation into adaptive and failing cardiomyocytes, and p53 signaling is specifically activated in late hypertrophy. Cardiomyocyte-specific p53 deletion shows that cardiomyocyte remodeling is initiated by p53-independent mitochondrial activation and morphological hypertrophy, followed by p53-dependent mitochondrial inhibition, morphological elongation, and heart failure gene program activation. Human single-cardiomyocyte analysis validates the conservation of the pathogenic transcriptional signatures. Collectively, cardiomyocyte identity is encoded in transcriptional programs that orchestrate morphological and functional phenotypes.

Key Words：Heart failure, single-cell RNA-seq, cardiomyocyte remodeling

Introduction

Organs respond appropriately to external and internal stress to maintain homeostasis, but excessive stress disrupts the adaptive response, leading to organ dysfunction. Hemodynamic stimuli such as pressure and volume overload to the heart initially induce cardiac hypertrophy to reduce wall stress and prevent cardiac dysfunction. However, sustained overload causes cardiac dysfunction leading to heart failure. During this process, cardiomyocytes activate various signaling cascades initially for adaptive morphological hypertrophy, followed by a transition to the failing phenotype characterized by elongation and contractile force reduction. Yet, it remains elusive how individual cardiomyocytes undergo molecular and morphological remodeling in response to stress, contributing to cardiac adaptation and dysfunction.

Results

Single-cardiomyocyte transcriptomic profiles in heart failure

We obtained single-cardiomyocyte transcriptomes from mice exposed to pressure overload. In our model, transverse aorta constriction (TAC) in 8-week-old C57BL/6 mice induced cardiac hypertrophy at 1–2 weeks after the operation and heart failure at 4–8 weeks. We isolated cardiomyocytes from the left ventricular free wall after sham operation and at 3 days and 1, 2, 4, and 8 weeks after TAC using Langendorff perfusion and obtained 396 single-cardiomyocyte transcriptomes (sham, 64 cardiomyocytes; day 3, 58; week 1, 82; week 2, 61; week 4, 73; and week 8, 58) in which >5,000

genes were detected (RPKM > 0.1). We next used Monocle to reconstruct the branched trajectory of cardiomyocyte remodeling after pressure overload, which consisted of 3 cell states and 1 branch point. Cardiomyocytes of the early stage after TAC operation (D3 and W1) mainly belonged to State 1, suggesting that cardiomyocytes enter into State 1 immediately after TAC operation and were bifurcated into distinct cell fates (State 2 and State 3) after the branch point. Cardiomyocytes near the branch point were mainly from mice at 2 or more weeks after TAC operation, suggesting that the bifurcation occurs in the late stage of hypertrophy.

Modules and regulators of cardiomyocyte hypertrophy

To identify the gene modules involved in cardiomyocyte hypertrophy, we again isolated cardiomyocytes from mice at 1 week after TAC, measured their area, obtained their transcriptomes, and integrated them. Correlation analysis indicated that the expression of mitochondrial ribosome and oxidative phosphorylation genes is closely linked to the extent of cell hypertrophy, suggesting that pressure overload-induced mitochondrial activation might participate in mitochondrial biogenesis to match the increased energy demand during cardiac hypertrophy. We next performed chromatin immunoprecipitation followed by sequencing for histone H3 acetylated lysine 27 (H3K27ac) modification in cardiomyocytes from mice at 1 week after TAC and evaluated the enrichment of transcription factor recognition motifs to infer the regulatory factors for each module. Recognition motifs of ETS domain-containing protein (ELK1) and nuclear respiratory factors 1 and 2 (NRF1/2) were specifically enriched around M1 genes. Extracellular signal-regulated protein kinases 1 and 2 (ERK1/2) signaling induces cardiomyocyte hypertrophy via ELK1 phosphorylation and NRF1/2 signaling enhances mitochondrial biogenesis.

Signaling pathway inducing heart failure

We investigated how cardiomyocytes in the adaptive hypertrophy stage become failing cardiomyocytes. Pathway enrichment analysis revealed that genes involved in the cell cycle and p53 signaling pathways were enriched in late hypertrophy stage-specific gene modules. To assess whether p53 activation in cardiomyocytes is critical for the transition to failing cardiomyocytes and development of heart failure, we generated cardiomyocyte-specific p53 knockout (p53CKO) mice. Echocardiography demonstrated that p53flox/flox and p53CKO mice showed similar cardiac hypertrophy at 2 weeks after pressure overload. However, at 4 weeks after pressure overload, cardiac function was impaired in p53flox/flox, but not in p53CKO mice. Single-cardiomyocyte transcriptome analysis of p53flox/flox and p53CKO mice at 2 weeks after pressure overload showed that failing cardiomyocytes appeared in p53flox/flox mice, but rarely in p53CKO mice, suggesting that p53 activation is necessary for the induction of failing cardiomyocytes. Epigenomic profiling of murine cardiomyocytes in the heart failure stage revealed the enrichment of binding motifs of myocyte enhancer factor-2 (MEF2) and nuclear factor-erythroid 2-related factor 2 (Nrf2) at active regulatory elements around p53-regulated genes. We performed western blot analysis of heart tissues from p53flox/flox and p53CKO mice after sham operation and at 8 weeks after TAC operation (heart failure stage) to confirm that Nrf2 protein expression was increased after TAC operation in p53flox/flox mice, which was blocked in p53CKO mice. We also conducted chromatin immunoprecipitation followed by quantitative PCR of TAC cardiomyocytes to show the significant enrichment of Nrf2 at the Mef2a promoter, validating our hypothesis that the p53-Nrf2-Mef2a axis is essential for the induction of failing cardiomyocytes.

Discussion & Conclusion

Having established a system for the comprehensive analysis of multilayer cardiomyocyte responses to hemodynamic overload in vivo at the single-cell level, we elucidated the trajectory of cardiomyocyte remodeling in response to pathological stimuli, distinguished gene modules for cardiomyocyte hypertrophy and failure, and revealed the coordinated molecular and morphological dynamics of cardiomyocytes leading to heart failure.

Upon pressure overload, cardiomyocytes activated the mitochondrial ribosome and oxidative phosphorylation module, the activity of which is correlated with the extent of morphological hypertrophy and is linked to the ELK1 and NRF1/2 transcriptional networks. This suggests that ERK1/2-induced ELK1 phosphorylation and NRF1/2 activation cooperatively regulate mitochondrial biogenesis to generate more ATP, which is required for enhanced protein synthesis to adapt to the enlargement of cell size and for increased contractility to overcome pressure overload. We also revealed the association of morphological hypertrophy and the oxidative stress response, supporting the hypothesis that increased mitochondrial biogenesis is the source of oxidative stress.

Sustained stimuli induce the accumulation of oxidative DNA damage, leading to p53 signaling activation during hypertrophy. Single-cell analysis of cardiomyocyte-specific knockout mice provided strong evidence indicating that p53 in cardiomyocytes increases cell-to-cell transcriptional heterogeneity, induces morphological elongation, and drives pathogenic gene programs by disrupting the adaptive hypertrophy modules and activating the heart failure module, thereby elucidating how DNA damage accumulation leads to heart failure. Heterogeneous p53 activation in vivo may be related to recent live-cell imaging results showing stochastic p53 signaling activation for cell fate determination in vitro. Our single-cell analysis uncovered a small population of hypertrophy-stage cardiomyocytes with transient activation of p53 signaling. Heart failure stage-specific cells dominate in the failing heart, suggesting that p53 signaling might be activated in most cardiomyocytes to induce heart failure. This p53 signaling-induced cellular dysfunction might be associated with findings that p53 activation at the G2-M phase is necessary and sufficient for cellular senescence. The p53-induced heart failure gene program is orchestrated by MEF2 and Nrf2. We showed that p53 is necessary for Nrf2 activation in the heart failure stage, consistent with the previous finding of p21-mediated Nrf2 protection against Keap1-mediated ubiquitination. Bardoxolone methyl, an antioxidant Nrf2 activator, increases the risk of heart failure, suggesting that the p53-induced gene program might cause heart failure.

References

1. Nomura S, Satoh M, Fujita T, Higo T, Sumida T, Ko T, Yamaguchi T, Tobita T, Naito AT, Ito M, Fujita K, Harada M, Toko H, Kobayashi Y, Ito K, Takimoto E, Akazawa H, Morita H, Aburatani H, Komuro I. Cardiomyocyte gene programs encoding morphological and functional signatures in cardiac hypertrophy and failure. ***Nat Commun***. 9: 4435, 2018
2. Satoh M*, Nomura S*, Harada M, Yamaguchi T, Ko T, Sumida T, Toko H, Naito AT, Takeda N, Tobita T, Fujita T, Ito M, Fujita K, Ishizuka M, Kariya T, Akazawa H, Kobayashi Y, Morita H, Takimoto E, Aburatani H, Komuro I. High-throughput single-molecule RNA imaging analysis reveals heterogeneous responses of cardiomyocytes to hemodynamic overload. ***J Mol Cell Cardiol.*** 128: 77-89, 2019 *co-first authors

一般の皆様へ

【背景】

心臓に高血圧などの負荷がかかると心臓は肥大してポンプ機能を維持しようとしますが、負荷が持続すると心機能が低下して心不全を発症します。しかし、これまでその詳細なメカニズムはわかりませんでした。

【目的】

心筋シングルセル解析により心不全発症メカニズムを明らかにする。

【結果】

我々は、シングルセル解析・機械学習により世界で初めて心筋リモデリングの過程における分子プロファイルの挙動を明らかにしました。その結果、心筋細胞の肥大化にはミトコンドリア生合成の活性化が重要であること、肥大心筋細胞は代償性心筋細胞と不全心筋細胞へと分岐すること、不全心筋細胞への誘導にはDNA損傷（DNAに傷が入ること）とがん抑制遺伝子であるp53の活性化が重要であることを明らかにしました。さらに、遺伝子発現パターンから患者の予後・治療応答性を予測できることを実証しました。

【今後の発展性】

明らかとなった分子メカニズムを標的として心不全の新しい治療法の開発が進むと考えられます。また本研究の成果は、あらゆる心臓疾患の病態の解明に役立つだけでなく、個々の心不全患者さんの治療方針を決める上で実際の臨床の現場に応用されることが期待され、これにより循環器疾患の精密医療（個別化医療）が実現すると考えられます。

Development of the new organ lack model

Ayako Isotani
isotani@bs.naist.jp
Nara Institute of Science and Technology

Summary Abstract

In this study, to generate an organ-deficient animal model, we attempted to create new method by using the CRISPR/Cas9 genome editing technique. For this purpose, we established the mouse line that has gRNA that could induce cell death in the presence of the Cas9 protein. In future, it is expected that new organ-deficient animal models will be produced by modifying them with various organ-specific Cas9 proteins.
Key Words：organ formation, inducible cell death, genome editing, chimera

Introduction

Several studies have been performed in regenerative medicine research to solve the problem of the shortage of organs for transplantation, and specifically, to develop interspecies animal chimeras to generate organs of interest in an animal body. An organ-deficient animal model is essential to produce an organ in an interspecies chimeric animal body. Therefore, we attempted to develop a method for producing new organ-deficient animal models.

Results

We focused on the CRISPR/Cas9 system, a genome editing technique, as a method to generate a new organ-deficient animal model. In this study, we aimed 1) to identify a target sequence of guid RNA (gRNA) that induces cell death in the presence of the Cas9 protein and 2) to express the Cas9 protein in a specific organ to generate an organ-deficient model.

First, we selected candidates for the target sequence of gRNA and transiently expressed each of them with the Cas9 protein by transfection into ES cells to examine whether any of them induced cell death. Thus, we identified two suitable gRNA sequences.

Second, although gRNA is constitutively expressed, it does not work when the Cas9 protein is absent. Therefore, the expression sequences of the identified gRNAs were knocked-in the Rosa26 locus of mouse ES cells, and an attempt was made to establish ES cells that constitutively expressed gRNA. In the recent years, the CRISPR/Cas9 system has often been used to increase the efficiency of knock-in. However, in the present study, this strategy could not be employed because the expression of the Cas9 protein resulted in cell death. Therefore, knock-in was performed using a similar CRISPR/Cpf1 system to establish ES cells with gRNA in the Rosa26 region. To confirm if gRNA was expressed in the established ES cells and could induce cell death, a Cas9 expression vector was transfected into the ES cells. As expected, the Cas9-expressing ES cells did not survive (Figure 1).

Subsequently, to establish a genetically-modified mouse line using the established ES cells, the ES cells were injected into 8-cell-stage mouse embryos, which were then transferred into the uteri of pseudo-pregnant mice. This enabled us to obtain chimeric pups. Once they reached maturity, the chimeric mice were mated with the wild-type ones to allow germline transmission and the

establishment of a mouse line. Finally, we established a mouse strain that expressed gRNA and was capable of inducing cell death in the presence of the Cas9 protein.

Furthermore, we aimed to perform phenotypic analysis of the chimeric mice. Cas9 cDNA was knocked-in behind the promoter of a gene expressed in a specific organ, using gRNA-expressing ES cells gRNA successfully obtained from mice. Unfortunately, we could only obtain ES cells knocked-in both the alleles and gene-deficient ES cells with a mutation on the other side, even if knocked-in in just one allele. It is predicted that both types mutant ES cell lines had the gene knocked-out phenotype. Therefore, even if the organ-deficient phenotype appeared in the chimera following the use of established ES cells, it was difficult to judge whether it was a phenotype due to a gene defect or the system was functioning. Therefore, we decided to establish a mouse line and analyze this in the next generation. As described above, the established ES cells were injected into the mouse embryos and chimeric mice were obtained. Surprisingly, some chimeras were found to have the gene knocked-out phenotype, whereas some chimeras had no significant phenotype. This was dependent on which ES cell lines were used.

We are currently waiting for the growth of more chimeric mice to obtain the next generation.

Figure 1

Alkaline phosphatase staining shows surviving ESC upon transfection of mock plasmid (mock). No surviving ESC were detected in the non-transfected (control) and pX459 (Cas9) transfected cells.

Discussion & Conclusion

In this study, to generate an organ-deficient animal model, we attempted to induce cell death in an organ-specific manner using the CRISPR / Cas9 genome editing technique. We determined gRNA sequences that could induce cell death in the presence of the Cas9 protein. Thereafter, we established that gRNA was constitutively expressed in ES cells and confirmed whether cell death was induced by the expression of the Cas9 protein in established ES cell lines. In addition, using chimeric mice, mouse lines expressing gRNA were established gRNA.

In future, it is expected that new organ-deficient animal models will be produced by modifying them with various organ-specific Cas9 proteins.

一般の皆様へ

近年、再生医療研究において、動物の体内に臓器を作らせる、異種間キメラ動物が注目されつつあります。異種間キメラ動物体内で臓器を作らせるためには、臓器欠損モデルの作出が欠かせないため、本研究において、新たな臓器欠損モデル動物の作製法の開発を試みました。我々は、Crispr/Cas9システムに着目し、細胞死誘導する sgRNA を同定し、機能を細胞レベルで確認しました。さらに、この sgRNA を恒常的に発現するマウス系統を樹立しました。今後、Cas9を臓器特異的に発現するマウスと組合せる事で、臓器欠損モデルを作製することができると期待しています。

Molecular mechanism for the initial assembly of human procentriole.

Satoko Yoshiba
sayoshiba@mol.f.u-tokyo.ac.jp
Graduate School of Pharmaceutical Sciences, The University of Tokyo

Summary Abstract

The role of the cartwheel structure, a universal template of centriole across species, is further characterized using a combination of super-resolution microscopy and Crispr/Cas9-mediated auxin-inducible protein degradation (AID) system in human cells.
Key Words：centriole duplication, cartwheel, SAS-6, AID

Introduction

The centrosome is a major microtubule-organizing center of animal cells and comprises a pair of centrioles surrounded by pericentriolar material. The centriole duplicates once in a cell cycle, and its assembly is strictly regulated with cell cycle progression. At the onset of procentriole formation, a structure called the cartwheel is formed adjacent to pre-existing centriole. SAS-6 proteins are thought to constitute the hub of the cartwheel structure. In this study, we focused on the roles of human SAS-6 (HsSAS-6), and tried to elucidate its unveiled functions, using conditional protein knockout system.

Results

Establishment of HsSAS-6-AID human cell line. The cartwheel/SAS-6 is known to be essential for the initiation of procentriole formation. However, whether it has an additional role in the subsequent processes of procentriole formation remains to be elucidated. Therefore, to further investigate the possible functions of the cartwheel, we generated an HsSAS-6-AID human cell line, which enabled swifter removal of endogenous HsSAS-6 proteins than the conventional reverse-genetic approach using RNAi. We applied a combination of genome editing by CRISPR/Cas9 and the AID-based protein degradation systems to human HCT116 cells. In the HCT116 cells constitutively expressing osTIR1, which is an essential component of SCF/E3 ligase for AID-based degradation with the addition of auxin, both endogenous HsSAS-6 alleles were AID-tagged at their C-terminal ends. First we tested the degradation properties of HsSAS-6-AID proteins in these cells, and found that after addition of auxin, cytoplasmic HsSAS-6-AID proteins were quickly reduced within 1 h, whereas it took 6 h to completely remove HsSAS-6-AID proteins from the centrioles. Next, we examined whether centriole duplication occurs when HsSAS-6-AID is degraded before centriole formation starts in the late G1 phase. HsSAS-6-AID cells were synchronized in the G2/M phase by treatment with nocodazole, released and then simultaneously treated with auxin until the S phase or the next G1 phase. The recruitment of HsSAS-6-AID to the centriole was inhibited as a result of the addition of auxin, and centriole duplication was effectively blocked. These results confirmed that HsSAS-6 is required for the initiation of centriole formation. **HsSAS-6-AID removal from the centriole in the process of procentriole formation.** Next, we sought to analyze whether HsSAS-6 is dispensable after the early stages of procentriole assembly, or alternatively whether it is essential

for further elongation. Given that it normally takes 6 h to remove HsSAS-6-AID proteins from the centrioles in asynchronous cells, we arrested cells in the early S phase, and then treated them with auxin to remove HsSAS-6-AID from centrioles for the last 6 h prior to analysis. Unfortunately, we failed to completely remove HsSAS-6 from centriole, even in the S-phase arrested cells after 6 h of auxin treatment. We speculated this is presumably because continuous loading of HsSAS-6 at centrioles during the extended S phase. Centriolar loading of HsSAS-6 is known to be dependent on Plk4 kinase activity. Therefore, to completely remove HsSAS-6 from the centrioles, we combined auxin treatment with simultaneous transient Plk4 inactivation via the addition of centrinone, a Plk4 specific inhibitor. We found that the addition of auxin and centrinone for 3 h in the early S phase or for 4 h in mid-S phase, was sufficient to remove HsSAS-6 from the centrioles. We found that in the cells treated with auxin and transiently with centrinone in the early S phase, the number of cells with duplicated centrioles was dramatically decreased in the next G1 phase (24% duplicated). By contrast, in the cells treated in mid-S phase, the number of duplicated centrioles in the next G1 phase was significantly increased (83% duplicated) compared with that in the case of HsSAS-6 removal in early S phase. These data suggest that cartwheel/HsSAS-6 is necessary for the integrity of procentriole intermediates at least up to the early S phase, but are thereafter dispensable for subsequent centriole elongation and maturation. **Testing the loading of centriolar proteins through early S phase to G2 phase using super-resolution microscopy.** Cep295 is a conserved protein that is not required for the initiation of cartwheel assembly, but is necessary for the proper elongation and maturation of centrioles through recruitment of Cep135, Cep192, Cep152 and other PCM proteins. Among these proteins, we found that Cep135, which is known to be required for well-organized stacking of cartwheel, was frequently observed to start to localize at the procentriole in the mid-S phase, suggesting Cep135 loading may be a key event for stabilizing the procentriole structure.

Discussion & Conclusion

In this study, we characterized the novel function of the cartwheel/HsSAS-6 in centriole formation, by developing a system for inducible HsSAS-6 degradation in human cells. We demonstrated that HsSAS-6 is essential not only for the initiation of procentriole formation, but also for the stabilization of the proximal half of the procentriole. However, it seems that the cartwheel structure is dispensable for the subsequent steps for full elongation and maturation of centrioles. Such requirement of the cartwheel structure implies a stepwise procentriole assembly in the following way. Several layers of cartwheel structures that are stacked on the mother centriole wall establish the overall geometry of a procentriole. Thereafter, some critical components are incorporated into the intermediate, and facilitate arrangement of centriolar triplet microtubules and further procentriole elongation. In our previous study, we showed that Cep295 is required for the recruitment of Cep135 to the proentriole. Together with the findings in this study, it is possible that the acquisition of Cep135 leads to the stabilization of the centriole intermediate, and it would allow further elongation and maturation of the procentriole. Overall, our results experimentally demonstrated for the first time the importance of HsSAS-6 until the procentriole structure is stabilized for subsequent maturation.

References

Yoshiba, S., Tsuchiya, Y., Ohta, M., Gupta, A., Shiratsuchi, G., Nozaki, Y., Ashikawa, T., Fujiwara, T., Natsume, T., Kanemaki, M., Kitagawa, D. (2019). HsSAS-6-dependent cartwheel assembly ensures stabilization of centriole intermediates. *Journal of Cell Science*, in press.

Ran, F., Hsu, P., Wright, J. and Agarwala, V. (2013). Genome engineering using the CRISPR-Cas9 system. *Nat. Protoc*. 8, 2281–2308

Natsume, T., Kiyomitsu, T., Saga, Y. and Kanemaki, M. T. (2016). Rapid Protein Depletion in Human Cells by Auxin-Inducible Degron Tagging with Short Homology Donors. *Cell Rep.* 15, 210–218.

Tsuchiya, Y., Yoshiba, S., Gupta, A., Watanabe, K. and Kitagawa, D. (2016). Cep295 is a conserved scaffold protein required for generation of a bona fide mother centriole. *Nat. Commun.* 7, 12567.

一般の皆様へ

細胞のなかにある 1 組の中心体は、細胞が分裂し 2 つに分かれるときにそれぞれの極となって分裂を正しく導く重要な役割を持っています。中心体の数の増加や機能の異常は、がんの発症やさまざまな病気と密接に関係していることがわかっています。中心体がどのように形成されるのかについて研究することで、細胞のがん化のメカニズムや関連する病気の原因が明らかになり、将来的には治療に役立つことが期待されます。

Structural basis for inactivation of Na^+,K^+-ATPase by β-amyloid

Ryuta Kanai
ryuta-kanai@iam.u-tokyo.ac.jp
The University of Tokyo

Summary Abstract

Amylospheroid (ASPD) composed of amyloid β-proteins causes neurodegeneration correlating with Alzheimer's disease and inhibits the ATPase activity of the α3 isoform of Na^+,K^+-ATPase (NKAα3). In order to elucidate the mechanism of NKA inactivation by ASPD, we performed crystallographic analysis of NKA, constructed mammalian expression system for NKAα3, and carried out isothermal calorimetry experiments to determine thermodynamic parameters for the interaction between NKA and ASPD. (64 wrds)

Key Words : Na^+,K^+-ATPase, Amyloid β-protein, crystallography

Introduction

Amyloid β-proteins form neurotoxic oligomers correlating with Alzheimer's disease.

Recently, ASPD consisting of amyloid β-proteins have been reported to target neurospecific NKAα3 and eventually to cause neurodegeneration (Ohnishi, et al. (2015) PNAS). NKAα3 pumps three Na^+ ions out and two K^+ ions into the cell per molecule of ATP hydrolysed. Structural information about NKAα3 and ASPD is necessary for designing a drug to block the interaction between NKAα3 and ASPD but is not available yet.

Results

NKA consists of three polypeptides; the α- and β-subunits and a FXYD protein. ASPD is known to bind an extracellular loop L7/8 of the α subunit that is not the ATPase catalytic site or the transmembrane ion binding sites. However, as L7/8 appears close to outerleaflet of membrane and the ectodomain of the β subunit, we thought ASPD binding L7/8 results in destabilizing the interaction between the α and β subunits, or phospholipids. As a precise membrane position was unknown for NKA, we re-visited the crystal structures of NKA in E1~P·ADP·$3Na^+$ and E2·Pi·$2K^+$ reported previously, and built atomic models for missing parts of NKA and phospholipids surrounding NKA by re-refining the structure including more low resolution reflections.

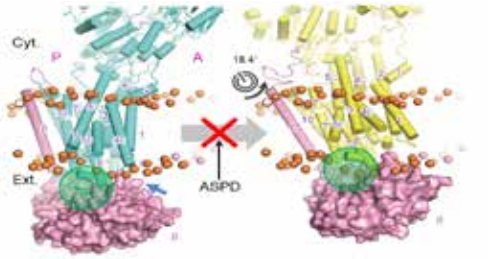

Fig. 1. ASPD would interfere with a rigid motion of NKA β subunit necessary to form an unphosphorylated E1 state. (left) the E2·P·$2K^+$ state of NKA (right) the E1~P·ADP·$3Na^+$ state inclined toward membrane plane by 18.4° like E1·$2Ca^{2+}$ of Ca^{2+}-pump. Cyan and yellow, α subunit; violet, β subunit; green circle, ASPD binding site; orange spheres, phosphorous atoms of phospholipid membrane. The membrane model is constructed by overlapping the membrane structure experimentally determined for Ca^{2+}-pump in its equivalent state (E1~P·ADP·$2Ca^{2+}$) onto the partial phospholipid membrane determined in this study. Please note the M1-2 helices in an unphosphaorylated E1 state would move down toward the extracellular side to avoid such energetically unfavorable conformation and to open the cytoplasmic gate.

We have succeeded in identifying 12-13 phospholipids (PLs) and a new glycosylation site of the β-subunit as well as extending N-terminal cytoplasmic region of the β-subunit. These partial membrane models in two states enabled to predict a membrane position in the crystals and raised a

possibility that the ectodomain of the β subunit in an unphosphorylated E1 state rigidly moves close to outerleaflet membrane and the closed extracellular gate composed of M1-4 helices of the α subunit (Fig. 1b). Such rigid motion of the β subunit indicates that the ectodomain contributes to close the extracellular gate by interacting with M1-2 helices and/or outerleaflet membrane. Therefore, ASPD binding to L7/8 may interfere with these interactions of the β subunit and the extracellular gate and/or outerleaflet membrane by blocking such movement of the β subunit.

For further structural studies for an inhibition mechanism of NKAα3β1 by ASPD, we are establishing mammalian expression system for human NKAα3β1 which atomic structure has not been determined yet. Here, we constructed a recombinant adenovirus to express human NKAα3β1, and tested several cell lines for optimal virus infection and NKA expression. A549 and AD293 cells showed better expression than the others. ATPase assay of the purified microsome including NKA showed that NKA from AD293 is active but not from A549. As AD293 cells are not suitable for protein production using the recombinant adenovirus, we are trying constructing a recombinant baculovirus to express NKA α3β1 in AD293 cells.

In addition, we are trying to determine thermodynamic parameters of the interaction between NKA and ASPD by using isothermal calorimetry (ITC). As ASPD is too large to stably be solubilized, truncated amyloid β-protein (Aβ1-42), which forms oligomers like ASPD, was used in this experiment. As an initial attempt, we titrated the purified membrane fraction containing NKA with Aβ1-42 solubilized in DMSO. However, the titration curves were very unstable because thermodynamic effect from DMSO appeared much larger than that of Aβ1-42 even when carefully measured the background using DMSO. Next, to minimize such noise effect, DMSO was added to the membrane fraction as same concentration as in the Aβ1-42 solution. This adjusting background dramatically improved the baseline but the signal occurred by titration was too weak to determine reliable K_d. Because, a thermal change caused in association of Aβ1-42 with NKA may be very small or Aβ1-42 used in this experiment may be inactive because of a solubilization problem. In fact, preparation of Aβ1-42 solution needs special cares like using DMSO with the highest grade, low humidity when solubilizing, and immediate use. Currently, we are carefully analyzing the solubilization condition of Aβ1-42.

Discussion & Conclusion

In this study, we re-constructed crystal structures of NKA in E1~P·ADP·$3Na^+$ and E2·P_i·$2K^+$ to predict inhibition mechanism of NKA by ASPD and suggested that ASPD appears to interfere with interactions of the β subunit with M1-2 helices and/or outerleaflet membrane.

For further structural study, we are establishing mammalian expression system for human NKAα3 and β1 and found that AD293, a substrain of HEK293T cells, is the best cell line for expression and activity of NKA.

We are performing ITC experiments for biochemistry of the interaction between NKA and ASPD but got some technical problems. We are trying to solve them but also planning of other biochemical tools like surface Plasmon resonance.

References

Ohnishi, et al. (2015) *PNAS*, **112**, E4466-E4474. Na, K-ATPase α3 is a death target of Alzheimer patient amyloid-β assembly.

一般の皆様へ

アルツハイマー病は脳内でアミロイドβの凝集・蓄積により発症します。近年、アミロスフェロイド (ASPD) と呼ばれる、アミロイドβの特定の凝集体がNKA α3と呼ばれる神経細胞に特異的な膜蛋白質に結合し、強い神経毒性を示すことが分かってきました。そこで、私達は将来的にアルツハイマー病の治療薬創出を目指して、ASPDがどのようにしてNKA α3に結合し、その機能を破壊するのかを研究しました。その結果、ASPDはNKA α3が機能する際に生じる構造変化を阻害しているらしいことが分かりました。実際の創薬にはまだ遠いですが、これからも研究を続けていきたいと思います。

Evolutionary development of fluorescent RNA sensors by droplet technology

Shigeyoshi Matsumura
smatsumu@sci.u-toyama.ac.jp
University of Toyama

Summary Abstract

We have established the directed evolution system for a fluorescent RNA using droplet microfluidics. Based on the developed technology, we are currently running the directed evolution experiments of the RNA. This effective method to engineer the fluorescent RNAs would lead much broader applications for life science.
Key Words：Fluorescent RNA, directed evolution, droplet microfluidics

Introduction

Recently a fluorescent RNA called “Spinach” was developed, binding with a fluorophore DFHBI to activate its GFP-like green fluorescence [1]. This enables any cellular RNAs to be labelled and visualized in vitro and in vivo. An effective method to engineer such fluorescent RNAs is desired for much broader applications. Our objective is establishment of such methodology by combining directed evolution strategy and droplet microfluidic technology.

Results

Droplet microfluidics is a technology which provides precise handling of tiny water droplets (emulsions) on microfluidic chips [2]. To evolve fluorescent RNAs, this technique is essential to encapsulate and evaluate each species of the RNA library. We have developed two microfluidic devices for encapsulation and sorting of the fluorescent RNAs. The one is for making droplets whose size is around 1 pL, which is 10 times smaller than that of the droplets prepared with a previous device. The other is for analyzing and sorting the 1 pL droplets. The new design of this device provides low false positive (miss-sorting), achieving higher throughput of the sorting (2000 events / sec.).

Next, a single-molecule fluorescent RNA needs to be encapsulated into one droplet, and be detected. But it is impossible since the RNA concentration under such condition (1 molecule / droplet) is too low. To enhance the fluorescent signal in droplets, we employed an RNA amplification technique called Nucleic Acid Sequence-Based Amplification (NASBA). In this way, transcription from DNA to RNA and reverse transcription from RNA to DNA proceed simultaneously in solution, enabling exponential amplification of RNA under isothermal condition [3]. The first test of the NASBA with the fluorescent RNA showed amplification, but its efficiency was quite low when the RNA template concentration is less than 10 pM. Improvement of the reaction condition including buffer compositions increased the yield at low template concentration. It was also verified that the fluorescent RNA is functional under the NASBA conditions.

We subsequently introduced the reaction above into the tiny droplets. The template, the NASBA enzymes and components, and the fluorophore DFHBI were compartmentalized into the 1 pL

droplets, and then incubated at 37 °C. After incubation, the droplets were re-injected into the sorting device, and then the individual fluorescence was analyzed on the chip. We have succeeded in detecting the green fluorescence originating from the fluorescent RNA, indicating that the amplification of the functional fluorescent RNA works nicely even in the tiny droplets, not only in the bulk solution.

To proceed into next evolution experiments, we constructed an initial library of the fluorescent RNA. Point mutations were introduced into the RNA sequence by mutagenic PCR. Furthermore, the randomness of the resulting library was analyzed and evaluated by next-generation sequencing. The data indicates that the mutations are uniformly introduced into the entire region of the fluorescent RNA sequence, which is likely suitable as a library for directed evolution experiment.

Discussion & Conclusion

As described above, we have established the directed evolution system for the fluorescent RNA using droplet microfluidics. We already achieved: (1) new microfluidic system and devices, (2) exponential amplification method for the fluorescent RNA, (3) the same reaction in droplets, (4) initial library construction by mutagenic PCR. Based on the above, we are currently running the evolution experiments of the RNA. If the enrichment of the active species is observed, we are going to analyze the enriched pool of RNA by next-generation sequencing (Illumina MiSeq), and then isolate the improved (evolved) variants. The NGS analysis would reveal the evolutionary dynamics of the RNA during the selection, which should be helpful to understand what kind of selection conditions are useful or not for successful evolution.

References

1) Paige, J. S. *et al.*, RNA mimics of green fluorescent protein. *Science*, 333, 642-646 (2011)
2) Matsumura, S. *et al.*, Transient compartmentalization of RNA replicators prevents extinction due to parasites. *Science*, 354, 1293-1296 (2016)
3) Compton, J., Nucleic acid sequence-based amplification. *Nature*, 350, 91-92 (1991)

一般の皆様へ

近年、蛍光を発する人工 RNA の開発が急速に進んでおり、細胞内の任意の RNA の蛍光標識および可視化、細胞内 RNA 動態のリアルタイム解析などへの応用が期待されている。本研究は、これらの蛍光 RNA を細胞サイズのマイクロドロップレットへ封入し、人為的に「進化」させることで、望みの特性をもつ蛍光 RNA を自在に創製する方法論を確立し、ライフサイエンスにおける RNA イメージングなどへの貢献を目指すものである。

Functional Analysis of Chk1 Targets for Breast Cancer Treatment

Midori Shimada
shimada@yamaguchi-u.ac.jp
Yamaguchi University

Summary Abstract

Triple-negative breast cancer (TNBC) is associated with poor prognosis and a high risk of relapse. A previous report showed that the calcineurin/NFATc pathway was activated in TNBC cells, and has an essential role in the tumorigenic and metastatic properties. The effect of FK506 has not been totally analyzed in TNBC cells. In this study, we demonstrate that expression of Chk1 was reduced and G1/S progression, but not G2/M, was inhibited in TNBC cells by FK506 treatment.
Key Words：Cell cycle, triple negative breast cancer, calcineurin

Introduction

FK506 (tacrolimus) is a major immunosuppressant agent widely used for the prevention of graft rejection in organ transplantation and the treatment of autoimmune diseases [1]. FK506 inhibits calcineurin protein phosphatase by binding to various FK506 binding proteins (FKBPs) [2]. Calcineurin activates the nuclear factor of activated T cell (NFATc) transcription factors, which induces T cell activation via expression of cytokines [3]. It has become increasingly apparent that two other macrolide immunosuppressants, cyclosporine A and rapamycin, as well as FK506, induce apoptosis in a wide variety of cancer cells [4-6]. Conversely, one study shows that a low concentration of FK506 promotes proliferation in vascular smooth muscle cells. Owing to their antiproliferative effects, these immunosuppressant agents are expected to provide new potential therapeutic approaches for cancer treatment. A recent study demonstrated that cyclosporine A and rapamycin decreased mRNA expression of *cyclin D1* and showed a defect in G1/S progression [7]. However, it is largely unknown whether FK506 has any effect on cell cycle progression.

Results

Given that the CN/NFATc pathway is activated in the ER-PR-HER2-triple-negative breast cancer (TNBC) subgroup [8], we investigated the effect of a CN/NFATc inhibitor, FK506, on cell proliferation in the TNBC, Hs578T, and MDA-MB-231 cell lines. FK506 (50 μM) efficiently inhibited TNBC cell growth, which was consistent with a previous report showing that FK506 induced apoptosis in the Jurkat human T cell line and other non-T cell lines [4-6]. In contrast, treatment of TNBC cell lines with FK506 (10 μM) did not produce growth defects. At 24 h after treatment with FK506 (50 μM), cells became rounded and detached from culture dishes. FACS analysis revealed that FK506 (50 μM) did not increase mitotic cells but increased the populations of G1 phase cells and the sub-G1 fraction. A low dose of FK506 (10 μM) did not change the cell cycle profile. To confirm that 50 μM FK506 stimulates apoptosis, we monitored two apoptotic markers, the cleaved form of caspase 3 and PARP1. We found that both caspase 3 and PARP1 were efficiently cleaved in the FK506-treated cells, suggesting that FK506 induced apoptosis in TNBC cells. Our results showed that FK506 induced G1/S arrest and apoptosis at a concentration of 50 μM.

The data above indicate that FK506 affected G1/S cell cycle progression. Next, we synchronized cells at the G1/S boundary using a double thymidine block and examined the effect of FK506. We added FK506 at 2 h just before the release from the thymidine block and the cells were released in the presence of FK506. FACS analysis revealed that cells treated with FK506 progressed to S phase more slowly than the control cells. At 8 h after release, about 70 % of the control cells entered into the G2/M phase, whereas most of the cells treated with FK506 were still in the G1/S or middle S phase, and less than 30 % of the cells showed progression into the G2/M phase. These results indicate that FK506 induces a delay in G1/S progression. Progression from the G1 to the S phase, and the S phase of the cell cycle is regulated by cyclins D and E, which are essential for the activation of cyclin-dependent kinases. A previous report showed that cyclin A2 is important for the continuation of the S phase, B1 for the G2/M phase, E for the S phase initiation, and D1 mainly for G1/S progression [9,10]. Next, we investigated the expression of these key cyclins. Treatment of cells with FK506 led to decreased cyclin D1 expression, whereas FK506 had no effect on cyclin E. Decreased expression of cyclin A2 and B1 by FK506 may be due to the altered cell cycle populations, because they were not changed in synchronized cells at G2. In addition, expression of Chk1 was reduced in FK506 treated cells.

Next we investigated whether FK506 post-translationally regulated cyclin D1. Inhibition of proteasome activity with MG132 reversed the FK506-induced reduction in cyclin D1, suggesting that FK506 induces the proteasomal degradation of cyclin D1. To investigate other possible effects of FK506, with potential influence on *cyclin D1* mRNA expression, we performed quantitative real-time PCR analysis and found that *cyclin D1* mRNA expression was not affected by treatment with FK506 or FK506 combined with MG132. Taken together, FK506 facilitates proteasomal degradation of cyclin D1, which may lead to delayed G1/S progression.

Discussion & Conclusion

In summary, we found that calcineurin inhibition promoted cyclin D1 degradation by impairing dephosphorylation, resulting in G1/S delay. It is worthy to note that overexpression of cyclin D1 is detected in more than 50% of human invasive breast cancers 32, and this may be partly due to deregulated proteasomal degradation. In TNBC as well, overexpression of cyclin D1 is relates to poor prognosis 33. In addition, it is reported that the calcineurin/NFAT pathway is frequently activated in TNBC subgroups, and has an essential role in the tumorigenic and metastatic properties 4. Similarly, mutation on T286 has been reported in esophageal and endometrial cancers 34. We therefore propose that therapeutic targeting of cyclin D1 could be useful for the prevention and treatment of cancers, such as TNBC, where cyclin D1 is overexpressed.

References

[1] J.R. Azzi, M.H. Sayegh, S.G. Mallat, Calcineurin inhibitors: 40 years later, can't live without, J Immunol, 191 (2013) 5785-5791.

[2] M.W. Harding, A. Galat, D.E. Uehling, S.L. Schreiber, A receptor for the immunosuppressant FK506 is a cis-trans peptidyl-prolyl isomerase, Nature, 341 (1989) 758-760.

[3] G.P. Mognol, F.R. Carneiro, B.K. Robbs, D.V. Faget, J.P. Viola, Cell cycle and apoptosis regulation by NFAT transcription factors: new roles for an old player, Cell Death Dis, 7 (2016) e2199.

[4] S.J. Choi, H.S. You, S.Y. Chung, Tacrolimus-induced apoptotic signal transduction pathway, Transplantation proceedings, 40 (2008) 2734-2736.
[5] Y. Hashimoto, N. Matsuoka, A. Kawakami, M. Tsuboi, T. Nakashima, K. Eguchi, T. Tomioka, T. Kanematsu, Novel immunosuppressive effect of FK506 by augmentation of T cell apoptosis, Clin Exp Immunol, 125 (2001) 19-24.
[6] K. Migita, K. Eguchi, Y. Kawabe, T. Tsukada, A. Mizokami, S. Nagataki, FK506 augments activation-induced programmed cell death of T lymphocytes in vivo, J Clin Invest, 96 (1995) 727-732.
[7] M. Weischer, M. Rocken, M. Berneburg, Calcineurin inhibitors and rapamycin: cancer protection or promotion?, Experimental dermatology, 16 (2007) 385-393.
[8] C.T. Quang, S. Leboucher, D. Passaro, L. Fuhrmann, M. Nourieh, A. Vincent-Salomon, J. Ghysdael, The calcineurin/NFAT pathway is activated in diagnostic breast cancer cases and is essential to survival and metastasis of mammary cancer cells, Cell Death Dis, 6 (2015) e1658.
[9] E.A. Musgrove, C.E. Caldon, J. Barraclough, A. Stone, R.L. Sutherland, Cyclin D as a therapeutic target in cancer, Nat Rev Cancer, 11 (2011) 558-572.
[10] P. Hydbring, M. Malumbres, P. Sicinski, Non-canonical functions of cell cycle cyclins and cyclin-dependent kinases, Nat Rev Mol Cell Biol, 17 (2016) 280-292.

一般の皆様へ

乳癌は日本人女性が罹患する悪性腫瘍の第 1 位であり、その罹患数ならびに死亡数は増加の一途を辿っています。ホルモン療法および抗 *HER2* 療法では効果がないトリプルネガティブ乳癌に対しては治療法は限定されており、予後は極めて不良であることから、有効な分子標的薬の創出が緊急に迫られています。本研究では、トリプルネガティブ乳癌で高発現している Calcineurin 脱リン酸化酵素を阻害する FK506が乳癌の増殖を抑制できることがわかりました。

Revealing a new red light signaling pathway for resetting the circadian clock in green algae

Takuya Matsuo
t-matsuo@gene.nagoya-u.ac.jp
Center for Gene Research, Nagoya University

Summary Abstract

In this study, a gene involved in a light response mechanism of circadian clock in the green alga *Chlamydomonas reinhardtii* has been identified. This gene provides a clue to understand an unknown light response mechanism in algae.

Key Words：alga, light response, circadian clock

Introduction

Most organisms are characterized by an endogenous clock that generates a ~ 24-hour rhythm of various processes from sleep/wake cycles in mammals, leaf movement in plants to phototaxis and chemotaxis in algae. This rhythm can be reset by signals such as light and temperature. In case of light resetting in C. reinhardtii, the light induced degradation of ROC15, a DNA binding clock protein, was identified as a crucial event. Here, by a forward genetics approach, we identified a green algae specific gene that plays a crucial role in the light induced degradation of ROC15.

Results

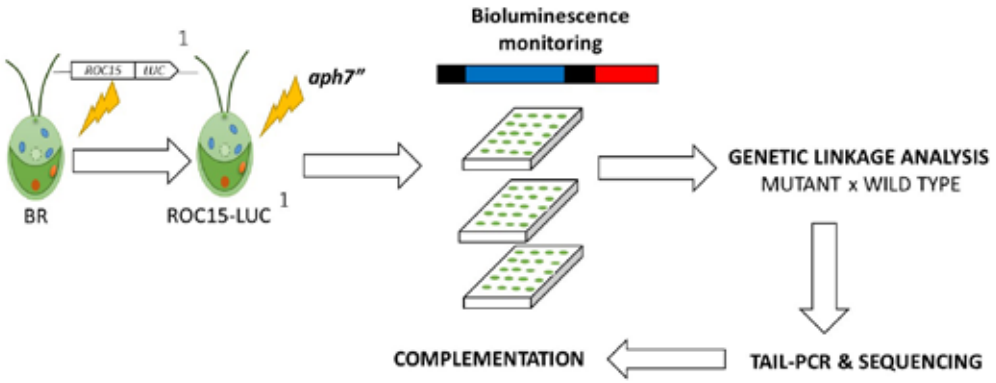

1. **Screening for mutants:** For the isolation of light response mutants, the ROC15-luciferase bioluminescence levels of the insertional mutants were monitored in response to red and blue light. From approximately 5000 mutants monitored, two mutants (M1 and M2) showing abnormal bioluminescence phenotypes were isolated. Both failed to show acute decrease in ROC15-luciferase bioluminescence levels in response to red and blue light, unlike in the WT, which shows an acute decrease in ROC15-luciferase bioluminescence level in response to both red and blue light. Therefore, M1 and M2 were selected as light response mutants and were pursued.
2. **Genetic linkage Analysis:** To confirm the linkage of hygromycin resistance and abnormal response to light, M1 and M2 were backcrossed with WT strain of opposite mating type. In case of M1 backcross, almost all progenies that were hygromycin resistant did not show an acute

decrease in bioluminescence after red light exposure. On the other hand, in case of M2 backcross, not all individuals that were hygromycin resistant had a decreased bioluminescence level in response to red light. In only M1, the cause of the abnormal bioluminescence response could be directly attributed to the insertion of the hygromycin resistance gene. The mutant in which almost all progeny were both hygromycin resistant and showed abnormal response to light in other words failed to show acute decrease in ROC15-luciferase bioluminescence levels in response to light were pursued. Hence, only M1 was pursued.

3. **Identification of disrupted gene:** In order to identify the insertion locus, TAIL-PCR and sequencing analysis was performed on M1. The secondary and tertiary downstream PCR products were used for sequencing. The resulting sequence was searched against the genome database and was found in the gene Cre07.g357500 on chromosome 7. This indicated that the insertion occurred in the gene Cre07.g357500 on chromosome 7 of the *Chlamydomonas* genome. To confirm the result of the TAIL- PCR, genomic PCR was performed around the insertion locus. The mutant band was heavier than the WT band by 1.7kb, thus confirming the result of TAIL-PCR.
4. **Complementation with Cre07.g357500 WT allele:** To clarify that Cre07.g357400 was the gene responsible for the abnormal bioluminescence response, M1 was transformed with WT Cre07.g357500 gene, and with only spectinomycin cassette were used as controls. ROC15-luciferase bioluminescence levels of 660 transformants (244 controls and 416 transformed with WT gene) were measured in response to red light and blue light. As expected, none of the 244 control were complemented, in other words, they still showed abnormal response to light, while 6 of 416 colonies transformed with WT gene were complemented, in other words, the ROC15-bioluminescence levels in response to both red and blue light were restored to WT levels. These results indicate that the Cre07.g357500 gene was responsible for the abnormal bioluminescence response.
5. **Protein Sequence analysis:** Cre07.g357500 was found to code for a protein of 2386 amino acids. The functional annotation tool in Phytozome 12.1 however did not reveal any known functional motifs. Conserved domains were also searched for (against all databases) (CD search service, NCBI) though no domain of significant similarity was obtained. On the other hand, a homology search (BLASTp, NCBI) revealed two possible homologs, XP_002956981.1 (*Volvox carteri*) and KXZ53772.1 (*Gonium pectorale*). The Cre07.g357500 peptide sequence was then aligned with the peptide sequences of the homologs (Clustal Omega, EMBL-EBI). From the alignment, the protein appears to have conserved regions in green algae.

Discussion & Conclusion

Cre07.g357500 which codes for a protein of 2298 amino acids was found to be disrupted as a result of insertional mutagenesis in the mutant M1. The disruption of this gene appears to affect the acute light induced degradation of ROC15. By analyzing the phosphorylation of ROC15 and interaction of this protein with other identified components of the light signaling pathway for resetting the circadian clock, the significance of this protein in the pathway can be further elucidated.

References

1. Kondo T, Johnson CH, Hastings JW .1991. Action spectrum for resetting the circadian phototaxis rhythm in the cw15 strain of *Chlamydomonas*. I. Cells in darkness. Plant Physiol 95: 197–205.
2. Niwa Y, Matsuo T, Onai K, Kato D, Tachikawa M, Ishiura M. 2013. Phase-resetting mechanism of the circadian clock in *Chlamydomonas reinhardtii*. Proc Natl Acad Sci U S A.;110: 13666–71.
3. Kinoshita A, Niwa Y, Onai K, Yamano T, Fukuzawa H, Ishiura M, Matsuo T. 2017. *CSL* encodes a leucine-rich-repeat protein implicated in red/violet light signaling to the circadian clock in *Chlamydomonas*. *PLoS Genetics*, 13(3), e1006645-e1006645.

一般の皆様へ

私はクラミドモナスという緑藻の一種を使って体内時計を研究しています。私たち人間と同様、緑藻の体内時計も光によってリセットされます。しかしその分子メカニズムはよく解っていませんでした。私はこの研究により、その未知のメカニズムに関わる遺伝子を明らかにしました。その遺伝子の解析から、緑藻は他の生物には見られない独特な光応答メカニズムを持つことが見えてきました。この研究成果は、生物の光応答メカニズムの進化の理解につながると考えています。

Elucidation of the role of fatty acid elongase Elovl6 in the pancreatic β-cell

Takashi Matsuzaka
t-matsuz@md.tsukuba.ac.jp
Faculty of Medicine, University of Tsukuba

Summary Abstract

To investigate the role of Elovl6 in pancreatic β-cell function and T2D, we generated and analyzed pancreatic β-cell specific Elovl6 deficient mice. We found that β-cell specific Elovl6 deficiency significantly improved hyperglycemia and increased plasma insulin concentration in diabetic db/db mice.

Key Words：Fatty acid composition, Type 2 diabetes, Conditional knockout mouse

Introduction

Elovl6 is a microsomal enzyme that elongates saturated- and monounsaturated-fatty acids (FAs) with 12, 14, and 16 carbons to FAs with 18 carbons such as stearic acid (C18:0), vaccenic acid (C18:1n-7), and oleic acid (C18:1n-9). Loss of Elovl6 function reduces stearate and oleate levels but increases palmitate, palmitoleate and vaccinate levels. We assessed the effects of Elovl6 deletion in leptin receptor-deficient db/db mice, a model of type 2 diabetes (T2D) and reported that db/db;Elovl6 KO mice showed improved glycemic control, an adaptive increase in insulin, and had a markedly increased β-cell mass. To further investigate the role of Elovl6 in pancreatic β-cell function and T2D, we generated pancreatic β-cell specific Elovl6 deficient mice and analyzed its effects in this study.

Results

Elovl6 lox/lox (Flox) mice were crossed to an insulin-1 promoter-Cre transgenic mice, which express Cre exclusively in β cells, to obtain Elovl6 lox/+;Cre+ mice. Subsequently, these mice were crossed to Flox mice to yield Elovl6 lox/lox;Cre+ (βE6KO) mice. The genotype of mice harboring the null allele was confirmed by PCR using tail genomic DNA. To confirm the deletion of Elovl6 in βE6KO mice, we analyzed mRNA levels of Elovl6 in various tissues by qPCR. The result indicated that the Elovl6 gene deletion was restricted to the pancreatic islet in βE6KO mice.

Oral glucose tolerance testing of a chow-fed βE6KO and Flox mice indicated that plasma glucose levels of Flox and βE6KO mice after overnight fasting or an oral glucose gavage was similar. Pancreatic islets isolated from βE6KO mice were morphologically compared with those from Flox mice. The number, size, and morphology of isolated islets were similar between chow-fed Flox and βE6KO mice. Isolated islets were tested for insulin secretion. Basal (low glucose) and glucose-stimulated (high glucose) insulin secretion was almost similar between Flox and βE6KO islets. Insulin content of βE6KO islets was also indistinguishable from that of Flox islets.

To investigate the role of β-cell Elovl6 in T2D development and progression, we next generated db/db;βE6KO mice. db/db and db/db;βE6KO mice both gradually gained body weight (BW) without any significant differences. Although obesity in db/db mice was not improved, Elovl6 deficiency in β-cell significantly improved hyperglycemia, increased plasma insulin concentration, and reduced

HbA1c levels. Immunostaining of pancreatic sections from 16-week-old animals with antibodies to insulin and glucagon revealed that β-cell Elovl6 deficiency in db/db mice resulted in a significant increase in β-cell mass.

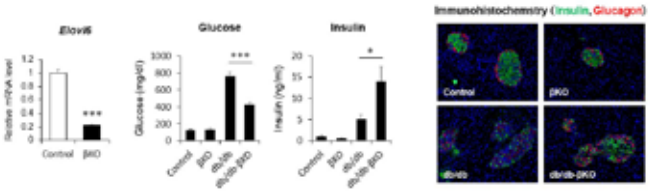

Figure. Elovl6 deficiency in β-cell ameliorates the development of type 2 diabetes in mice

Discussion & Conclusion

Current results indicated that Elovl6 deficiency in β cells did not affect the development of β cells and capacity of the insulin production and secretion in β cells under the normal chow diet fed condition. These results are consistent with the phenotype of Elovl6 global knockout mice.

In contrast, we demonstrated that β-cell-specific Elovl6 deletion in db/db mice significantly reduced circulating blood glucose levels without affecting obesity. This result suggests that Elovl6-mediated modulation of FA composition in β cells was essential in preserving proper β-cell function and preventing the development of T2D in obesity.

References

Zhao H, Matsuzaka T, Nakano Y, Motomura K, Tang N, Yokoo T, Okajima Y, Han SI, Takeuchi Y, Aita Y, Iwasaki H, Yatoh S, Suzuki H, Sekiya M, Yahagi N, Nakagawa Y, Sone H, Yamada N, Shimano H. Elovl6 Deficiency Improves Glycemic Control in Diabetic db/db Mice by Expanding β-Cell Mass and Increasing Insulin Secretory Capacity. ***Diabetes.*** 2017 Jul;66(7):1833-1846. doi: 10.2337/db16-1277.

一般の皆様へ

本研究では、パルミチン酸（C16:0）からステアリン酸（C18:0）への伸長を触媒する酵素Elovl6に着目し、2型糖尿病モデル db/db マウスの膵β細胞でこの酵素を欠損させると、2型糖尿病の発症・進展が抑制される可能性があることが示唆されました。本研究をさらに進めることにより、膵β細胞における Elovl6の阻害や脂肪酸バランスの管理が、2型糖尿病の新規治療法となることが期待されます。

Development of regenerative therapy and novel therapeutic drugs for renal anemia using human iPS cell-derived erythropoietin-producing cells

Kenji Osafune
osafu@cira.kyoto-u.ac.jp
iPS Cell Research and Application (CiRA), Kyoto University

Summary Abstract

In this study, we identified one small molecule that increase the mRNA expression and protein secretion of erythropoietin (EPO) from human iPS cell-derived EPO-producing cells (hiPSC-EPO cells). This compound may contribute to the development of cell therapy and new therapeutic drugs for renal anemia.

Key Words：iPS cell, erythropoietin, EPO, small molecule, screening

Introduction

An increasing number of patients with end-stage renal failure (ESRF) start dialysis therapy, which cause medical and economical problems. Renal anemia in ESRF have been treated with recombinant human erythropoietin (rhEPO) agents. However, physiological control of renal anemia is still difficult. To overcome the problem, we previously developed the differentiation method for hiPSC-EPO cells and demonstrated that cell therapy using hiPSC-EPO cells ameliorates renal anemia in mice (Hitomi H. et al., 2017). In this study, we aimed to identify small molecules that facilitate the production of EPO from hiPSC-EPO cells towards the development of cell therapy and drug discovery against renal anemia.

Results

(1) Screening of chemical compounds that increase EPO secretion from hiPSC-EPO cells.

We had developed the directed differentiation method to induce hiPSCs into EPO-producing cells by modifying the previously reported hepatocyte differentiation protocols (Hitomi H. et al., 2017). In our differentiation method for EPO cells, hiPSCs were first induced to differentiate into definitive endoderm cells expressing SOX17 and HOXA2 by the combination treatment with activin A and a glycogen synthase kinase (GSK)3 inhibitor, CHIR99021, and then treated with dimethyl sulfoxide (DMSO) to generate AFP(+) hepatoblasts. We found that the hepatoblasts also expressed EPO and that the prolonged treatment with DMSO more efficiently generates hiPSC-EPO cells. We then set up the screening system for chemical compounds, in which AFP(+)EPO(+) hepatoblasts differentiated from an hiPSC line, 585A1, were split into 96-well plates and individual compounds were added to different wells. The effects of individual compounds were analyzed by enzyme-linked immunosorbent assay (ELISA) for EPO protein in the culture supernatants. By using the unbiased screening system for chemical compounds, we have identified one hit compound that increase the secretion of EPO protein from hiPSC-EPO cells.

(2) Evaluation of hit compound.

We next confirmed the reproducibility of effects of the hit compound in 24-well plate settings that increased the EPO mRNA expression and protein secretion from hiPSC-EPO cells and found that the hit compound increases the EPO mRNA expression and protein secretion in a concentration dependent manner. We also optimized the treatment protocol using the hit compound to maximize the EPO expression and secretion from hiPSC-EPO cells. The main regulators of EPO expression in our body are known to be hypoxia, hypoxia inducible factors (HIFs) and prolyl hydroxylase domain-containing protein (PHD). We thus examined whether the hit compound increases the secretion of EPO synergistically with hypoxia and confirmed that the compound additionally increases the EPO production from hiPSC-EPO cells under hypoxic conditions.

We had previously established the renal anemia mouse model induced by oral addition of adenine (Hitomi H. et al., 2017). We are currently examining the in vivo effects of the hit compound by intraperitoneally injecting the hit compound to the renal anemia mice.

(3) Elucidation of the mechanisms of action of hit compound.

We purchased several analogs of the hit compound and examined the effects of the analogs on the EPO expression and secretion from hiPSC-EPO cells. The results showed that the analogs also increased the EPO expression and secretion, which help providing the information of target molecules of the hit compound.

In an attempt to elucidate the mechanisms of action by which the hit compound increases the EPO production from hiPSC-EPO cells, we performed RNA sequencing analyses and compared the expression profiles between hiPSC-EPO cells treated with or without the hit compound. Consequently, we identified several molecules whose expression levels are upregulated by the hit compound. We are currently examining the knockdown experiments for the molecules by using siRNAs to see which molecules work downstream of the hit compound. Based on the data, we will eventually elucidate the mechanisms of action of the hit compound.

Discussion & Conclusion

Although the rhEPO agents have been successfully used to treat renal anemia in ESRF patients, the physiological control of renal anemia is still difficult and the cost of rhEPO therapy is becoming huge burden on health care system. In this study, we have identified one small molecule that facilitate the EPO expression and protein secretion from hiPSC-EPO cells. This small molecule may be used to develop new therapeutic drugs for renal anemia, which facilitate EPO secretion from EPO-producing cells in our body. From basic research aspects, our small molecule may elucidate the detailed mechanisms of EPO production or secretion from EPO-producing cells. It is well known that EPO production in our body is regulated by HIF-PHD axis. Future studies should elucidate the relationship between our small molecule and the axis.

References

Hitomi H, Kasahara T, Katagiri N, Hoshina A, Mae SI, Kotaka M, Toyohara T, Rahman A, Nakano D, Niwa A, Saito MK, Nakahata T, Nishiyama A, Osafune K. Human pluripotent stem cell-derived erythropoietin-producing cells ameliorate renal anemia in mice. Science Translational Medicine, 2017; 9(409). pii: eaaj2300.

一般の皆様へ

現在、慢性腎臓病の進行によって慢性腎不全となり透析療法を受けている多くの患者さんがいます。慢性腎不全の合併症として腎性貧血があり、遺伝子組換えヒトエリスロポエチン製剤投与による治療が行われておりますが、貧血の生理的なコントロールは依然として困難です。本研究において、我々はヒト iPS 細胞からエリスロポエチンを産生する細胞を作る方法を開発し、さらに本細胞からのエリスロポエチン分泌を促進する活性を有する化合物を発見しました。今後、本化合物を用いた腎性貧血に対する再生医療と新規治療薬の開発が期待されます。

Mechanism that controls the neuronal survival/ death in the developing brain

Kazunori Nakajima
kazunori@keio.jp
Department of Anatomy, Keio University School of Medicine

Summary Abstract

We found a unique pattern of neuronal cell death that occurs when cerebral hemispheres are cultured under a certain condition. The neuronal cell death progresses from the lateral cortex to the dorsomedial cortex in a very reproducible manner. Interestingly, we found that a very potent "cell survival factor" with a relatively small size is endogenously produced and secreted from the cerebral hemispheres and can completely prevent this neuronal cell death.
Key Words：neuronal cell death, cerebral cortex, cell survival factor

Introduction

We previously established a whole-mount culture system of mouse developing cerebral hemispheres. Using this system, we can cultivate the entire cerebral hemispheres for 1-2 days in vitro. Under a certain condition, however, we found that some developmental events were disturbed and massive neuronal cell death was induced in an interesting and unusual sequence. In this study, we have analyzed the detailed profile of this cell death.

Results

Cerebral hemispheres including cerebral cortex and ganglionic eminences were dissected out from embryonic day (E) 15.5 ICR mouse brain, and cultured individually in a glass culture tube attached to a rotation disk of the whole embryo culture system (Ikemoto Rika Kogyo, Tokyo, Japan) containing a 2 ml DMEM/F12 medium supplemented with N2 supplement (Invitrogen, Carlsbad, CA) and several other components. The rotation disk was maintained in a 37 ℃ incubator and rotated at 20 rpm. As a result, we found that culturing the brain in this condition resulted in bumpy brain surface in all the analyzed hemispheres. Immunohistochemical analyses showed ectopic invasion of cells into the marginal zone, retraction and disorganization of radial glial fibers, abnormal layer formation in the cortical plate, malalignment of Cajal-Retzius cells, and reduction of the MAP2 and Reelin immunoreactivity. Since the massive reduction of MAP2 and Reelin immunoreactivity and severe disruption of layer structures suggested cell death of cortical plate neurons and marginal zone cells, we then evaluated the cell viability using a membrane-impermeant chromatin dye Propidium Iodide (PI) as a fluorescent viability indicator: cells with intact membranes (live cells) would exclude PI; cells with damaged membranes (dead cells) would be stained with PI. After 2 days in the rotation culture (days *in vitro*, DIV), coronal slices of the cerebral hemispheres were prepared and stained with PI. As the result, we observed widespread and massive cell death in the cortical plate and marginal zone. Interestingly, there was a clear border between the PI-negative region and the PI-positive region. Furthermore, whole mount staining of the cerebral hemispheres using PI revealed that the PI-positive dead cells formed island-like clusters, separated by PI-negative linear zones that

appeared along the rostro-caudal axis with relatively constant intervals. These unique features of a cobblestone-like brain surface were observed in all the analyzed hemispheres. To determine when and where the cell death begins, the time course of the cell death was then examined. Each cerebral hemisphere was collected at 0.5, 1, or 2 DIV and their viability was analyzed using PI. At 1 DIV, PI-positive dead cells were observed only in the lateral region of the telencephalon, and by 2 DIV the PI-positive region extended to reach the dorsomedial region of the telencephalon, suggesting that the cell death progressed in a lateral-to-medial direction with a clear boundary between the dead region and the live (intact) region. Interestingly, this massive neuronal cell death was almost completely rescued when multiple cerebral hemispheres were co-cultured in a single culture tube. To examine whether there is a "secretory cell survival factor", we next put a single hemisphere into a dialysis membrane tube and cultured with several other hemispheres that were placed outside of the dialysis membrane. As the result, neuronal cell death in the hemisphere in the dialysis membrane tube was also clearly rescued, suggesting that this "cell survival factor" is indeed secreted from the cultured hemispheres. We have then repeated this coculture experiments using dialysis membranes that had various molecular weight cut-off. The results indicated that this endogenous "cell survival factor" is a relatively small molecule.

Discussion & Conclusion

In the whole-mount cerebral hemisphere cultures, we found a unique pattern of neuronal cell death that progresses from the lateral cortex to the dorsomedial cortex in a very reproducible manner. Interestingly, although almost all neurons died in the "dead" region, a "live (intact)" region exists next to the "dead" region and is clearly demarcated from the "dead" region. The border between the "dead" and "live" regions moves medially until almost the entire cortex became dead eventually.

The putative "cell survival factor" that is secreted from the cerebral hemispheres seems to have a very potent function to prevent this neuronal cell death that occurs in the whole-mount cerebral hemisphere cultures. The identification of this molecule would be important, especially because it is an endogenous and small size molecule with a very strong preventive effect on neuronal cell death.

一般の皆様へ

マウス胎生期の大脳半球をある条件下で培養すると、神経細胞死が外側から背内側に向かって進行し最終的に全体が死滅することを見出した。その際、死んだ領域とまだ生き残っている領域の境界は極めて明瞭であり、かつ細胞死が起こらない筋状の領域が前後方向にほぼ一定間隔で現れた。複数の脳を半透膜で包んで共培養する実験から、この神経細胞死を完全に防ぐことのできる強力かつ低分子量の内在性因子が脳から分泌されていることを発見した。この因子を今後の研究で同定できれば、発生期の脳に内在する低分子量の強力な神経細胞死抑制因子として、臨床応用も視野に入ると期待される。

Direct reprogramming into cardiac pacemaker cells for a novel regeneration therapy for arrhythmias

Shu Nakao
snakao@fc.ritsumei.ac.jp
Ritsumeikan University

Summary Abstract

Severely slow heart rate requires transplantation of a mechanical pacemaker, which has disadvantage in infection, mechanical failure, and medial economy. This proposal aims to develop an alternative heart rhythm therapy using reprogrammed cells by gene introduction of some molecules from somatic cells of the patients. In a whole genome expression analysis, the cardiac pacemaker tissue in arrhythmia model mice exhibited decreased expression of more than 4,000 genes by the modelling. In particular, 42 transcription factors were downregulated that suggests these factors are possibly important to maintain the expression of pacemaking ion channels. We are now working on in silico analysis to figure out what transcription factors really regulate heart rate through modification of ion channel functions. This work will provide insights into cardiac regenerative medicine.

Key Words：Cardiac pacemaker, cell reprogramming, transdifferentiation, arrhythmias

Introduction

Heart rate is decreased age-dependently, and severe bradycardia causes respiratory distress and syncope, which requires pacemaker implantation. Mechanical pacemaker is broadly available over the world, however, there are a risk of infection and mechanical failure in those millions of patients and an impact on medical economy, so that an alternative therapy has been sought.

Results

1. Transcriptomic analysis of the pacemaker tissue in arrhythmia model mice

We first established a mouse model of pacemaker dysfunction characterized by slow heart rate. The model was induced by swim training which designated twice 60 min sessions/day, 6 days/week for 4 weeks (Fig. 1). We next collected the sinoatrial node region (the primary pacemaking site in the heart) and the neighbouring right atrial wall tissue for the transcriptomic analysis using a next generation sequencing, which can measure the expression level of 41,195 genes. 19,679 genes were expressed in the sinoatrial node of sedentary mice. There were 655 genes upregulated (> 2-fold) and 4,306 genes downregulated (< 1/2) by exercise(Fig. 2). We particularly focused on the result of transcription factors as candidates of the reprogramming factor, and found 42 transcription factor genes downregulated.

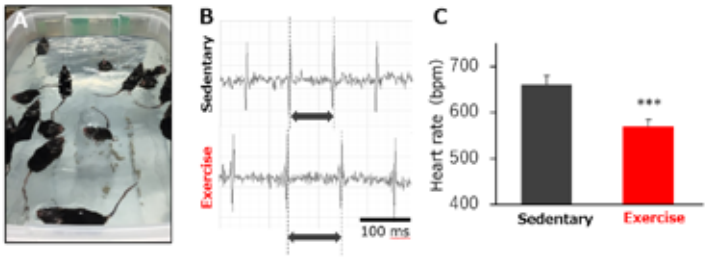

Fig 1. Exercise-induced bradycardia in mice. Mice in swim exercise (A) and slowed heart rate by training (B and C).

2. In silico analysis of binding motif of the transcription factors to pacemaking molecules.

As these 42 transcription factors could be involved in the regulation of transcription and/or functions in cardiac ion channels, we have been working on the bioinformatics analysis to figure out theoretical binding sites of the transcription factors in the genomic region of ion channels such as HCN pacemaker channels and voltage-gated Ca^{2+} channels.

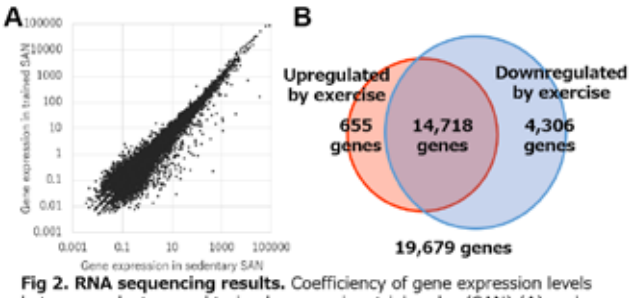

Fig 2. RNA sequencing results. Coefficiency of gene expression levels between sedentary and trained mouse sinoatrial nodes (SAN) (A) and a number of genes changed by exercise (B).

Further analyses including luciferase reporter assay in vitro and reprogramming experiments using viral vectors encoding those transcription factors will be performed.

3. Built a platform for reprogramming somatic cells into pacemaker-like cells

Direct reprogramming of somatic cells to cardiomyocytes was first reported by Ieda et al. in 2010. They introduced Gata4, Mef2c, and Tbx5 (GMT), known as the master regulator genes of cardiac development, into fibroblasts to convert to cardiomyocyte-like cells. As for development of the cardiac conduction system, there are several key transcription factors as seen in cardiac development. So far, we have tried to induce pacemaker-like cells using transduction of these transcription factors in combination with GMT. Fig. 3 shows the result that little changes of the expression level of pacemaker channel HCN4 were observed in contrast to upregulation of a cardiac marker gene cardiac α-actin. This tells us the necessity to further find novel transcription factors to produce pacemaker-like cells.

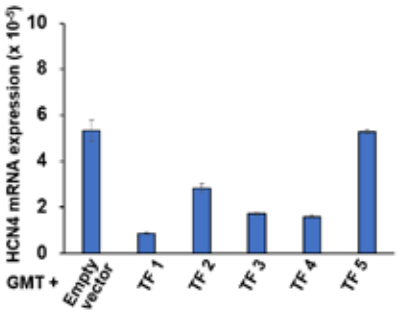

Fig 3. Expression levels of a dominant pacemaker ion channel HCN4 in cells introduced with known cardiac reprogramming factors "GMT" and a transcription factor (TF1-5) for cardiac conduction system development.

Discussion & Conclusion

RNA sequencing of the whole genome from the sinoatrial node region in sedentary and trained mice revealed that transcription factors downregulated by swim exercise would be candidates of the reprogramming factor for production of pacemaker cells. We are now working on identification of the reprogramming factors with an *in silico* approach. To pursue this project, other mouse models of pacemaker dysfunction such as heart failure models may be required to find common transcription factors changed by pathology. Similar to GMT, typical transcription factors for development of the cardiac conduction system may also be important for cell reprogramming into pacemaker cells, so we are seeking novel molecules regulating pacemaker development. Induced pacemaker cells developed from this project have potential to restore the heart rate as a regenerative therapy. This study will also gain understanding of the bradycardia pathophysiology and sinoatrial node development.

References

D'Souza A et al. Circ Res 2017;121:1058-1068
Ieda M et al. Cell 2010;142:375-386
Wiese C et al. Circ Res 2009;104:308-397

一般の皆様へ

加齢に伴う心拍数の低下（徐脈）は、ときに息切れや動悸、失神を生じるほどに進行し、その主な治療法である機械式ペースメーカーの移植には、感染、故障、高額などの問題が残されている。本研究では、徐脈性不整脈に対する新たな再生医療の開発を展望として、心臓ペースメーカー細胞を体細胞から作り出す方法の確立を目的とする。この方法は、iPS 細胞などの未分化細胞へ脱分化させる過程をスキップできることから、時間と費用を大きく節約できる特長がある。また、ペースメーカー細胞の性質を獲得させるための因子を特定するための手掛かりとして、病気モデルや胎児期の心臓形成に着目し、データの集積・解析を進めている。

Structure determination of formosalide A by the combined technology of the NMR calculation and total synthesis

Daisuke Urabe
urabe@pu-toyama.ac.jp
Department of Biotechnology, Faculty of Engineering, Toyama Prefectural University

Summary Abstract

We have applied computational techniques to predict the structure of a bioactive polyketide, formosalide A. An exhaustive conformational search was performed using molecular mechanics, semi-empirical MO, and DFT methods on model compounds of formosalide A. NMR chemical shifts of the model compounds were simulated to predict the gross structure of formosalide A. Synthetic approaches to the C9-C18 fragment and the C19-C30 side chain have also been established toward a complete structure determination of formosalide A.

Key Words：Natural products, structure determination, NMR calculation, total syntheiss

Introduction

Marine dinoflagellates are a rich source of bioactive secondary metabolites. Formosalide A is a cytotoxic macrolide, which was isolated from the cultured dinoflagellate Prorocentrum sp. by Lu and coworkers.[1)] The unique structural features including tetrahydrofuran and pyrane moieties embedded in a 17-membered ring and the C19-C30 tetraene side chain were elucidated by extensive NMR studies, while the stereochemical relationship among the *anti*-C2,C5, *syn*-C16,C18 and C8-C12 pyrane residue remained to be determined. In this study, we aimed at a complete determination of the structure of formosalide A by using both computational and experimental approaches.

Results

Since formosalide A has 3 structural motifs whose stereochemical relationships are unknown, we must consider the possibility of 4 isomers for determination of the gross structure of formosalide A. Thus, we planned to predict the structure by NMR calculations before starting the total synthesis. To simplify the calculations, 4 isomeric model compounds lacking the C19-C30 acyclic side chain were designed. The procedure for calculating the NMR chemical shifts of an isomer was as follows. The geometry of the model compound was optimized by molecular mechanics (MMFF/MCMM), semi-empirical MO (PM6) and DFT (pcm/M062X/6-31g(d)) methods, giving a number of conformers within 2.0 kcal/mol from the minimum energy conformer. Clustering of conformers with RMSDs of 0.1 Å removed similar geometries from the library and then the selected conformers were subjected to a DFT-based NMR calculation (pcm/mPW1PW91/6-31+g(d,p)). The calculated NMR chemical shifts were Boltzmann-weighted to afford the simulated NMR chemical shifts for the model compound. This computational procedure was applied to the other 3 isomers. DP4+ comparison of the simulated NMR chemical

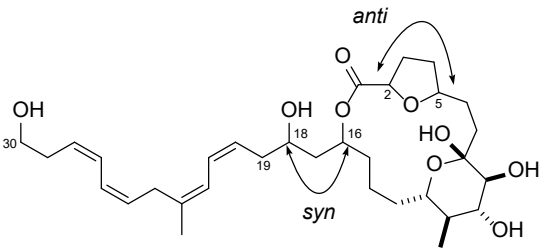

formosalide A

shifts for the 4 model compounds with the experimental NMR spectrum of formosalide A successfully predicted the stereochemical relationship for the 3 structural motifs to determine the true structure of formosalide A with 100% probability.[2)] The results of the NMR calculations prompted us to embark on the total synthesis of the predicted structure of formosalide A. A series of catalyst-controlled asymmetric syntheses enabled us to prepare the C9-C18 fragment in enantiopure form. Furthermore, an efficient approach to the C19-C30 acyclic side chain featuring SN2 displacement and partial reduction of multiple alkynes to Z-alkenes was established.

Discussion & Conclusion

A challenge in the present study was how to simulate NMR chemical shifts for a conformationally flexible natural product. Formosalide A possesses a 17-membered ring and a C19-C30 tetraene side chain, which generate a number of conformational isomers, and thereby complicate the NMR calculation. We used a sequential approach to select the important conformers for the NMR calculations. Specifically, MMFF was first used to perform an exhaustive conformational search, followed by optimization with semi-empirical and DFT methods. Subsequent clustering of the optimized geometries allowed us to generate the important conformers with reasonable computational costs. Consequently, we succeeded in predicting the gross structure of formosalide A. We expect that the stereoselective total synthesis of the predicted structure of formosalide A will complete the structure determination.

References

1) Grimblat, N.; Zanardi, M. M.; Sarotti, A. M. J. Org. Chem. **2015**, 80, 12526.
2) Lu, C.-K.; Chen, Y.-M.; Wang, S.-H.; Wu, Y.-Y.; Cheng, Y.-M. T*etrahedron Lett.* **2009**, *50*, 1825.

一般の皆様へ

天然には、抗がん活性や抗菌活性など創薬において魅力的な生物活性を有する有機化合物が数多く存在します。一方で、天然から得られる量が限られている希少天然物の基礎研究は進展していません。本研究では、渦鞭毛藻から単離された希少天然物ホルモサリドAの初期段階の基礎研究として、その構造決定に取り組みました。現在までに、コンピューターを使ったホルモサリドAの構造推定に成功し、有機合成による推定構造の確認に着手しています。近い将来ホルモサリドAの構造が決定できると考えています。

Development of apoptosis induction method with spatiotemporal control using microRNAs.

Kazunori Watanabe
k_watanabe@okayama-u.ac.jp
Okayama University

Summary Abstract

The methods of cell functions regulated by light have been developed. Previously, we developed photo-dependent RNA delivery method called PCDR [1, 2]. In addition, we identified a novel pre-miR-XX inducing apoptosis. In this study, we attempted to develop a spatiotemporally controllable apoptosis-inducing method using pre-miR-XX and PCDR.

As a result, we have demonstrated the efficient and selective induction of apoptosis by the combination of pre-miR-XX-U1A and PCDR.

Key Words：photo-regulation, apoptosis, miRNA

Introduction

The methods of cell functions regulated by light have been developed. For instance, photo dynamic therapy using photosensitizer can induce photo-dependently apoptosis.

It is reported that microRNAs (miRNAs) regulate apoptosis. We identified a novel pre-miR-XX inducing apoptosis (prepared paper). In addition, we developed photo-dependent RNA delivery method called PCDR [1, 2]. In this study, we attempted to develop a spatiotemporally controllable apoptosis-inducing method using pre-miR-XX and PCDR.

Results

Apoptosis-inducing method using miR-XX and PCDR has one problem. The RNA carrier used in PCDR recognizes RNA having hairpin structure which contains specific sequence. Pre-miRNA has hairpin structure. Therefore, pre-miRNA-U1A which was replaced with specific sequence recognized by the RNA carrier was prepared. In this study, pre-miR-XX-U1A identified as a novel apoptosis-inducing miRNA was prepared. In addition, pre-miR-16-U1A and pre-miR-218-U1A which induce apoptosis were also prepared. We attempted to induce apoptosis by the combination of pre-miR-XX and PCDR. As a result, all pre-miRNA-U1A could induce apoptosis, especially apoptosis induction efficiency by pre-miR-XX was highest. In addition, PCDR could induce apoptosis more efficiently than lipofection method.

We attempted to control region specific apoptosis induction by the combination of pre-miR-XX-U1A and PCDR. Pre-miR-XX-U1A entered into the cells only within the photo-irradiated area, and then apoptosis was induced only within the irradiated area (Fig 1, lower panel).

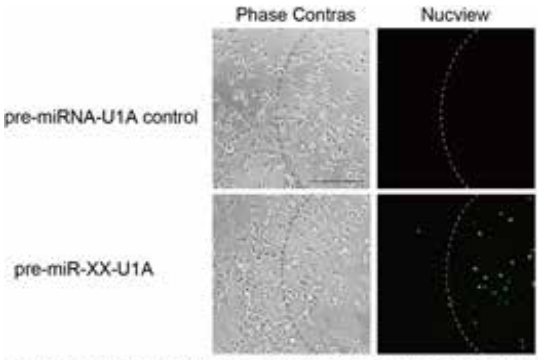

Fig 1 Region specific apoptosis induction. Cells at the right region of the dotted line were photo-irradiated. Apoptosis was detected by using NucView.

In contrast, while pre-miRNA-U1A control, which is non-targeting, entered into the cells only within the photo-irradiated area, apoptosis was not induced (Fig 1, upper panel). These results indicate that apoptosis can be spatially controlled by the combination of pre-miR-XX-U1A and PCDR.

PCDR can transiently deliver RNA into the cells [3]. Therefore, the cells delivered miR-XX-U1A by PCDR might be induced apoptosis faster than the cells delivered by lipofection method. We validated this hypothesis. As a result, the cells delivered miR-XX-U1A by PCDR were induced apoptosis faster than the cells delivered by lipofection method.

Discussion & Conclusion

In conclusion, we have demonstrated the efficient and selective induction of apoptosis by the combination of pre-miR-XX-U1A and PCDR. PCDR is not observed cytotoxicity [1, 2]. Therefore, this method using pre-miR-XX-U1A and PCDR has the potential to develop as a treatment with lower side effect than photo dynamic therapy.

Target mRNAs of pre-miR-XX has not been clarified. Thus, to understand the apoptosis induction mechanism by pre-miR-XX, further studies will be necessary.

References

(1) T. Endoh, M. Sisido and T. Ohtsuki, “Cellular siRNA delivery mediated by a cell-permeant RNA-binding protein and photoinduced RNA interference” ***Bioconjug. Chem.*** 19, 1017-1024, (2008).
(2) Y. Matsushita-Ishiodori, M. Morinaga, K. Watanabe and T. Ohtsuki, “Near-infrared light-directed RNAi using a photosensitive carrier molecule” ***Bioconjug. Chem.*** 24, 1669-1673, (2013).
(3) K. Shiraga, T.H. Soe, S. Matsumoto, K. Watanabe and T. Ohtsuki, “Red and near-infrared light-directed cytosolic delivery of two different RNAs using photosensitive RNA carriers” ***Bioconjug. Chem.*** 29, 3174-3179, (2018)

一般の皆様へ

国内外の研究者により光による細胞機能制御法が開発されている。本研究では、申請者らが同定したアポトーシスを誘導するマイクロ RNA である pre-miR-XX と、光依存的に RNA を細胞内に輸送できる PCDR 法を組み合わせることで、アポトーシスを時空間的に制御することを目的とした。

その結果、PCDR 法で pre-miR-XX を細胞内で導入することで、アポトーシスを高効率に誘導できるだけでなく、アポトーシスを時空間的に制御できることも明らかになった。本手法は副作用の小さいがん治療法として発展していく可能性を秘めている。

Study on the enantioselective total synthesis of dragmacidin E: a natural product with high potential for medicinal chemistry researches

Tetsuhiro Nemoto
tnemoto@faculty.chiba-u.jp
Graduate School of Pharmaceutical Sciences, Chiba University

Summary Abstract

Synthetic studies of dragmacidin E have been performed. A strategy for constructing the core structure of this natural product was developed. In addition, a novel synthetic method for the 3,4-fused tricyclic indoles and benzofurans was developed based on a radical cascade cyclization strategy.
Key Words：dragmacidin E, total synthesis, heterocycles, catalysis

Introduction

Dragmacidin E was isolated from an Australian marine sponge by Capon et al. in 1998. The structure features a 7-membered ring-fused tricyclic indole skeleton functionalized with an indolyl pyrazinone motif and two contiguous stereocenters. Because of its unique structure, dragmacidin E is an attractive target for synthetic organic and medicinal chemists. It is noteworthy that this natural product exhibits serine-threonine phosphatase inhibitory activity. Dragmacidin E cannot be efficiently obtained from natural sources (0.01% yield from the natural source), however, hampering detailed investigation into its biological activities. This background led us to initiate synthetic studies of this natural product.

Results

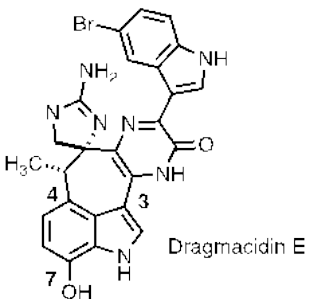

Dragmacidin E

We already reported a synthetic study of dragmacidin E, which provided an access to the core skeleton of this natural product (ref 1). To extend the present method to the total synthesis, we examined the key reaction for constructing the 3,4-fused tricyclic indole skeleton using a densely functionalized substrate. The requisite tetra-substituted aromatic ring substrate was prepared using a regioselective nitration reaction. After condensation of the corresponding aldehyde with dimethyl malonate, a methyl group was introduced by Cu-mediated conjugate addition. Coupling with an allenyl tosylate with the malonate derivative provided a substrate for the Pd-catalyzed cascade cyclization. The key reaction was performed using 10 mol % of Pd catalyst and 24 mol % of phosphine ligand and the corresponding tricyclic product was obtained in 70% yield, revealing that the present Pd catalysis could be applied to the synthesis of a suitably functionalized synthetic intermediate.

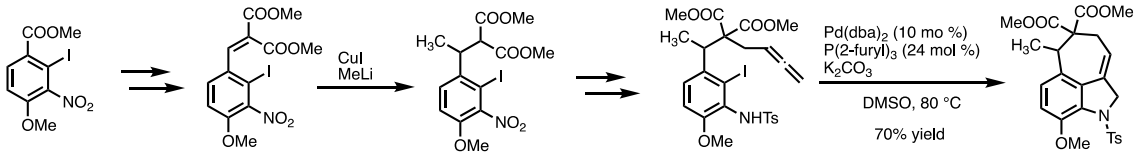

We next examined the construction of the contiguous stereocenters in an asymmetric fashion. Asymmetric hydrogenation of tri- and tetra-substituted olefin substrates was first investigated. However, high asymmetric induction could not be accomplished when substrates with a tetra-substituted aromatic ring were utilized. In addition, we examined catalytic asymmetric allenylation of benzophenone imine type prochiral nucleophiles to construct the tetra-substituted carbon center using chiral phase transfer catalysis. Products with high enantiomeric excess were not obtained as well. To overcome the current situation, biocatalytic processes will be examined as a collaborative study with Prof. Harald Gröger in Bielefeld University in Germany. We have already started discussions for this project and the reactions in the below scheme are under investigation.

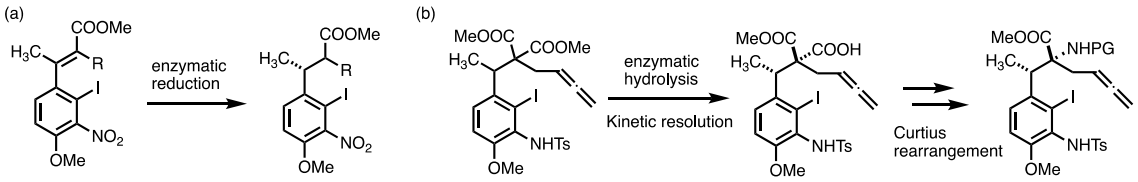

In addition to the synthetic method based on transition metal catalysis, we tried to develop an alternative synthetic method for 3,4-fused tricyclic indoles and related benzofuran derivatives using a radical cascade cyclization strategy. As shown in the scheme below, when O-allyl iodophenol type substrates were heated in toluene in the presence of HSnBu3 (hydride source) and AIBN (radical initiator), the radical cascade cyclization proceeded smoothly to give the corresponding tricyclic product in excellent yield. Acid-promoted isomerization proceeded well to give benzofuran type compound. This method was also applicable to the synthesis of 3,4-fused tricyclic indoles by using N-allyl iodoanilines as substrates. These results will be reported in due course (ref 2).

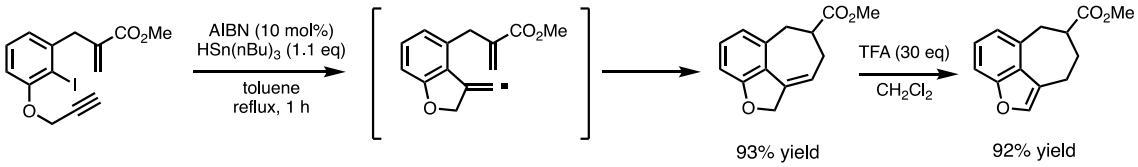

In addition to the experimental works, we wrote a review article on the synthesis of 3,4-fused tricyclic indoles (ref 3).

Discussion & Conclusion

Pd-catalyzed cascade cyclization developed by our group could be applied to the synthesis of suitably functionalized tricyclic ring system of dragmacidin E. We thus concentrated on the construction of contiguous stereocenters on the seven-membered ring. Initial trials using chemo-catalytic asymmetric reactions were not successful. Therefore, enzymatic enantioselective processes are currently investigated. A collaborator: Prof. Harald Gröger possesses a series of enzymes libraries for this purpose. Enzyme screening for a couple of candidate transformations will be examined. A radical cascade cyclization for synthesizing 3,4-fused tricyclic indoles and related benzofuran derivatives was also developed.

References

1) Synthetic Study of Dragamcidin E: Construction of the Core Structure Using Pd-Catalyzed Cascade Cyclization and Rh-Catalyzed Aminoacetoxylation
Naoya Inoue, Shun-ichi Nakano, Shingo Harada, Yasumasa Hamada, Tetsuhiro Nemoto
J. Org. Chem. **2017**, 82, 2787–2793.

2) Radical Cascade Cyclization for Synthesizing 3,4-Fused Tricyclic Benzofuran Derivatives
Masaya Nakajima, Yusuke Kondo, Shun-ichi Nakano, Yusuke Adachi, Robert Franzén, Tetsuhiro Nemoto
Manuscript in preparation.

3) Synthetic Methods for 3,4-Fused Tricyclic Indoles via Indole Ring Formation
Tetsuhiro Nemoto, Shingo Harada, and Masaya Nakajima
Asian J. Org. Chem. **2018**, 7, 1730–1742.

一般の皆様へ

ドラグマシジン E は、生体内で重要な役割を果たすセリン - スレオニンホスファターゼの阻害作用を示す化合物として知られているが、天然から得られる量はごく微量であり、詳細な研究には合成化学的な供給法の開発が不可欠となっている。私たちは、本天然有機化合物の合成法を開発し、医薬品開発への可能性を調査するために研究を進めている。これまでに、本化合物の主要骨格の構築法は開発したものの、鏡像異性体の作りわけに関しては一層の検討を要する。標的分子骨格の新規合成法開発を含めた、網羅的な研究を進めることで、本天然有機化合物の供給法を今後開発していきたい。

Understanding the neural mechanism underlying flexible decision making by the combination of neurophysiology and deep neural networks

Hironori Kumano
hkumano@yamanashi.ac.jp
University of Yamanashi

Summary Abstract

Flexible behavior based on multiple rules is a hallmark of human cognition. To understand the role of the prefrontal cortex in flexible task switching, we recorded electrocorticogram signals in wide areas of the prefrontal cortex while a monkey performed task switching. Representation of task rules was first observed in the orbitofrontal cortex. We suggest that rule signal is first encoded in the orbitofrontal cortex and propagates in wide areas of the prefrontal cortex.
Key Words：Macaque monkey, Electrocorticogram

Introduction

Switching behavior based on multiple rules is a fundamental ability of flexible behavior. We have previously shown that neurons in the lateral intraparietal area (LIP) integrate relevant information preferentially depending on rule (Kumano et al., 2016). We hypothesized that the prefrontal cortex (PFC) control the speed of integration depending on task rule. In this study, We examined neural activity of a wide range of PFC by recording electrocorticogram (ECoG) signals while a monkey performed the reaction time task switching.

Results

A Japanese macaque (*Macaque fuscata*) was trained to switch between discriminating motion direction and stereoscopic depth of a random-dot stimulus. In each trial, the color of the fixation point (FP) indicated which discrimination task the monkey had to perform. In the direction discrimination task, the monkey was required to saccade to the lower target when the dots moved down and to the upper target when the dots moved up. In the depth discrimination task, the monkey was required to saccade to the lower target when the dots were nearer than the plane of fixation and to the upper target when the dots were farther. The two tasks were randomly interleaved from trial to trial so that the monkey was unable to predict the task rule of the upcoming trial. The monkey was allowed to make a saccade as soon as a decision was made. Difficulty of the tasks was varied by changing the percentage of coherently moving and binocularly correlated dots in the random-dot stimulus.

We first customized ECoG electrodes that can cover all surfaces of the prefrontal cortex including the lateral PFC (64 channels), the medial PFC (32 channels), and the orbitofrontal cortex (OFC; 32 channels). After implanting these electrodes using aseptic procedures, we recorded ECoG signals while the monkey performed the reaction time task switching.

We analyzed how well the monkey switched between the two tasks by calculating the switch ratio (SR, Sasaki and Uka, 2009). If the monkey switched between the two tasks perfectly, then the SR

would be 1, whereas if the monkey was ignoring the task cue and solving the task the same way on each trial, then the SR would be 0. The mean SR for the direction discrimination task was 0.85 and the mean SR for the depth discrimination task was 0.91 (n = 53 sessions). The SRs were in agreement with our previous studies (Sasaki and Uka, 2009; Kumano et al., 2016) and indicated that the monkey switched successfully between the two tasks, although not perfectly.

During the task, visual response and saccade related response were observed in various areas within the PFC. We explored whether neural activity in the PFC represented task-related signals using a decoding-based approach. We examined whether task rule can be decoded from the event related potentials (ERPs). In our task switching paradigm, the color of the FP indicates which task the monkey should perform. We thus used a linear Support-Vector-Machine (SVM) to decode task rule by classifying the ERP in a 20-ms window that slid every 10ms from 100 ms before FP onset to 400 ms after FP onset. We found that ERP in all areas of the PFC encoded the task rule (significantly above the pre-FP period). Peak classification accuracy was observed as early as 80 ms after the FP onset in the OFC. Medial PFC exhibited peak accuracy at around 100 ms after the FP onset. The peak accuracy in the lateral PFC was delayed compared to other areas and was observed at 200 - 300 ms after the FP onset.

Discussion & Conclusion

The results suggest that information about task rules is first represented within the OFC and propagates in wide areas of the PFC. Statistical analysis of neural signals such as Granger Causality analysis and coherence measurement between electrode channels would be needed to test this hypothesis. Examining whether the manipulation of rule-selective activity in the PFC alter the decision related activity in area LIP is essential for understanding the role of the PFC in flexible decision making.

Neural activity in the PFC, including ECoG signals examined in this study, is known to have complex and diverse response properties. Trained neural network models may provide insights into complex neural representations in the PFC.

References

Kumano H, Suda Y, Uka T. Context-dependent accumulation of sensory evidence in the parietal cortex underlies flexible task switching. J Neurosci 36, 12192-12202, 2016.

Sasaki R, Uka T. Dynamic readout of behaviorally relevant signals from area MT during task switching. Neuron 62, 147-157, 2009.

一般の皆様へ

ヒトは環境に応じて柔軟に判断を切り替え、そのときの環境に応じた行動をとることができる。これまでに我々は、判断を切り替える際には、判断をくだすのに必要な情報を収集する過程が環境に応じて異なることを見出した。本研究では、前頭前野がどのようにダイナミックに情報収集過程を制御しているかを理解するために、前頭前野の広い範囲から皮質脳波を計測した。その結果、環境に関する情報は眼窩前頭皮質で最初に現れ、前頭前野の広い領域に伝播する可能性が示唆された。今後は、前頭前野に存在する環境情報がどのように判断をつかさどる神経回路に作用し柔軟な行動が可能になるのかを、神経生理学的手法と深層学習を併用して明らかにしたい。

Drug development of DYRK1A inhibitors: targeting excess phosphorylation in Alzheimer's disease

Masashi Asai
euterpeoleracea@rs.tus.ac.jp
Tokyo University of Science

Summary Abstract

Alzheimer's disease (AD) is the most common cause of dementia in elderly people. Currently, there is no disease-modifying drug for AD. Dual-specificity tyrosine-phosphorylation-regulated kinase 1A (DYRK1A), encoded in chromosome 21 Down syndrome critical region, is involved in the progression of AD through the phosphorylation of AD-related molecules. Therefore, DYRK1A inhibitors would be a potent anti-AD drug. Indeed, harmine and epigallocatechin gallate, natural products, led to upregulated the activity of neprilysin, the dominant amyloid-β peptide (Aβ)-degrading enzyme in the brain.

Key Words：Alzheimer's disease, Down syndrome, Chromosome 21, DYRK1A, Neprilysin

Introduction

Alzheimer's disease (AD) is the most common cause of dementia in elderly people [1]. Despite the increasing prevalence of AD, no effective therapeutic agent is available [2]. Dual-specificity tyrosine-phosphorylation-regulated kinase 1A (DYRK1A) is a member of the protein kinase family that plays a role in several signaling pathways for developmental processes and cell homeostasis in physiological and pathological conditions [3-5]. It has been reported that DYRK1A phosphorylated tau and APP, leading to development of AD pathology. Since DYRK1A is an excellent target to effectively treat AD, we focused the relationship between DYRK1A and amyloid-β peptide (Aβ), and tried to develop its inhibitors.

Results

First, to determine whether the expression of genes located on chromosome 21 is increased in two cell lines of fibroblasts form DS patients (DS fibroblasts), we performed quantitative real-time PCR analysis. The mRNA levels of APP and DYRK1A were significantly higher in the DS fibroblasts than in fibroblasts from healthy controls (control fibroblasts) (Fig. 1A). Also, the protein level of DYRK1A was significantly elevated in the DS fibroblasts, compared with the control fibroblasts (Fig. 1B).

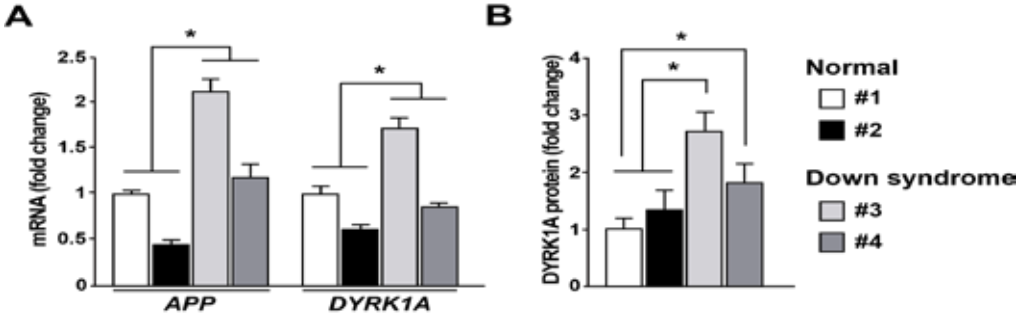

Fig. 1. Expression levels of APP and DYRK1A in fibroblasts from healthy controls and people with DS.

Aβ is currently the primary therapeutic target in attempts to arrest AD. In the brain, secreted Aβ is rapidly degraded by neprilysin (NEP), the dominant Aβ-degrading enzyme in the brain [6]. Although DYRK1A promotes to produce Aβ through phosphorylation of APP by DYRK1A [7], it is unclear the effect of DYRK1A on the Aβ-degrading system, especially NEP.

Next, we analyzed the protein level and activity of NEP in cell lysates of control and DS fibroblasts using the quantitative western blot method and an indirect coupled enzyme assay, respectively. The protein levels of NEP were remarkably decreased in the DS fibroblasts, compared with the control fibroblasts (data not shown). The peptidase activity of NEP in DS fibroblasts is significantly lower than that in control fibroblasts (Fig. 2).

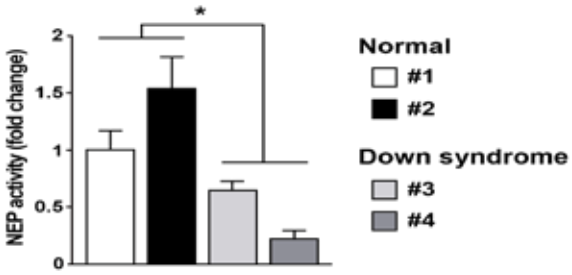

Fig. 2. NEP activity in fibroblasts from healthy controls and people with DS.

Then, to rescue NEP activity, we treated the two DS fibroblast cell lines from different DS patients with a DYRK1A inhibitor, harmine, to inhibit the catalytic activity of DYRK1A (Fig. 3). The pharmacological inhibition of DYRK1A at a concentration of at least 5 μM enhanced NEP activity by 1.5–2.0-fold in both DS fibroblasts. It has been reported that harmine is capable of inhibiting recombinant monoamine oxidase A (MAO A) and DYRK1B, a DYRK1A homologue [8]. In a test-tube, the IC50 values for MAO A and DYRK1B are 2 nM and 166 nM, respectively, whereas for DYRK1A it is 33 nM. To exclude the involvement of these molecules in the modulation of NEP activity, we evaluated the knockdown effects of DYRK1A in the two DS fibroblast lines using a specific siRNA (data not shown). We confirmed using western blot analysis that DYRK1A expression in the DS fibroblasts was suppressed by the knockdown. The knockdown of DYRK1A significantly increased NEP activity and protein amount by 1.5–2.0-fold in both DS fibroblasts. The level of increase was almost the same as that observed by the harmine treatment, of which the effective dosage was much higher than the IC_{50} value for DYRK1A in the test-tube.

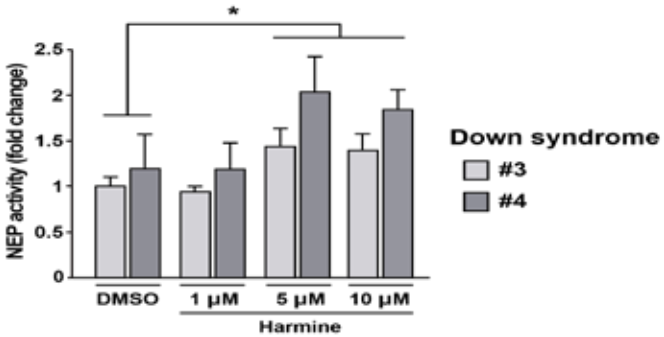

Fig. 3. Rescue of NEP activity by a DYRK1A inhibitor in fibroblasts from people with DS.

Moreover, to determine the phosphorylation sites of NEP by DYRK1A, we performed an in vitro kinase assay with recombinant DYRK1A and synthetic NEP intracellular domain peptide as a substrate. The phosphorylations by recombinant DYRK1A were detected by dot blot analysis using specific anti-phosphorylated

NEP antibodies. As a result of this kinase assay, DYRK1A is capable of catalyzing the phosphorylation of NEP at Thr11, Thr15, and Thr25 in a direct way.

Epigallocatechin gallate (EGCG), a key member of the family of catechins originating from tea, has many biological activities beneficial for human health, including anti-cancer, anti-diabetes, anti-infectious, and neuroprotective effects [9,10]. It has been reported that EGCG had an inhibitory effect on DYRK1A [11]. Finally, our in vitro kinase assay was performed to determine whether EGCG can inhibit the phosphorylation of NEP by DYRK1A in a similar way. EGCG inhibited the phosphorylation of NEP at Thr25 by DYRK1A (data not shown). Interestingly, NEP activity in neuronal cultured cells treated with EGCG was significantly increased, compared with the cells treated with vehicle (data not shown).

Discussion & Conclusion

DYRK1A phosphorylates APP as well as tau, leading to an increase in Aβ levels. Taken together with our results, DYRK1A appears to have multiple sites of action and to exacerbate AD pathology at multiple stages of the disease development. Thus, DYRK1A may act as a triple modulator, affecting both production and degradation of Aβ, and tau phosphorylation. Inhibition of DYRK1A may be a promising target for the development of drugs against AD and DS.

Nevertheless, in vivo studies using mouse model treated with a DYRK1A inhibitor [12,13] and clinical trials for administration of EGCG [12,14] have been successful. Because of increased expression of DYRK1A in the brains of not only people with DS but also AD patients [15] and induction of DYRK1A expression by Aβ [15], drugs targeting DYRK1A could address the cause of exacerbation of AD with few adverse effects. Although further studies are required, future research should be devoted to the development of DYRK1A inhibitors for the treatment of AD.

References

[1] Alzheimer's Association. 2017 Alzheimer's disease facts and figures. Alzheimers Dement. 2017; 13: 325–373.

[2] Agatonovic-Kustrin S, Kettle C, Morton DW. A molecular approach in drug development for Alzheimer's disease. *Biomed Pharmacother* 2018; 106: 553–565.

[3] Aranda S, Laguna A, de la Luna S. DYRK family of protein kinases: evolutionary relationships, biochemical properties, and functional roles. *FASEB J* 2011; 25: 449–462.

[4] Tejedor FJ, Hämmerle B. MNB/DYRK1A as a multiple regulator of neuronal development. *FEBS J* 2011; 278: 223–235.

[5] Wegiel J, Gong CX, Hwang YW. The role of DYRK1A in neurodegenerative diseases. *FEBS J* 2011; 278: 236–245.

[6] Nalivaeva NN, Turner AJ. Targeting amyloid clearance in Alzheimer's disease as a therapeutic strategy. *Br J Pharmacol* in press.

[7] Ryoo SR, Cho HJ, Lee HW, Jeong HK, Radnaabazar C, Kim YS, Kim MJ, Son MY, Seo H, Chung SH, Song WJ. Dual-specificity tyrosine(Y)-phosphorylation regulated kinase 1A-mediated phosphorylation of amyloid precursor protein: evidence for a functional link between Down syndrome and Alzheimer's disease. *J Neurochem* 2008; 104: 1333–1344.

[8] Brierley DI, Davidson C. Developments in harmine pharmacology--implications for ayahuasca use and drug-dependence treatment. Prog Neuropsychopharmacol *Biol Psychiatry* 2012; 39: 263–272.

[9] Mandel SA, Amit T, Weinreb O, Reznichenko L, Youdim MB. Simultaneous manipulation of multiple brain targets by green tea catechins: a potential neuroprotective strategy for Alzheimer and Parkinson diseases. *CNS Neurosci Ther* 2008; 14: 352–365.

[10] Pae M, Wu D. Immunomodulating effects of epigallocatechin-3-gallate from green tea: mechanisms and applications. *Food Funct* 2013; 4: 1287–1303.

[11] Bain J, McLauchlan H, Elliott M, Cohen P. The specificities of protein kinase inhibitors: an update. *Biochem J* 2003; 371: 199–204.

[12] De la Torre R, De Sola S, Pons M, Duchon A, de Lagran MM, Farré M, Fitó M, Benejam B, Langohr K, Rodriguez J, Pujadas M, Bizot JC, Cuenca A, Janel N, Catuara S, Covas MI, Blehaut H, Herault Y, Delabar JM, Dierssen M. Epigallocatechin-3-gallate, a DYRK1A inhibitor, rescues cognitive deficits in Down syndrome mouse models and in humans. *Mol Nutr Food Res* 2014; 58: 278–288.

[13] Neumann F, Gourdain S, Albac C, Dekker AD, Bui LC, Dairou J, Schmitz-Afonso I, Hue N, Rodrigues-Lima F, Delabar JM, Potier MC, Le Caër JP, Touboul D, Delatour B, Cariou K, Dodd RH. DYRK1A inhibition and cognitive rescue in a Down syndrome mouse model are induced by new fluoro-DANDY derivatives. *Sci Rep* 2018; 8: 2859.

[14] de la Torre R, de Sola S, Hernandez G, Farré M, Pujol J, Rodriguez J, Espadaler JM, Langohr K, Cuenca-Royo A, Principe A, Xicota L, Janel N, Catuara-Solarz S, Sanchez-Benavides G, Bléhaut H, Dueñas-Espín I, Del Hoyo L, Benejam B, Blanco-Hinojo L, Videla S, Fitó M, Delabar JM, Dierssen M; TESDAD study group. Safety and efficacy of cognitive training plus epigallocatechin-3-gallate in young adults with Down's syndrome (TESDAD): a double-blind, randomised, placebo-controlled, phase 2 trial. *Lancet Neurol* 2016; 15: 801–810.

[15] Kimura R, Kamino K, Yamamoto M, Nuripa A, Kida T, Kazui H, Hashimoto R, Tanaka T, Kudo T, Yamagata H, Tabara Y, Miki T, Akatsu H, Kosaka K, Funakoshi E, Nishitomi K, Sakaguchi G, Kato A, Hattori H, Uema T, Takeda M. The *DYRK1A* gene, encoded in chromosome 21 Down syndrome critical region, bridges between beta-amyloid production and tau phosphorylation in Alzheimer disease. *Hum Mol Genet* 2007; 16: 15–23.

一般の皆様へ

認知症患者は、団塊世代が75歳以上となる2025には700万人に達すると見積られており、その最大の原因疾患はアルツハイマー病である。アルツハイマー病の根本的治療薬は存在せず、多くの化合物の治験が中止となっている。本研究では、治療薬開発の着眼点を変え、早期からアルツハイマー病を発症するダウン症からヒントを得て、21番染色体に存在するリン酸化酵素に辿り着いた。この酵素はアルツハイマー病に増悪的に作用し、患者脳で発現が亢進していることから、その阻害剤は複数の作用点を有し、副作用が少ない治療薬になり得る。茶カテキン等が阻害活性を有していることから、さらなる開発が望まれる。

Development of combination therapy targeting on tumor endothelial cells

Takahisa Murata
amurata@mail.ecc.u-tokyo.ac.jp
The University of Tokyo

Summary Abstract

We found that the inhibition of a lipid mediator synthase increases the sensitivity against anti-cancer drugs of vascular endothelial cells in tumor.
Key Words：Tumor endothelial cell, Angiogenesis, Drug resistance

Introduction

Tumor cells produce cytokines and/or growth factors to stimulate the formation of new vessels, by a process called angiogenesis. Since tumor vessels are indispensable for tumor growth, normalizing and reducing tumor vessels can be developed into a potential anti-tumor therapy.

Tumor vessels mainly comprise vascular endothelial cells (ECs), which possess completely different characteristics compared to normal ECs. For example, tumor ECs have fenestrations and they are widened intercellular junctions. They also obtain drug resistance against anti-cancer drugs.

In the preliminary study using comprehensive analysis of mRNA expression, we found that tumor ECs strongly express one type of lipid mediator synthase. In this project, we attempted to reveal its function especially focusing on drug resistance in tumor ECs.

Results

1. We performed gene expression analysis and found a marked increase of one type of lipid synthase (PYP2) expression in tumor ECs derived from mice melanoma.

2. Immunostaining of mice melanoma revealed protein expression of PYP2 in the tumor ECs. *In situ* hybridization also showed PYP2 mRNA expression in the ECs of human melanoma and oral squamous cell carcinoma .

3. We generated systemic or endothelial specific PYP2 deficient mice and examined the anti-cancer drug sensitivity of tumor grown on these mice. Administration of low dosage (1 mg/kg) of doxorubicin or 5-FU was not effective against the growth of lung carcinoma or melanoma on WT mice. In contrast, these regimens were beneficial against tumor growth on PYP2 deficient mice.

4. We also found that pharmacological inhibition of PYP2 also significantly increased the sensitivity of tumor against anti-cancer drugs in WT mice.

5. Morphological studies showed tumor on PYP2$^{-/-}$ mice possessed more hyper-permeable and apoptotic ECs suggesting increased extravasation of anti-cancer drugs into tumor mass.

6. *In vitro* studies showed PYP2 inhibition decreased while stimulation of its signaling pathway increased the mRNA expressions of transporters which eliminate drugs in ECs. The inhibition of PYP2 significantly attenuated the elimination of doxorubicin and increased the apoptosis of ECs.

Discussion & Conclusion

Taken together, 1) inflammatory stimuli in tumor microenvironment seems to increase PYP2 expression specifically in ECs, 2) the inhibition or deficiency of PYP2 makes ECs hyper-permeable and increased the sensitivity against anti-cancer drugs by inhibiting the expressions of transporters in tumors.

References

Hematopoietic prostaglandin D synthase-derived prostaglandin D2 ameliorates adjuvant-induced joint inflammation in mice. Tsubosaka Y, Maehara T, Imai D, Nakamura T, Kobayashi K, Nagata N, Fujii W, Murata T. FASEB J. 2019 Feb 27:fj201802153R.

L-PGDS-derived PGD2 attenuates acute lung injury by enhancing endothelial barrier formation. Horikami D, Toya N, Kobayashi K, Omori K, Nagata N, Murata T. J Pathol. 2019 Feb 8.

Inhibition of stromal cell-derived factor-1α/CXCR4 signaling restores the blood-retina barrier in pericyte-deficient mouse retinas. Omori K, Nagata N, Kurata K, Fukushima Y, Sekihachi E, Fujii N, Namba-Hamano T, Takabatake Y, Fruttiger M, Nagasawa T, Uemura A, Murata T. JCI Insight. 2018 Dec 6;3(23).

Epithelial cell-derived Prostaglandin D2 inhibits Chronic Allergic Lung Inflammation in mice. Maehara T, Nakamura T, Maeda S, Aritake K, Nakamura M, Murata T. FASEB J 2019 in press.

一般の皆様へ

がん細胞と同様に、がんに伸びて酸素や栄養を届ける血管細胞も抗癌剤耐性能を獲得することが知られている。私たちは、このがんの血管に特異的に発現している酵素を発見し、この酵素の阻害ががん血管の薬剤耐性を解除することを発見した。この酵素の阻害剤と抗癌剤を同時に投与することで、がんに伸びる血管を効率よく抑えて、がんの増殖をとめることが可能となる可能性がある。

Molecular mechanism of store-operated Ca^{2+} entry signalosome and its physiological significance

Yoshihiro Baba
babay@bioreg.kyushu-u.ac.jp
Division of Immunology and Genome Biology,
Department of Molecular Genetics Medical Institute of Bioregulation, Kyushu University

Summary Abstract

A chief Ca^{2+} entry pathway in immune cells is store-operated Ca^{2+} (SOC) influx, which is triggered by depletion of Ca^{2+} from the endoplasmic reticulum (ER). STIM1 functions as the chief ER-resident protein to activate SOC influx by detecting ER Ca^{2+} depletion in many cells. However, the activation mechanism of STIM1 and the identity of SOC influx signalsome remain elusive. Here, we have identified a novel STIM1-binding protein, STBP1, as a component of SOC influx signalsome. Furthermore, our data suggest that STBP1 regulates STIM1 activity and cell viability.
Key Words：Store-operated calcium influx, B cells

Introduction

SOC influx is essential for a wide variety of physiological responses. Previous studies have identified STIM1, a Ca^{2+}-binding membrane protein localized in the ER, as the ER Ca^{2+} sensor and critical SOC influx activator (1-5). Subsequent studies have identified Orai1 as a calcium channel. The interaction of STIM1 with Orai1 is essential to induce SOC influx. In addition to Orai1, STIM1 has been reported to make signalsome by interacting with several proteins. However, the molecular machinery modulating STIM1 activity remains poorly understood. Here, we aimed to identify novel binding partners of STIM1 that can regulate SOC influx.

Results

To identify novel regulators of SOCE, affinity purification for STIM1 was conducted by using DT40 B cells stably expressing Flag-STIM1. We used in vivo cross-linking of cells to preserve STIM1 protein complexes and to validate possible STIM1-interacting proteins. This cross-linker is reactive with primary amines to one another and is easily reversible, which is used to preserve protein – protein complexes. To identify the binding proteins of Flag-STIM1, the STIM1 complexes in cross-linked cells were immunoprecipitated with anti-FLAG mAb and eluted with the FLAG peptide. Then, multidimensional protein identification technology (MudPIT) analysis was performed to identify proteins containing STIM1 complexes. This analysis identified many STIM1- associated proteins and we focused on a novel protein and named it as STBP1, (STIM1-binding protein 1).

To further investigate the interaction between STBP1 and STIM1, immunoprecipitation was conducted in 293T cells transiently transfected with plasmids encoding STBP1 and STIM1. We found that STBP1 was co-immunoprecipitated with STIM1 and its association was not affected when stimulated with TG, an ER calcium pump inhibitor.

Next, we investigated where STBP1 is localized in cells. After STBP1-YFP was transfected transiently in HeLa cells, the images of STBP1-YFP were obtained by confocal fluorescence

microscope. We found that STBP1 was localized in the ER. To assess the spatial relationship between STIM1 and STBP1, the distribution of these proteins was investigated in HeLa cells transiently expressed with STBP1-YFP and mCherry-STIM1. At steady state, a large portion of STBP1-YFP colocalized with mCherry-STIM1 in the ER. Store depletion induced by histamine and TG resulted in co-redistribution of mCherry-STIM1 and STBP1-YFP into puncta in the immediate vicinity of the ER near the PM. Thus, these results strongly suggest that STBP1 binds with STIM1 in the ER.

To examine the molecular function of STBP1, we established conditional STBP1-deficient DT40 B cells by using CreERT2 system. At first, we searched chicken homolog of stbp1 using the expressed sequence tag database and obtained the genomic clone by PCR using oligonucleotides, and DT40 genomic DNA was used as a template. The targeting vectors were constructed and transfected by electroporation. A floxed stbp1 construct was transfected at the same time. Homologous recombination was identified by PCR. This tamoxifen-inducible method allows us to delete STBP1 gene when the cells was treated with tamoxifen. Deletion of STBP1 was verified by genomic PCR and RT-PCR in tamoxifen-dependent manner. After tamoxifen treatment, we examined the cell viability. Unexpectedly, we found that the deletion of STBP1 in DT40 B cells induced cell death. Furthermore, to determine the effects of STBP1 on calcium signal, we monitored cytosolic Ca^{2+} in wild-type and STBP1-deficient DT40 B cells after tamoxifen treatment. Conditional STBP1-deficient DT40 B cells showed a significant increase of cytosolic Ca^{2+} concentration compared with STBP1-intact cells. These results collectively suggest that STBP1 regulates cell survival, death or growth, and may modulate calcium mobilization.

Now we are establishing the B cell specific STBP1 deficient mice to understand the physiological function of STBP1.

Discussion & Conclusion

Our findings identify a novel STIM1-binding protein STBP1 as a component of STIM1-mediated SOC influx signalsome. We showed that STBP1 is colocalized and physically associated with STIM1 in the ER. It has been reported that STIM1 interacts with several proteins, but it is unclear how these molecules modulate STIM1 activity. Our study by using STBP1-conditional deficient B cells suggest that STBP1 may be important for calcium-dependent cell survival or death, which is a unique effect among STIM1-binding partners. Whether the binding of STBP1 with STIM1 regulate SOC influx awaits further studies. In addition, the physiological function of STBP1 will be uncovered by analysis of our STBP1 conditional knock out mice.

References

1. Parekh, A.B. & Penner, R. Store depletion and calcium influx. Physiol. Rev. 77, 901–930 (1997).
2. Parekh, A.B. & Putney, J.W., Jr. Store-operated calcium channels. Physiol. Rev. 85, 757–810 (2005).
3. Roos, J. et al. STIM1, an essential and conserved component of store-operated Ca^{2+} channel function. J. Cell Biol. 169, 435–445 (2005).
4. Liou, J. et al. STIM is a Ca^{2+} sensor essential for Ca^{2+}-store-depletion-triggered Ca^{2+} influx. Curr. Biol. 15, 1235–1241 (2005).
5. Baba, Y. et al. Coupling of STIM1 to store-operated Ca^{2+} entry through its constitutive and inducible movement in the endoplasmic reticulum. Proc. Natl. Acad. Sci. USA □103, 16704–16709 (2006).

一般の皆様へ

本研究の目的はカルシウム流入に必須の分子であるSTIM1の活性を制御する新規分子を同定することです。免疫細胞の分化や活性においてカルシウム流入は極めて重要であり、免疫不全、自己免疫疾患、アレルギーの発症にも関与します。そこで、本研究成果はこれら疾患に対する新規薬剤の創薬につながる可能性があります。本研究では新規のSTIM1結合分子を同定でき、カルシウム流入に関与する可能性が示唆されたことから、今後さらに研究を進めていきたい。

Decoding the epigenome program which defines normal and tumor endothelial cells

Hiromu Suzuki
hsuzuki@sapmed.ac.jp
Department of Molecular Biology, Sapporo Medical University School of Medicine

Summary Abstract

Angiogenesis plays an essential role in tumor development and is an important therapeutic target. In this study, we identified that adipocyte enhancer binding protein 1 (AEBP1) promotes tumor angiogenesis in colorectal cancer (CRC), and that it could be a potential therapeutic target.
Key Words：colorectal cancer, tumor endothelium, AEBP1

Introduction

Tumor angiogenesis plays essential role in the development and progression of cancer. In colorectal cancer (CRC), clinical effectiveness of anti-VEGF treatment demonstrates that angiogenesis is a promising therapeutic target. To unravel novel factors involved in angiogenesis of CRC, we isolated epithelial cells and endothelial cells from primary CRC tissues and adjacent normal tissues, and performed RNA-sequencing analysis. We identified a series of genes upregulated in tumor endothelial cells including adipocyte enhancer binding protein 1 (AEBP1). We aimed to unravel the molecular function of AEBP1 in tumor endothelium, and to clarify its usefulness as a therapeutic target.

Results

Elevated expression of AEBP1 in CRC

We first tested the expression of AEBP1 in a series of epithelial cells and endothelial cells isolated from pairs of CRC tissues and corresponding normal colonic mucosa (n = 10). We found that AEBP1 was specifically upregulated in tumor endothelial cells. By using The Cancer Genome Atlas (TCGA) dataset, we analyzed the association between AEBP1 expression and clinicopathological features, and we found that higher AEBP1 expression is associated with poorer overall survival of CRC patients.

Functional analysis of AEBP1 in endothelial cells

We next analyze the function of AEBP1 cells in endothelial cells. Quantitative RT-PCR analysis revealed that AEBP1 is expressed in human umbilical vein endothelial cells (HUVECs) and human microvascular endothelial cells (HMVECs), while it is undetectable in CRC cell lines. We found that co-culture of HUVECs with CRC cells or treatment of HUVECs with conditioned medium derived from CRC cells upregulated AEBP1 expression in HUVECs.

By transfecting HUVECs with siRNAs targeting AEBP1, we found that knockdown of AEBP1 in HUVECs induced cell cycle arrest and suppressed cell proliferation, migration and in vitro tube formation by HUVECs. We next injected CRC cells with HUVECs with or without AEBP1 knockdown in nude mice subcutaneously. We found that AEBP1 knockdown in HUVECs suppressed

microvascular formation in xenograft tumors. These results suggest that AEBP1 expression in endothelial cells is induced by CRC cells, and that AEBP1 promotes tumor angiogenesis.

AEBP1 is a potential therapeutic target in CRC

To evaluate whether AEBP1 could be a therapeutic target, we next performed further xenograft experiments. We found that co-transplantation of CRC cells with HUVECs with AEBP1 overexpression promoted xenograft formation in nude mice. We next inoculated CRC cells into nude mice, and administered intratumoral injection of a siRNA targeting mouse Aebp1 or a control siRNA every 4 days, and found that Aebp1 siRNA suppressed xenograft tumor growth. We also observed that treatment with Aebp1 siRNA inhibited microvascular formation in the xenograft tumors.

Downstream targets of AEBP1 in endothelial cells

To clarify the intracellular localization of AEBP1, we performed fluorescent immunocytochemistry in HUVECs, and found that AEBP1 is located in both cytoplasm and nucleus. To unravel downstream targets of AEBP1, we next assessed the effect of AEBP1 knockdown on gene expression profiles in endothelial cells. We transfected HUVECs with either one of 2 different siRNAs targeting AEBP1 or a control siRNA, and harvested total RNA 48h or 72h after transfection. We performed gene expression microarray analysis and found that AEBP1 knockdown led to significant changes in gene expression profile. Gene ontology analysis suggested that genes associated with cell cycle are significantly enriched among genes affected by AEBP1 knockdown. Moreover, we found that a series of genes reportedly associated with tumor angiogenesis including aquaporin 1 (AQP1) and periostin (POSTN) were downregulated by AEBP1 knockdown in HUVECs. We validate the results by qRT-PCR, and found that 2 different siRNAs targeting AEBP1 could suppress expression of the putative target genes. We also confirmed that overexpression of AEBP1 in HUVECs led to opposite results. These results suggest that AEBP1 may regulate tumor angiogenesis through inducing downstream target genes which promote angiogenesis.

Discussion & Conclusion

In this study, we analyzed the role of AEBP1 in CRC. We found that expression of AEBP1 in vascular endothelial cells was induced by CRC cells, and that AEBP1 promotes proliferation, migration and tube formation of endothelial cells. Tumor xenograft experiments suggested that AEBP1 facilitates tumor angiogenesis, and that AEBP1 is a potential therapeutic target in CRC.

AEBP1 was originally identified as a transcriptional repressor that negatively regulate adipogenesis. Role of AEBP1 in cancer is not well understood, but recent studies show oncogenic function of AEBP1. For instance, a study reported that AEBP1 is upregulated in glioblastoma and promotes cell survival. Another study showed that AEBP1 upregulation confers chemoresistance in melanoma cells. However, its role in tumor angiogenesis has not been reported.

We also found that AEBP1 may regulate angiogenesis via inducing multiple target genes. AQP1 is a water channel protein expressed in vascular endothelial cells, and that its disruption impairs angiogenesis. POSTN is reportedly upregulated in various types of tumor, and promotes tumor angiogenesis and metastasis. Thus, AEBP1 may play as a transcription factor which upregulate angiogenesis promoting genes in endothelial cells.

References

1. He GP, Muise A, Li AW, Ro HS. A eukaryotic transcriptional repressor with carboxypeptidase activity. Nature. 1995 Nov 2;378(6552):92-6.
2. Ladha J, Sinha S, Bhat V, Donakonda S, Rao SM. Identification of genomic targets of transcription factor AEBP1 and its role in survival of glioma cells. Mol Cancer Res. 2012 Aug;10(8):1039-51.
3. Hu W, Jin L, Jiang CC, Long GV, Scolyer RA, Wu Q, Zhang XD, Mei Y, Wu M. AEBP1 upregulation confers acquired resistance to BRAF (V600E) inhibition in melanoma. Cell Death Dis. 2013 Nov 7;4:e914.
4. Saadoun S, Papadopoulos MC, Hara-Chikuma M, Verkman AS. Impairment of angiogenesis and cell migration by targeted aquaporin-1 gene disruption. Nature. 2005 Apr 7;434(7034):786-92.
5. Zhu M, Fejzo MS, Anderson L, Dering J, Ginther C, Ramos L, Gasson JC, Karlan BY, Slamon DJ. Periostin promotes ovarian cancer angiogenesis and metastasis. Gynecol Oncol. 2010 Nov;119(2):337-44.

一般の皆様へ

腫瘍血管新生はがんの発生や成長に重要な役割を担っており、有望な治療標的と考えられています。我々は大腸がん組織の遺伝子発現解析から新たな腫瘍血管関連因子として AEBP1を同定しました。我々の研究から AEBP1は大腸がん組織の血管内皮細胞で高発現していること、そして AEBP1が腫瘍血管新生を促進することが分かりました。マウスを用いた実験で AEBP1の阻害ががん組織の成長を抑制する効果が認められたことから、AEBP1はがん治療標的となりうる可能性が示されました。

Elucidation of long non-coding RNA family induced by molecular targeting anti-cancer drugs

Shigetada KONDO
kondoshi@rehab.osakafu-u.ac.jp
Graduate School of Comprehensive Rehabilitation, Osaka Prefecture University

Summary Abstract

In this research, we identified novel long noncoding RNAs (lncRNAs), which were induced in tumor cells by treatment with anti-VEGF agent (bevacizumab) and VEGFR tyrosine kinase inhibitor. The lncRNAs (lncRNA-1 and -2) were specifically expressed in colorectal cancer cells of patients who were treated with bevacizumab. Since the lncRNA-1 silenced tumor suppressor mRNAs (gene-A and gene-B) expression, induction of this lncRNA may not only promote tumor growth, but also render tumors more refractory against VEGF/VEGFR-targeted therapies.
Key Words：acquired drug resistance, molecular targeted therapy, long noncoding RNA

Introduction

Molecular targeted therapies are promising novel treatment options for patients with cancer. Different targeted therapies have achieved various degrees of success in cancer treatment. However, in many cases patient response is limited by acquired resistance to the drugs. The mechanisms of acquired resistance can be classified as three types: target gene mutation, bypass signaling pathway activation and down-stream pathway activation (1-3). We recently identified a novel mechanism of acquired resistance mediated by long noncoding RNAs (lncRNA-1 and -2).

Results

In the present study, we aimed to investigate lncRNAs (lncRNA-1 and -2) expression profiling in colorectal cancer tissues and to identify the molecular target of lncRNAs.

(1) Expression profiles of lncRNA-1 and -2 in human colorectal cancer tissues

Expression of lncRNA-1 and -2 was evaluated by RNA-FISH analysis. In colorectal cancer tissues from the untreated patients, lncRNA-1 and lncRNA-2 were insignificantly expressed. By contrast, in colorectal cancer tissues from the bevacizumab-treated patients, lncRNA-1 and lncRNA-2 were highly expressed. However, those lncRNAs were not expressed in the adjacent normal colorectal epithelial cells.

(2) Identification of target molecule of lncRNA-1 and -2

To identify target molecule of lncRNA-1 and -2 in colon cancer cells, RNA pull-down experiments using the lncRNA-1 or lncRNA-2 as bait and RNA-seq analysis were performed. We identified that molecular targets of lncRNA-1 were the tumor suppressor A mRNA and the tumor suppressor B mRNA. We further demonstrated that lncRNA-1 contained partial complementary sequence to the mRNAs and that lncRNA-1 could silence the both mRNAs in colon cancer cells.

Discussion & Conclusion

In this research, we identified novel lncRNAs, which were induced in tumor cells by treatment with bevacizumab and VEGFR tyrosine kinase inhibitor. Since the lncRNA-1 silenced tumor suppressor genes, induction of this lncRNA may not only promote tumor growth, but also render tumors more refractory against VEGF/VEGFR-targeted therapies. The gene status of the tumor suppressor A and B plays important roles in anti-tumor effects of VEGF-targeted therapy. However, how tumor cells lose the gene products during VEGF-targeted therapy remains unknown. Our findings may, at least in part, provide one of the mechanisms by which tumor cells lose the expression of the tumor suppressors and promotes their malignancy during anti-VEGF/VEGFR therapy.

References

(1) Alexander PB, Wang XF. Resistance to receptor tyrosine kinase inhibition in cancer: molecular mechanisms and therapeutic strategies. Front Med. 2015; 9:134-138.
(2) Mirone G, Shukla A, Marfe G. Signaling mechanisms of resistance to EGFR- and Anti-Angiogenic Inhibitors cancer. Crit Rev Oncol Hematol. 2016; 97: 85-95.
(3) Simon T, Gagliano T, Giamas G. Direct Effects of Anti-Angiogenic Therapies on Tumor Cells: VEGF Signaling. Trends Mol Med. 2017; 23: 282-292.

一般の皆様へ

現在、がん関連分子を標的とした分子標的薬治療は悪性腫瘍の標準化学療法となっている。しかしながら、がん細胞は分子標的薬に対して抵抗性を獲得することが臨床的に大きな問題となっている。これまでに、３つの分子標的薬耐性メカニズム〔① 標的分子の耐性変異獲得、② バイパス経路の活性化、③ 標的分子の下流経路の活性化〕が明らかとされている。本研究では全く新しい耐性獲得メカニズムの可能性を見出した。

Development of anti-metastatic therapy based on the regulation of vascular integrity.

Takayuki Shindo
tshindo@shinshu-u.ac.jp
Shinshu University School of Medicine

Summary Abstract

Controlling vascular integrity is expected to be a novel therapeutic target of cancers as well as cardiovascular diseases. Adrenomedullin (AM) and its receptor-modulating protein, RAMP2, have been identified as essential mediators of cardiovascular homeostasis. In this study, we used inducible vascular endothelial cell-specific RAMP2 knockout (DI-E-RAMP2-/-) mice to clarify the contribution made by the endogenous AM-RAMP2 system to angiogenesis and metastasis.

Subcutaneously transplanted melanoma cells showed less growth and angiogenesis in DI-E-RAMP2-/- than control mice. On the other hand, after transplantation of B16BL6 melanoma cells into hindlimb footpads, spontaneous metastasis to the lung was enhanced in DI-E-RAMP2-/- mice. Early after RAMP2 gene deletion, DI-E-RAMP2-/- mice showed enhanced vascular permeability, endothelial-mesenchymal transition (EndMT)-like change, and systemic edema. Within the lungs of DI-E-RAMP2-/- mice, pulmonary endothelial cells were deformed, and inflammatory cells infiltrated the vessel walls and expressed the chemotactic factors S100A8/9, which attract tumor cells and mediate formation of a pre-metastatic niche. Conversely, overexpression of RAMP2 suppressed tumor cell adhesion to endothelial cells, tumor metastasis, and improved survival.

These findings indicate that the AM-RAMP2 system regulates vascular integrity, whereas RAMP2 deletion promotes vascular permeability and EndMT-like change within primary lesions and formation of pre-metastatic niches in distant organs by destabilizing the vascular structure and inducing inflammation. Vascular integrity regulated by the AM-RAMP2 system could thus be a hopeful therapeutic target for suppressing tumor metastasis.

Key Words：Adrenomedullin (AM), RAMP2, tumor metastasis, vascular integrity

Introduction

Controlling vascular integrity is expected to be a novel therapeutic target of cancers as well as cardiovascular diseases. Adrenomedullin (AM) and its receptor-modulating protein, RAMP2, have been identified as essential mediators of cardiovascular homeostasis. In this study, we used inducible vascular endothelial cell-specific RAMP2 knockout (DI-E-RAMP2-/-) mice to clarify the contribution made by the endogenous AM-RAMP2 system to angiogenesis and metastasis.

Results

Using tumor transplantation models with DI-E-RAMP2-/- mice and control mice, we analyzed the effects of deleting the RAMP2 gene from vascular endothelial cells on tumor angiogenesis and growth. In the transplantation of B16F10 melanoma cells, tumor weights were significantly lower in DI-E-RAMP2-/- than control mice. Interestingly, B16F10 melanoma tumors excised from DI-E-RAMP2-/- mice showed signs of self-destruction. We thought that the self-destruction of the transplanted tumor was triggered by a lack of blood flow due to poor angiogenesis.

To assess the effect of RAMP2 deletion on tumor metastasis, B16BL6 melanoma cells were transplanted into the hindlimb footpads of DI-E-RAMP2-/- mice and control mice, and 3 weeks later the primary lesions were resected. Spontaneous lung metastasis was then analyzed 4 weeks after resection of the primary tumor. Contrary to our expectation, the incidence of metastasis and the number of metastatic lesions were higher in DI-E-RAMP2-/- mice than control mice.

Endothelial-mesenchymal transition (EndMT) has recently attracted attention as a phenomenon associated with tumor cell intravasation and metastasis. By immunostaining of primary B16F10 melanoma lesions, we detected abnormal growth of α-smooth muscle actin (αSMA)-positive mesenchymal cells within vascular walls in DI-E-RAMP2-/- mice, whereas the numbers of CD31-positive endothelial cells were decreased, which strongly suggests the occurrence of an EndMT-like change. To further confirm that RAMP2 gene deletion enhanced the EndMT-like change, we isolated vascular endothelial cells from DI-E-RAMP2-/- and control mice and then assayed EndMT induced by TGF-β in vitro. Our findings confirmed that among VE-cadherin-positive endothelial cells, cells also positive for fibroblast-specific protein-1 (FSP-1), a mesenchymal cell marker, were greatly increased in DI-E-RAMP2-/- mice as compared to control mice.

Recently, it is suggested that a favorable environment within a distant organ increases the likelihood that cancer metastasis will occur. This is the so-called pre-metastatic niche. We speculated that changes to the lung vasculature caused by RAMP2 deletion leads to formation of a pre-metastatic niche. Electron microscopic observation revealed the pulmonary endothelial cells in DI-E-RAMP2-/- mice to be deformed and to extend into the vascular lumen. Moreover, we detected prominent invasion of the lungs by macrophages, which were detected mainly along vascular lumens, in DI-E-RAMP2-/- mice. In addition, oxidative stress indicated by the accumulation of 4HNE, an unsaturated fatty acid peroxide, was enhanced in the lungs of DI-E-RAMP2-/- mice. Recently, S100A8 and S100A9 have been identified as tumor chemoattractant factors enhancing tumor metastasis to distant organs, and their expression was elevated in the lungs of DI-E-RAMP2-/- mice. These observations indicate that RAMP2 deletion from vascular endothelial cells enhances pre-metastatic niche formation in the lung, through invasion of the vasculature by inflammatory cells with increases in oxidative stress, and production of tumor chemoattractant factors.

Finally, to determine whether tumor cell metastasis could be suppressed by stimulating the AM-RAMP2 system, we generated endothelial cell-specific RAMP2-overexpressing transgenic mice (E-RAMP2 Tg). As expected, after transplantation of B16BL6 melanoma cells into the hindlimb footpads, there was less spontaneous lung metastasis in E-RAMP2 Tg mice than WT mice. Moreover, E-RAMP2 Tg mice showed greater survival in a spontaneous lung metastasis model

Discussion & Conclusion

Our findings indicate that deletion of RAMP2 from endothelial cells suppresses growth of locally transplanted tumors by reducing tumor angiogenesis. Contrary, metastasis was exacerbated in DI-E-RAMP2-/- mice. To elucidate the mechanism by which this process is enhanced in DI-E-RAMP2-/- mice, we examined the vascular structure within primary tumors to determine whether it possesses features. Within primary B16F10 melanomas in DI-E-RAMP2-/- mice, abnormal overgrowth of αSMA-positive mesenchymal cells in the vascular walls was accompanied by reduced numbers of CD31-positive endothelial cells, which suggests the occurrence of EndMT-like change.

Cancer metastasis depends on the microenvironment in distant organs as well as the primary tumor. We examined the effect of RAMP2 deletion on the formation of a pre-metastatic niche in the lung, and found S100A8/9 expression was elevated in the lungs of DI-E-RAMP2-/- mice. The elevated S100A8/9 expression is induced in distant organs prior to metastasis, which may enhance the recruitment of tumor cells from the primary lesion.

Conversely, endothelial cell-specific RAMP2 overexpression in E-RAMP2 Tg mice reduced lung metastasis and promoted survival in a lung metastasis model. We previously reported that stable overexpression of RAMP2 in endothelial cells enhances their barrier function through formation of intercellular tight-junctions. Thus, activation of the AM-RAMP2 system in endothelial cells enhances vascular integrity, which may suppress tumor cell adhesion and invasion.

AM is a peptide with a very short half-life in the bloodstream, which limits its usefulness for treatment of chronic diseases. It is noteworthy that we are able to modulate AM function in the vasculature by modulating RAMP2. RAMP2 could be a useful therapeutic target to suppress metastasis by controlling vascular integrity.

References

Shindo T, Tanaka M, Kamiyoshi A, Ichikawa-Shindo Y, Kawate H, Yamauchi A, Sakurai T.
Regulation of cardiovascular development and homeostasis by the adrenomedullin-RAMP system
Peptides. 111:55-61. 2019

Xian X, Sakurai T, Kamiyoshi A, Ichikawa Y, Tanaka M, Koyama T, Kawate H, Yang L, Liu T, Imai A, Zhai L, Hirabayashi K, Dai K, Tanimura K, Liu T, Cui N, Igarashi K, Yamauchi A, Shindo T.
Vasoprotective activities of the adrenomedullin-RAMP2 system in endothelial cells.
Endocrinology 158(4): 1–14, 2017

Tanaka M, Koyama T, Sakurai T, Kamiyoshi A, Ichikawa-Shindo Y, Kawate H, Liu T, Xian X, Imai A, Zhai L, Hirabayashi K, Owa S, Yamauchi A, Igarashi K, Taniguchi S, Shindo T.
The endothelial adrenomedullin-RAMP2 system regulates vascular integrity and suppresses tumor metastasis
Cardiovasc Res. 111(4):398-409. 2016

Koyama T, Ochoa-Callejero L, Sakurai T, Kamiyoshi A, Ichikawa-Shindo Y, Iinuma N, Arai T, Yoshizawa T, Iesato Y, Yang Lei, Uetake R, Okimura A, Yamauchi A, Tanaka M, Igarashi K, Toriyama Y, Kawate H, Adams R.H, Kawakami H, Mochizuki N, Martínez A, Shindo T.
Vascular endothelial adrenomedullin-RAMP2 system is essential for vascular integrity and organ homeostasis
Circulation. 127(7) 842-53. 2013

一般の皆様へ

血管の恒常性は、液性因子とその受容体システムによって制御されています。私達は、アドレノメデュリン (AM) が主として血管から分泌され、様々な生理作用を有することを明らかとしてきました。AM とその受容体活性調節タンパクである RAMP2は、血管恒常性維持に重要な働きをしています。この研究において、私達は、血管内皮細胞特異的な RAMP2ノックアウトマウスや、RAMP2過剰発現マウスを用いて、AM-RAMP2系の癌転移における意義をはじめて明らかとしました。

注目すべきは、血管内皮細胞に RAMP2を過剰発現したマウスでは、癌の転移が抑制され、生存率が改善したことです。この結果から、血管の恒常性維持に注目することで、癌転移を抑制する新しい治療法につながることが期待されます。

Mechanisms underlying commitment to thymic epithelial cells preventing onset of autoimmune diseases

Taishin Akiyama
taishin.akiyama@riken.jp
RIKEN Center for Integrative Medical Sciences

Summary Abstract

Medullary thymic epithelial cells (mTECs) are critical for preventing onset of autoimmune diseases by promiscuously expressing tissue-specific antigens. mTECs differentiate from stem/progenitor cells that have a capability of differentiating into cortical TECs. To data, mechanisms determine the fate of the common stem/progenitor of TECs into mTECs and cTECs are largely unknown. We asked possible role of interferon regulatory factor 6 (IRF6) in mTEC differentiation. Although regulating epithelial cell differentiation of skin, IRF6 does not have non-redundant function in differentiation and gene expression of TECs

Key Words：Thymus, autoimmunity, epithelial cells, transcription factor

Introduction

Medullary thymic epithelial cells (mTECs) are critical for preventing onset of autoimmunity (ref1). mTECs express many kinds of tissue specific antigens ectopically, which in part regulated by transcriptional regulator Aire. Previous several studies suggested that both mTECs and cortical TECs differentiate from common stem/progenitor cells (ref1). However, mechanisms regulating differentiation of mTECs remain to be determined. In this study, we aimed to find transcriptional regulators that determines fate of common stem/progenitor cells into mTECs.

Results

We previously reported two different precursor cells of mTECs expressing Aire (ref2). Then we performed microarray analysis of gene expressing these precursor cells and identified transcription factors expressing in all of mTECs and their precursor cells, but not in cTECs and their precursor cells. We obtained three candidate transcription factors, IRF6 and other two transcription factors with similar domain structure (tentatively named MTF1 and MTF2). We next asked if these transcription factors are necessary for mTEC differentiation.

We first analyzed role of IRF6 in mTEC differentiation. IRF6 is reportedly necessary for skin epithelial cells differentiation (ref3). Deficiency of IRF6 in whole body caused death just after birth due to defect of skin epithelium development. Therefore, we used IRF6 flox/flox mouse line, which are kindly provided by Dr. Kinoshita in Nagasaki University. We crossed Foxn1-Cre, which allows deletion of flox allele in thymic epithelial cells and hair follicles (IRF6 cKO mice). IRF6 cKO mice were born normally and showed a hair loss after around 3 weeks old age. Body weight of IRF6 cKO mouse are normal. Weight of thymus and spleen was also normal in IRF6 cKO mice as compared to littermate control mice. We further detailed development of thymocytes and TECs in IRF6 cKO. Thymocytes are largely classified by expression of surface markers CD4 and CD8 by flow cytometer.

The IRF6 deletion in TECs did not influence cellularity and ratio of CD4+CD8+, CD4+CD8-, CD4-CD8+, CD4-CD8- thymocytes, suggesting that IRF6 in TECs is not required for TEC function regulating differentiation and development of thymocytes. We performed flow cytometric analysis of TECs. EpCAM-positive TECs were separated by expression of UEA-1 lectin ligand, CD80, and Ly51 in CD45-negative TER119-negative cell fraction. Cell number and frequency of mTECs and cTECs were not changed in IRF6 cKO, indicating that IRF6 is not essential for differentiation of mTECs. We further analyzed gene expression of mTECs and cTECs in IRF6 cKO mice. EpCAM+ cells were separated into mTECs (UEA-1+ Ly51-) and cTECs (UEA-1- Ly51+) and sorted by flow cytometry. Expression of mRNA in mTECs and cTECs of IRF6 cKO and control mice was evaluated by high-throughput sequencing (RNA-seq). Gene expression level was determined by using CLC Genomics Workbench. Unexpectedly, RNA-seq showed that mRNA expression in IRF6 deficient mTECs and cTECs is almost identical with that in control. Taken together, we concluded that IRF6 does not have non-redundant role in TEC differentiation and gene expression even if IRF6 is expressed in mTECs.

We next tried to address role of MTF1 and MTF2 on mTEC differentiation. Because MTF-1 deficient mice had never been established yet, we first prepared MTF-1 deficient mice. Because public database suggest that MTF-1 is expressed in epithelial cells of several organ, we chose to establish MTF-1 flox/flox conditional mice of which MTF-1 gene is deleted in TECs by crossing with Foxn1-Cre. Moreover, MTF-1 expression can be detected by beta-galactosidase (LacZ) activity in these reporter mice. We first checked MTF-1 expression in murine organs by monitoring LacZ activity. We found that MTF-1 is expressed in mTECs, intestinal epithelial cells, and lung epithelial cells. In mTECs, MTF-1 is highly expressed in a part of mTECs. We are currently analyzing TEC differentiation of MTF1 cKO, MTF2 cKO, and double cKO of MTF1 and MTF2.

Discussion & Conclusion

In this study, we are trying to identify “master regulator” for mTEC differentiation. IRF6 is reportedly critical for epithelial cell differentiation in skin (ref3). However, we found that IRF6 does not have non-redundant role in differentiation of both mTECs and cTECs. IRF family consists of 9 members. Database analysis and previous study suggested that, beside IRF6, several other IRF family members are expressed in TECs. It is possible that other IRF family member compensate the deletion of IRF6. For instance, a previous study suggested that IRF7 partially contribute to development of mTECs (ref4). It is important future work to address such possible redundant role of IRF family proteins in differentiation and function of mTECs.

References

1. Abramson J and Anderson G., Annu. Rev. Immunol. 35:85-118 (2017)
2. Akiyama N., J. Exp. Med. 213:1441-1458 (2016)
3. Nat. Genet. 38:1335-1340 (2006)
4. J Immunol. 190:3289-3298 (2013)

一般の皆様へ

免疫応答の司令塔であるＴリンパ球のほとんどが胸腺で産生されます。胸腺でＴ細胞が産生する際、自己の組織に応答するＴリンパ球も生じます。そのほとんどは胸腺であらかじめ除かれますが、それらがうまく除かれない場合、自己免疫疾患の原因になると考えられています。本研究では、胸腺で自己組織応答性Ｔリンパ球を除去し、自己免疫疾患の発症を抑制する上皮細胞に着目し、それらの細胞がどのような機構で発生するのか調べます。本研究の成果は、将来的に自己免疫疾患の発症予防や治療に貢献することが期待されます。

Regulation of cellular functions by the nucleolus as a stress sensor

Keiji Kimura
kekimura@tara.tsukuba.ac.jp
University of Tsukuba

Summary Abstract

The nucleolus is a dynamic nuclear body whose structure changes in response to cellular stresses. The nucleolar structure is also changes during mitosis. We found that a novel nucleolar protein complex, which we called the NWC complex, translocates from interphase nucleoli to the periphery of mitotic chromosomes during mitosis. The NWC complex regulates centromeric function of mitotic chromosomes by regulating centromeric enrichment of Aurora B.
Key Words：nucleolus, cellular stress, mitosis, nucleolar disruption, chromosome periphery

Introduction

The nucleolus is the largest nuclear body and is the site of ribosome biogenesis. In addition, recent studies have revealed that the nucleolus in involved in various cellular processes (1). In response to various stresses, the nucleolar structure changes and many of the nucleolar factors (proteins and RNAs) are released from the nucleolus and induce stress response (2-4). The nucleolar structure is also changes during mitosis in higher eukaryotes, which leads to translocation of nucleolar proteins to the cytoplasm or periphery of mitotic chromosomes. In this project, we have characterized the role of the novel nucleolar protein complex involved in mitotic progression.

Results

In the previous study, we found that depletion of a nucleolar protein called nucleolar protein 11 (NOL11) or induced nucleolar disruption during interphase, which in turn delayed activation of cyclin-dependent protein kinase 1 (cdk1) and mitotic entry (5). We also noticed that NOL11 depletion increased mitotic index, suggesting that NOL11 has the functions in the progression of mitosis (5).

In this project, we first examined the subcellular localization of NOL11 to test the mitotic function of NOL11. We found that NOL11 localized at the periphery of mitotic chromosomes (PR). Then we tested whether NOL11 forms a protein complex because NOL11 has no functional motif. By tandem affinity purification approach, we found that NOL11 formed a novel protein complex with WDR43 and Cirhin, both of which are nucleolar component. This complex, which we call the NWC (NOL11-WDR43-Cirhin) complex, localized in the nucleolus during interphase and translocated to the PR of condensed mitotic chromosomes during mitosis when the nucleolus disassembles. Treatment of RNase A led to dissociation of the NWC complex from the PR. Furthermore, the NWC complex interacted with pre-rRNA in mitotic cells. These result shows that the NWC complex localized the PR pre-rRNA, which is consistent with the report that newly synthesized pre-rRNA associates with the PR and act as a binding scaffold of several nucleolar proteins.

To address the roles of the NWC complex, we depleted of each component of the NWC complex using siRNAs. Depletion of the NOL11, WDR43, or Cirihin (The NWC component) spent longer time progressing prophase to metaphase. Consistent with this results, depletion of the NWC complex

severely compromised chromosome alignment on the metaphase plate, showing activation of spindle assembly checkpoint and metaphase arrest. Because chromosome alignment depends on the regulated interaction between microtubules and kinetochores (MT-KT), we tested whether the NWC complex were involved in the process by monastrol release assay. We found that regulated MT-KT interaction was defective in the cells depleted of the NWC complex.

Mitotic phenotypes induced by the NWC complex depletion are similar to those induced by inhibition of Aurora B, a kinase involved in multiple mitotic events and the centromeric localization is essential. Therefore, we tested the effects of the NWC depletion on the localization and activity of Aurora B. We found that the NWC depletion had little influenced the activity and total amount of Aurora B but severely reduced Aurora B signals at centromere, showing that the NWC complex is essential for centromeric enrichment of Aurora B. In addition, we found that depletion of the NWC complex markedly reduced centromeric localization of histone H3 phosphorylated at threonine 3 (H3T3ph) that is the histone mark to recruit Aurora B at centromere. However, depletion the NWC complex little affected total levels of H3T3ph. Taken together, we speculate that the NWC complex prevents H3T3ph from spreading from centromeres to chromosome arms, thereby contributes to centromeric enrichment of Aurora B.

Finally, we tested the effect of NWC depletion on sister chromatid cohesion, which depends on centromeric localization of Aurora B. We found that depletion of the NWC complex caused defects in mitotic chromosome cohesion, showing the NWC complex is essential for centromere organization and the maintenance of sister chromatid cohesion.

Discussion & Conclusion

In this project, we identified a novel nucleolar protein complex, consists of NOL11, WDR43, and Cirhin, which plays an essential role in regulating centromeric function of mitotic chromosomes. The NWC complex existed in nucleoli during interphase and associated with the PR of mitotic chromosomes. The NWC complex was required for centromeric enrichment of Aurora B through the phosphorylation of histone H3 at threonine 3, thus contributing to regulated interaction between microtubules and kinetochores and establishment of sister chromatid cohesion.

There are several proteins that dynamically shuttles between nucleoli and the PR of chromosomes in a cell cycle dependent manner and are considered to be involved in regulation of mitosis. In this project, we have characterized that the NWC complex, one of these nucleolar-perichromosome shuttling proteins, regulates chromosome function in mitosis through facilitating centromeric concentration of Aurora B.

References

1) F. M. Boisvert, S. van Koningsbruggen, J. Navascues, A. I. Lamond. The multifunctional nucleolus.
Nat. Rev. Mol. Cell Biol. (2007) 8, 574-585.

2) Nishimura K, Kumazawa T, Kuroda T, Katagiri N, Tsuchiya M, Goto N, Furumai R, Murayama A, Yanagisawa J, and Kimura K. Perturbation of ribosome biogenesis drives cells into senescence through 5S RNP-mediated p53 activation.
Cell Rep. (2015) 10:1310-1323

3) Katagiri N, Kuroda T, Kishimoto H, Hayashi Y, Kumazawa T, and Kimura K. The nucleolar protein nucleophosmin is essential for autophagy induced by inhibiting Pol I transcription. *Sci. Rep.* (2015) 5:8903
4) Kumazawa T, Nishimura K, Katagiri N, Hashimoto S, Hayashi Y, and Kimura K. Gradual reduction in rRNA transcription triggers p53 acetylation and apoptosis via MYBBP1A. *Sci. Rep.* (2015) 5:10854
5) Hayashi Y, Fujimura A, Kato K, Udagawa R, Hirota T, Kimura K. Nucleolar integrity during interphase supports faithful Cdk1 activation and mitotic entry. *Science Adv.* (2018) 4:eaap7777

一般の皆様へ

核小体は核内に存在する多種類のタンパク質と RNA から成る構造体で、リボソーム生合成やストレス応答など多くの細胞機能に関与します。細胞が種々のストレスに細胞がさらされた際には、核小体が崩壊しそれに伴って局在を変化させた核小体因子が種々の細胞機能に関与します。また、細胞分裂に伴って核小体が崩壊し多くの核小体因子が局在を変えることから、核小体と細胞分裂の関連性が示唆されてきましたが、その実態は分かっていませんでした。本研究で我々は、核小体因子である NWC 複合体が、分裂期の染色体周辺に結合し動原体の機能を制御することにより正常な細胞分裂に寄与することを見出しました。

Transomics approach to elucidate cellular signaling pathways in vascular development, morphogenesis and disease

Osamu NAKAGAWA
osamu.nakagawa@ncvc.go.jp
National Cerebral and Cardiovascular Center Research Institute

Summary Abstract

Proper formation and function of cardiovascular network are essential for embryonic development, and mutations of the genes involved in cardiovascular signaling often cause intractable human diseases. We have performed various experiments that examine transcriptome, proteome and phosphoproteome profiles in endothelial cells to clarify the influences of vascular signal activation or inhibition upon downstream signaling pathways and endothelial functions. These studies provide a clue to understand mechanisms of normal cardiovascular development and etiologies of human diseases.

Key Words：Vascular development, Cellular signaling, Bone morphogenetic protein, ALK1 receptor complex, protein kinase

Introduction

Formation of cardiovascular network is essential for embryonic development, and neovascularization is associated with various adult diseases such as ischemic heart diseases, retinopathy and cancer (1). Vasculogenesis occurs as a de novo organization of endothelial cell plexus, followed by a series of processes for vascular remodeling and maturation, including endothelial cell migration, proliferation and tubular reorganization, collectively called angiogenesis. In addition, the structure of blood vessels is established by the stabilization of endothelial cells, acquirement of arterial or venous identity, and recruitment of mural cells to vascular walls (2).

Results

A variety of cellular signaling pathways controlling vascular development involve cytokines and growth factors, such as vascular endothelial growth factors (VEGF), angiopoietins, transforming growth factor β (TGFβ) and bone morphogenetic proteins (BMPs) (3,4). BMP9 and BMP10 mainly act through the endothelium-specific ALK1 receptor and promote arterial endothelial maturation and quiescence (5-8). Mutations in the genes involved in the ALK1 receptor signaling cause hereditary hemorrhagic telangiectasia and are implicated in the pathogenesis of pulmonary arterial hypertension (9-10). ALK1 signal induces SMAD1/5/9-dependent transcription of target genes, including its own signaling components, transcription factors and membrane ligands/receptors. To clarify the downstream events of ALK1 signal activation, we performed a transcriptome analysis of human umbilical artery endothelial cells stimulated with BMP9. Various genes showed an increase in mRNA expression following the ALK1 receptor activation, most of which had SMAD binding in their putative enhancer regions in the in silico analysis. These genes are likely new target genes that serve for endothelial differentiation and vascular morphogenesis downstream of the BMP-ALK1-SMAD signaling pathway.

Among them, we found that the SGK1 gene encoding Serum/glucocorticoid-regulated kinase 1 showed a rapid and significant increase in mRNA expression by the stimulation with BMP9 (11). At embryonic day 9.5, the Sgk1 mRNA expression was clearly enriched in vascular endothelial cells, which was significantly down regulated in Alk1/Acvrl1 null embryos. ALK1 signal was known to evoke post-translational activation of protein kinases such as TAK1 and ERK as a non-canonical pathway, but SGK1 was the first example of protein kinases whose expression was controlled by the SMAD-dependent canonical pathway. SGK1 belongs to the AGC (named after PKA, PKG and PKC) superfamily of protein kinases often involved in cardiovascular development and disease (12). Interestingly, the transcriptome analysis demonstrated that only SGK1 showed BMP9-dependent induction of gene expression among the genes encoding AGC kinases. *Sgk1* null mice with a particular genetic background exhibit severe abnormalities of vascular development and embryonic lethality (13-14), suggesting its role in the mechanisms of angiogenesis defects due to the ALK1 signaling deficiency.

While there were a couple of SGK1 substrates that were implicated in the control of vascular formation and maintenance, such as the Foxo family of transcription factors and the NDRG proteins (12), the detailed mechanisms of SGK1 actions in endothelial cells were yet to be clarified. We therefore employed a proteomic approach to search for possible endothelial-enriched SGK1 substrates using the mass spectrometry analysis of phosphorylated proteins in cultured endothelial cells expressing constitutively-activated SGK1. We have identified several proteins as candidates for novel SGK1 substrates, which show specific phosphorylation of consensus-matched serine or threonine residues. Further studies are ongoing to examine whether these proteins are functionally important in endothelial cell differentiation and vascular morphogenesis, and how SGK1-dependent phosphorylation influences their actions.

We have also started omics analyses using vascular endothelial cells of mouse embryos. Endothelial cells were isolated using anti-CD31 antibody for the application to RNA sequencing and protein mass spectrometry. mRNA and protein expression in endothelial cells of wild type embryos and gene knockout embryos of vascular signaling factors is currently under study. In addition to the analysis of individual layers of signaling network, such as transcriptome, proteome and phosphoproteome, the comparison of multiple omics data will be performed to clarify the global interrelationship of signaling events in endothelial cells.

Discussion & Conclusion

Elucidating cellular signaling pathways involved in endothelial cell differentiation and vascular morphogenesis is important for the mechanistic dissection of normal embryonic development. In addition, such information helps understand the pathogenesis of various congenital cardiovascular diseases. We have studied the regulation of transcriptome, proteome and phosphoproteome downstream of ALK1 and other vascular signaling pathways in cultured endothelial cells as well as in mouse embryos. Particularly, identification of SGK1 as a novel downstream target gene of ALK1 signaling is of high interest (11), and characterization of additional SGK1 substrates in endothelial cells provides a clue to better understanding of endothelial signaling during normal and abnormal vascular development.

References

1. Herbert, S.P. and D.Y. Stainier, Molecular control of endothelial cell behaviour during blood vessel morphogenesis. Nat Rev Mol Cell Biol, 2011. 12(9): p. 551-64.
2. Potente, M., H. Gerhardt, and P. Carmeliet, Basic and therapeutic aspects of angiogenesis. Cell, 2011. 146(6): p. 873-87.
3. Miyazono, K., Y. Kamiya, and M. Morikawa, Bone morphogenetic protein receptors and signal transduction. J Biochem, 2010. 147(1): p. 35-51.
4. Cai, J., et al., BMP signaling in vascular diseases. FEBS Lett, 2012. 586(14): p. 1993-2002.
5. Garcia de Vinuesa, A., et al., BMP signaling in vascular biology and dysfunction. Cytokine Growth Factor Rev, 2016. 27: p. 65-79.
6. Urness, L.D., L.K. Sorensen, and D.Y. Li, Arteriovenous malformations in mice lacking activin receptor-like kinase-1. Nat Genet, 2000. 26(3): p. 328-31.
7. Oh, S.P., et al., Activin receptor-like kinase 1 modulates transforming growth factor-beta 1 signaling in the regulation of angiogenesis. Proc Natl Acad Sci U S A, 2000. 97(6): p. 2626-31.
8. Li, D.Y., et al., Defective angiogenesis in mice lacking endoglin. Science, 1999. 284(5419): p. 1534-7.
9. Tillet, E. and S. Bailly, Emerging roles of BMP9 and BMP10 in hereditary hemorrhagic telangiectasia. Front Genet, 2014. 5: p. 456.
10. Ma, L. and W.K. Chung, The role of genetics in pulmonary arterial hypertension. J Pathol, 2017. 241(2): p. 273-280.
11. Araki M., et al., Serum/glucocorticoid-regulated kinase 1 as a novel transcriptional target of bone morphogenetic protein-ALK1 receptor signaling in vascular endothelial cells. Angiogenesis, 2018. 21(2):415-423.
12. Di Cristofano, A., SGK1: The Dark Side of PI3K Signaling. Curr Top Dev Biol, 2017. 123: p. 49-71.
13. Zarrinpashneh, E., et al., Ablation of SGK1 impairs endothelial cell migration and tube formation leading to decreased neo-angiogenesis following myocardial infarction. PLoS One, 2013. 8(11): p. e80268.
14. Catela, C., et al., Serum and glucocorticoid-inducible kinase 1 (SGK1) is necessary for vascular remodeling during angiogenesis. Dev Dyn, 2010. 239(8): p. 2149-60.

一般の皆様へ

細胞分化・増殖・移動など多様な生命現象の組み合わせにより、複数の起源を有する前駆細胞から心臓・血管の発生・形態形成が行われ、多様な細胞群が協調して働く成熟機能システムを実現するメカニズムは非常に複雑であり、その破綻が先天性心疾患・遺伝性血管疾患のみならず成人の循環器疾患の病因に深く関わることは明らかです。心血管系の発生・形態形成過程において様々な細胞間・細胞内シグナル伝達系が働くことが知られていますが、私たちはそれらシグナル伝達系の活性化や阻害によって内皮細胞の遺伝子発現様式・タンパク質分子発現様式などがどのような影響を受けるかを検討しました。今後も心血管形成におけるシグナル伝達機構の研究を続け、ヒト心血管疾患の病因・病態解明と診断法・治療法開発を目指したいと考えております。

Studies on formation and function of extracellular DNA fibers

Hisato Saitoh
hisa@kumamoto-u.ac.jp
Faculty of Advanced Science and Technology (FAST), Kumamoto University

Summary Abstract

Although the genomic DNA is compacted and sheltered in the nucleus in nearly all eukaryotic cells, DNAs can be detected in the extracellular spaces in many species, including humans. Such observations suggest existence of the mechanism that generates extracellular DNAs in eukaryotic cells. In this study, using cultured human cells, we investigate formation and function of genomic DNA which are extruded from the nucleus and are discharged to the extracellular environment.
Key Words：extracellular DNA, chromatin, nucleus, neutrophil extracellular traps (NETs)

Introduction

Eukaryotic cells, including human myeloid cells, are known to extrude their nucleus and DNAs in response to intrinsic or environmental cues. For instances, erythroid precursor cells efficiently separate the cytoplasmic compartment from the nucleus by squeezing the nucleus to extracellular spaces during the final erythroid maturation step, known as “enucleation” [1, 2]. Other example is observed in subsets of leucocytes, such as neutrophils and macrophages, undergoing extracellular trap-cell death (NETosis) [3, 4]. During NETosis, decondensed chromatin fibers are discharged from the nucleus to extracellular spaces, resulting in formation of the complex fibrous network which have a potential to capture and immobile pathogens. Mechanisms to generate such extracellular nucleus and/or chromatin fibers in the myeloid cellular lineages remain largely uninvestigated.

Results

1. The nuclear extrusion to extracellular spaces in TN-exposed HL-60 cell culture

To elucidate the effect of tunicamycin (TN) [5-7] on human myeloid cell lines under the FBS-free conditions, exponentially growing HL-60 cells were cultured in the presence or absence of TN under the FBS-free medium conditions at 37oC. More than 80% of the TN-exposed cells exhibited the ovoid-shape after the 60 min incubation. Our time-lapse analysis of a TN-exposed cell revealed that the ovoid-shaped object appeared suddenly with no premonitory sign and indicated that such ovoid-shaped objects emerged in a very rapid manner, which was completed within less than 5 min. Since these ovoid-shaped objects were readily stained by the DNA-staining fluorescent dyes, such as SYTOX Green and DAPI, without any detergent treatment, we considered that the TN-induced ovoid-shaped objects might represented the nucleus of HL-60 cells, which were somehow extruded from the cultured cells to the extracellular spaces under our experimental settings.

2. Generation of extracellular chromatin/DNA fibers

When TN-exposure was continued for 120 min, the numbers of SYTOX Green-positive ovoid-shaped objects reduced in the culture dish. Instead, the numbers of SYTOX Green-positive fiber-like structures increased in the culture medium, suggesting that DNA fibers were extruded from the nucleus. We isolated DNA from the fiber-like structures and performed agarose-gel electrophoresis,

confirming that the fiber-like structures were consisted of DNAs. We also detected that the TN-induced fiber-like structures were susceptible to MNase-digestion, generating 160-200 DNA ladder bands on agarose gel. These results indicated that TN-exposure of HL-60 cells under the FBS-free conditions resulted in generation of extracellular chromatin fibers, at least, in part of which consisted of MNase-sensitive structural units. This scenario was feasible, since SDS-PAGE analysis of the proteins associated with the fiber-like structure revealed existence of a large amount of histone proteins on the fiber-like structures.

3. Time-lapse observation of the extracellular chromatin formation

We performed the time-lapse images of representative TN-exposed cell and DMSO-treated control cells. In the time-lapse images of the TN-exposed cell, it appeared to squeeze large ovoid-shaped objects to the extracellular space, followed by discharge of fiber-like structures to extracellular space from the nucleus. In contrast, the control cells exhibited neither extrusion of the ovoid-shaped objects nor fiber-like structures during our time-lapse observation period. Together, these data indicated the sequential order of two events; extrusion of fiber-like structures to extracellular space proceeded following the nuclear extrusion.

4. TN-induced nuclear and chromatin extrusion in other myeloid cell lines

To elucidate TN-effect on other cell-types besides HL-60 cell line, we tested human myelomonocytic lymphoma U937 and human acute monocytic leukemia THP-1 cells. We found that both U937 and THP-1 cells exhibited a phenotype similar to TN-exposed HL-60 cells at either time point; they extruded ovoid-shaped objects were detected at 30~60 min-incubation, suggesting that TN-induced the nuclear extrusion in both cell lines, and the formation of SYTOX Green-positive extracellular fiber-like structures were discharged to extracellular spaces at 120 min-incubation, implying the formation of extracellular chromatin fibers in both cell lines.

Discussion & Conclusion

We found a unique effect of TN on a range of cultured myeloid cell lines to induce extracellular nucleus and chromatin fibers in a previously unappreciated fashion. Given that apoptosis prevents discharge of genetic and epigenetic materials of the dying cells, our discovery of the TN-induced cellular event provides quite different concept with respect to fate of genetic and epigenetic materials after cell death. At the same time, the discovery of this unique phenomenon will open the door to the investigation of the mechanism of the nuclear and chromatin discharge to extracellular environment, which are often observed in myeloid cellular lineage, such as enucleation during erythroid maturation and formation of NETs in leukocytes during pathogen infection. We anticipate that the identification of candidate regulators and effectors in the TN-induced pathway will enable to elucidate the factors which regulate 4D structure of chromatin in the nucleus and cells. Additionally, we expect that the extruded nucleus and chromatin in the TN-exposed cells will be suitable for the *in vitro* analyses of DNA replication, transcription, nuclear scaling and mitotic chromosome condensation. The TN-induced extracellular chromatin fibers will be beneficial for researchers studying interaction of chromatin with pathogens *in vitro.*

References

[1] Ji P. New insights into the mechanisms of mammalian erythroid chromatin condensation and enucleation. Int Rev Cell Mol Biol. 2015;316:159-82.
[2] Kalfa TA, Zheng Y. Rho GTPases in erythroid maturation. Curr Opin Hematol. 2014;21:165-71.
[3] Brinkmann V, Zychlinsky A. Neutrophil extracellular traps: is immunity the second function of chromatin? J Cell Biol. 2012;198:773-83.
[4] Castanheira FVS, Kubes P. Neutrophils and NETs in modulating acute and chronic inflammation. Blood. 2019;133: 2178-2185.
[5] Oakes SA, Papa FR. The role of endoplasmic reticulum stress in human pathology. Annu Rev Pathol. 2015;10:173-94.
[6] Prescher JA, Bertozzi CR. Chemical technologies for probing glycans. Cell. 2006;126(5):851-4.
[7] van Galen P, Kreso A, Mbong N, Kent DG, Fitzmaurice T, Chambers JE, et al. The unfolded protein response governs integrity of the haematopoietic stem-cell pool during stress. Nature. 2014;510:268-72.

一般の皆様へ

DNA は核内に保持されるだけでなく、細胞外に放出されることがある。例えば、白血球が細胞外に形成する Neutrophil Extracellular Traps（NETs）の DNA は、細菌の侵入とシグナル因子の拡散を調節することで、免疫応答に関わる。しかしながら、細胞外 DNA の形成と機能についての詳細は、不明な点が多い。本研究では、白血病由来細胞 HL-60を小胞体ストレス誘導剤 Tunicamycin で処理することで細胞外 DNA を誘導する実験系を構築した。細胞外 DNA に関する未踏破の研究領域に踏み込んだことで、遺伝暗号やエピジェネティクス以外の DNA 機能の重要性を指摘し、新たな保健医療技術を開拓するための知的基盤を構築した。

Serotonin 5-HT_{2A} receptor agonist in treatment to psychiatric disorders

Daisuke Ibi
ibid@meijo-u.ac.jp
Meijo University, Department of Chemical Pharmacology

Summary Abstract

Ketamine, a NMDA antagonist, has been available as an antidepressant for treatment-resistant depression in USA, but it has psychiatric-like symptom and a potential for addiction. Therefore, its use is restricted. Recent clinical studies demonstrated that psilocybin known as a serotonin 5-HT_{2A} receptor (5-HT2A) agonist as well as a psycedelic also has a therapeutic effect to treatment-resistant depression although its mechanisms remains unclear. Therefore, we investigated that mechanisms involved in antidepressant effect of a 5-HT2A agonist. We demonstrated that a 5-HT2A agonist showed the anti-depressant effect in mice, which occurred in a dose-dependent manner. Further, acute injection of a 5-HT2A agonist increased the c-Fos-positive cells in GABAergic neurons in the lateral septum of mice, which was suppressed by pre-treatment of a 5-HT2A antagonist. These results suggest that a 5-HT2A agonist may have an antidepressant effect through the activation of GABAergic neurons in the lateral septum.

Key Words：serotonin 5-HT_{2A} receptor, depression, psychiatric disorder, lateral septum

Introduction

Depression (major depressive disorder or clinical depression) is a common but serious mood disorder. It causes severe symptoms that affect how you feel, think, and handle daily activities, such as sleeping, eating, or working. To be diagnosed with depression, the symptoms must be present for at least two weeks. A various antidepressant have been developed for many decades. However, about 30% of the patients are considered treatment resistant, and will continue to depressive symptoms despite the optimal use of available antidepressants. Ketamine, a NMDA antagonist, has been available as an antidepressant for treatment-resistant depression in USA. The antidepressant effect of ketamine occurs rapid-acting and long-lasting, but it also has aversive effect such as psychiatric-like symptom and a potential for addiction. Recent clinical studies reported that 5-HT2A agonist also has rapid-acting and long-lasting anti-depressant effect[1]. Further, occurrence frequency of 5-HT2A agonist adverse effect such as hallucination would be less than ketamine[2] although the molecular mechanisms underlying antidepressant effect of 5-HT2A agonist remains unclear. Here, we investigated about mechanisms of a 5-HT2A agonist antidepressant effect.

Results

We examined the effect of antidepressant effect of 5-HT2A agonists in mice, for which the forced-swim test was employed. The immobility time of mice in FST was shorten after 24 hr after acute treatment of a 5-HT2A agonist, DOI, which was inhibited by a 5-HT2A antagonist, volinanserin (Fig. 1).

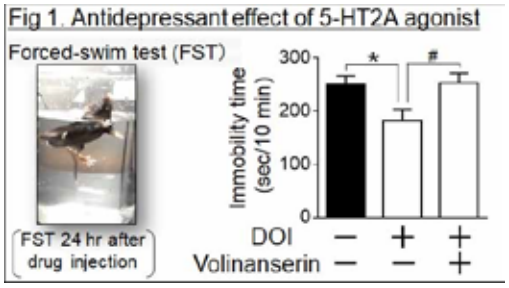

Next, we investigated the brain region involved in the antidepressant effect of 5-HT2A agonists, for which mice with 5-HT2A agonist treatment were sacrificed for c-Fos staining 60 min after FST. We found that increase in the number of c-Fos-positive cells in GABAergic neurons of the lateral septum (LS) of mice treated with DOI, which was also suppressed by volinanserin (Fig. 2).

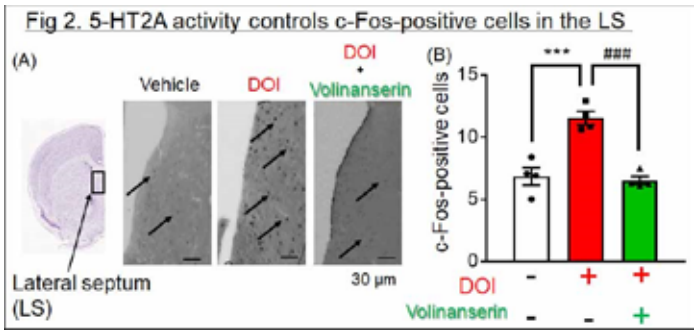

Discussion & Conclusion

Together with the results as described above, the shorten immobility time in FST and increase in the number of c-Fos-positive cells in the LS after FST occur dependency of 5-HT2A stimulation, suggesting that antidepressant effect of 5-HT2A agonist is associated with activation of GABAergic neurons in the LS. Thus, the lateral septum activation may inhibit the brain region projected from lateral septum, for which further study is required. Ketamine that has therapeutic effect for treatment-resistant depression has some problem such as psychosis-like behavior as well as the limitation of the route of administration[3]. So, new therapeutic strategy is required instead of ketamine. Given that occurrence frequency of 5-HT2A agonist adverse effect such as hallucination would be less than ketamine[2], 5-HT2A may be available for a new target of treatment-resistant depression.

References

1. Carhart-Harris RL, Bolstridge M, Rucker J, Day CM, Erritzoe D, Kaelen M, Bloomfield M, Rickard JA, Forbes B, Feilding A, Taylor D, Pilling S, Curran VH, Nutt DJ. Psilocybin with psychological support for treatment-resistant depression: an open-label feasibility study. *Lancet Psychiatry* 3:619-627, 2016.
2. Reiche S, Hermle L, Gutwinski S, Jungaberle H, Gasser P, Majić T. Serotonergic hallucinogens in the treatment of anxiety and depression in patients suffering from a life-threatening disease: A systematic review. Prog *Neuropsychopharmacol Biol Psychiatry* 81:1-10, 2018.
3. Berman RM, Cappiello A, Anand A, Oren DA, Heninger GR, Charney DS, Krystal JH., Antidepressant effects of ketamine in depressed patients. *Biol Psychiatry* 47:351-4, 2000.

一般の皆様へ

うつ病患者の30％は既存の抗うつ薬が効きにくい難治性である。最近の臨床研究から幻覚薬でセロトニン5-HT_{2A} 受容体（5-HT2A）刺激薬のシロシビンが、難治性うつ病患者に対して、即効的かつ持続的な抗うつ作用を示した。そこで我々は、5-HT2A 刺激薬による抗うつ作用についてマウスを用いて調べたところ、5-HT2A 刺激薬は、うつ病モデルマウスにおいて、即効的かつ持続的な抗うつ作用を示した。さらにその作用には外側中隔核における GABA 神経の活性化が関与していることが証明された。本研究によりうつ病治療における5-HT2A 刺激薬の有用性が示されれば、本研究が新たな抗うつ研究の礎となることが期待できる。

RopGEF in the regulation of planar cell polarity in plants

Teh Ooi Kock
okteh@oia.hokudai.ac.jp
Hokkaido University

Summary Abstract

This research proposal addresses the involvement of ROP guanine nucleotide exchange factor (RopGEFs) in the regulation of planar cell polarity (PCP). Using homologous recombination technology, we generated single knock-out mutants for all six RopGEFs (RopGEF1~RopGEF6) in Physcomitrella patens. We found that ropgef1 showed multiple and misplaced protonema protrusions. This suggests that RopGEF1 has a direct role in the regulation of PCP. In the future, we will focus on the molecular mechanisms of RopGEF1 in mediating moss protonema PCP.
Key Words：Physcomitrella patens, RopGEF, planar cell polarity

Introduction

One of the major unanswered questions in developmental biology is how multicellular organisms take its shapes by coordinating and integrating internal as well as external environmental cues. An essential feature of multicellular organisms is their ability to undergo cellular differentiation and polarized growth within the plane of a cell sheet-this planar morphogenesis is termed “planar cell polarity (PCP)[1]”. The underpinning hypothesis of this proposal is: PCP signaling pathways in plants are analogous to that in the animals but involved distinctively different players. We propose that RopGEFs modulate moss PCP by relaying auxin-dependent signals from upstream receptors to downstream effectors via regulation of membrane trafficking steps.

Results

The moss genome encodes 6 RopGEFs, RopGEF1~ RopGEF6. To determine which RopGEF(s) are involved in the moss PCP, we generated single knock-out mutants for all RopGEFs. We are surprised to find that only ropgef1 mutant showed compromised PCP, with multiple protrusions emerged within a single protonema cells. More importantly, the positions of these new protrusions are misplaced and switched from apical-end to middle- or basal-end. The following figure shows representative images of protonemata from ropgef1 and ropgef2. Arrow heads indicate the apical-end of cells where protrusions normally emerged in wild-type.

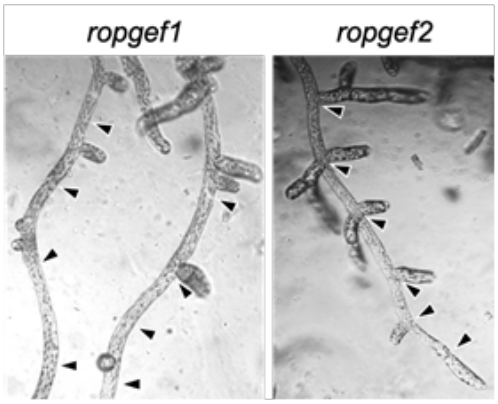

We also attempted to generate yellow fluorescent protein (YFP)-fused reporter lines for all the RopGEFs. YFP N-terminal fusions of RopGEFs, YFP-RopGEFs driven by an overexpression promoter did not produce any detectable signal. This hampers our subsequent effort to perform live cell imaging and co-immunoprecipitation experiments.

Discussion & Conclusion

Although the ROP signaling pathway has been implicated in the polarized tip growth of Arabidopsis root hair, its roles remain obscure in the basal land plant. Our genetic evidence demonstrates that RopGEF1 is the only RopGEF necessary to mediate PCP in Physcomitrella patens. Whether other RopGEFs have redundant or overlapping functions with RopGEF1 remains to be determined through analyses of double mutants. Failure to observe fluorescence in our YFP-RopGEFs reporter lines suggests that the N-terminal of RopGEFs may be involved in post-translational modification for membrane anchorage. Obstructing this anchorage by fusing a fluorescent protein may therefore hinder the RopGEF attachment to cell surface and inhibits its subsequent functions.

References

1. Devenport, D. The cell biology of planar cell polarity. *Journal of Cell Biology* (2014). doi:10.1083/jcb.201408039

一般の皆様へ

Our study highlights the importance of ROP signaling pathway in the regulation of body plant development in early land plants.

（我々の研究は初期陸上植物の植物体の発生調節における ROP シグナル伝達経路の重要性を強調している。）

A novel oxytocin neuronal system for regulating lactating behavior in mice

Yoshikage Muroi
muroi@obihiro.ac.jp
Obihiro University of Agriculture and Veterinary Medicine

Summary Abstract

Mammalian dams nurture their pups by lactation. In this study, we examined whether oxytocin is involved in regulating nurturing behavior in a nutritional state-dependent manner. We found a novel function of oxytocin to facilitate nurturing behavior under negative energy conditions. Oxytocin acts in the dorsal raphe nucleus. In addition, oxytocin may be released from the paraventricular nucleus of the hypothalamus in response to presentation with pups outside the nest under mildly negative energy conditions. Our data suggest that oxytocin facilitates milk delivery to pups by the behavioral control as well as milk ejection even under negative energy conditions.
Key Words：oxytocin, nurturing behavior, dorsal raphe nucleus, paraventricular nucleus

Introduction

Mammalian newborns, which can obtain energy only from milk before weaning, are delivered prematurely. Mothers need to partition their energy for the survivals of themselves and their pups. Nurturing behavior as well as milk production in mammary gland is suppressed under food-restricted conditions. These biological responses are understood as a self-defense from energy deficiency. However, dams do not abandon their pups even under negative energy states. In the present study, we examined how dams can continue to display nurturing behavior under negative energy conditions.

Results

To examine whether nurturing behavior alters in dependence on energy states of dams, we first compared the effect of different period of fasting on nurturing behavior. The fed dams or 3-h-fasted dams displayed nurturing behavior including nest maintenance, retrieval of pups into the nest, and crouching over the pups during the behavioral test. In contrast, 4-h-fasted or 8-h-fasted dams decreased the display of nurturing behavior. Dams obtained 0.61 ± 0.05 g of food pellets for 3 h under fed conditions. These results means that dams display nurturing behavior, regardless of lacking energy intake for 3 h. To examine the involvement of oxytocin in the dorsal raphe nucleus (DRN) with nutritional state-dependent regulation of nurturing behavior, dams were treated with an oxytocin receptor antagonist, L-368899. The injection of 2 pmol L-368899 into the DRN did not affect all of the parameters for nurturing behavior in fed dams, compared to saline injection. However, L-368899 inhibited retrieving behavior and crouching behavior in 3-h-fasted dams. These results indicate that oxytocin in the DRN is required for displaying nurturing behavior under the 3-h-fasted, but not fed, condition. To confirm that oxytocin in the DRN has an antagonistic effect on the inhibition of nurturing behavior by food deficiency, oxytocin was injected into the DRN in 8-h-fasted dams. The injection of 100 pmol oxytocin into the DRN recovered nurturing behavior in 8-h-fasted dams. These results indicate that oxytocin in the DRN counteracts the inhibition of nurturing behavior under

negative energy conditions.

The paraventricular nucleus (PVN) and supraoptic nucleus (SON) in the hypothalamus are the major nucleus where oxytocin neurons are distributed. We asked whether oxytocin is released from the PVN and/or SON in response to presentation with pups following 3-h-fasting. In the immunohistochemistry, presentation with pups decreased the number of oxytocin-positive cells and the intensity of oxytocin-positive signals in the PVN of 3-h-fasted dams. To determine whether the decrease in the number of oxytocin-positive cells and the intensity of oxytocin-positive signals in the PVN, we investigated the changes in the content of oxytocin in the PVN by using enzyme-linked immunosorbent assay. Presentation with pups decreased the content of oxytocin in the PVN of 3-h-fasted dams. These results indicate that oxytocin may be released from the PVN in response to presentation with pups following 3-h-fasting. We investigated how oxytocin is released from the PVN. Because presentation with pups did not affect the concentration of oxytocin in the serum in 3-h-fasted dams, oxytocin is unlikely to be released as a hormone in response to presentation with pups under the 3-h-fasted condition. We next examined whether oxytocin is transported from the PVN into the DRN by the synaptic transmission. In the dams that were injected with a retrograde tracer fluorogold into the DRN, few oxytocin neurons were positive to fluorogold in the PVN, it is unlikely that oxytocin is transported from the PVN into the DRN by synaptic transmission.

Discussion & Conclusion

In the present study, we found that oxytocin in the DRN is required for displaying nurturing behavior under a mildly negative energy state in lactating female mice. Oxytocin recovered the display of nurturing behavior inhibited by 8-h-fasting. These results suggest that oxytocin in the DRN counteracts the inhibitory effect of fasting on the display of nurturing behavior. Oxytocin may be released from the PVN in response to presentation with pups under negative energy conditions. Oxytocin is likely to reach the DRN by the styles other than endocrine or synaptic transmission. Oxytocin may be released by volume transmission to diffuse from the PVN into the DRN. More researches are required for clarifying how oxytocin reaches from the PVN into the DRN.

一般の皆様へ

哺乳類の母親は乳で仔を育てます。エネルギーを失うことは自分の生存に不利なことですが、母親は授乳により自分のエネルギーを自ら進んで仔に分け与えます。本研究ではそんな母親の性質を司る仕組みを明らかにすることを目指しました。今回の研究で、低エネルギー状態でもオキシトシンが脳に作用することで母親は授乳し続けることがわかりました。これまでにオキシトシンは乳腺に作用し射乳を促すことがわかっていましたが、母親の行動にも影響し授乳を促すことが明らかになりました。オキシトシンが自己犠牲的なお母さんの性質の一面を担っていると考えられます。

Molecular mechanisms for the bifurcation of thymic epithelial cells

Izumi Ohigashi
ohigashi@genome.tokushima-u.ac.jp
Division of Experimental Immunology, Institute of Advanced Medical Sciences,
University of Tokushima

Summary Abstract

To better understand molecular mechanisms that govern the differentiation and development of cortical thymic epithelial cells (cTECs) and medullary TECs (mTECs) in the thymus, we carried out omics analysis of these epithelial cells. Here we report the transcriptome and proteome profiling of TECs. We also report the functional significance of a molecule that is highly expressed in cTECs than mTECs in the thymus.
Key Words：Thymus, Thymic epithelial cells

Introduction

cTECs and mTECs characterize T cell-producing and -selecting functions of the thymus. We have previously reported that cTECs and mTECs are derived from bipotent TEC progenitors that transcribe beta5t, which is a component of thymoproteasome specifically expressed in cTECs and important for the positive selection of CD8T cells[1-3]. However, molecular mechanisms regulating the development of bipotent TEC progenitors into cTECs and mTECs is unclear. In this study, we aimed to better understand molecular mechanisms that govern the differentiation and diversification of bipotent TEC progenitors into cTECs and mTECs.

Results

We carried out transcriptome and proteome analysis of cTECs and mTECs isolated from wild-type mice and compared those profiles. We also compared profiles between wild-type cTECs and beta5t-deficient cTECs. We found that transcriptomic and proteomic profiles were sharp contrast between cTECs and mTECs, whereas those are similar between wild-type cTECs and beta5t-KO cTECs. However, proteomic profiles exhibited the reduction of proteasome components in protein amount in cTECs by beta5t-deficiency. We also confirmed the reduction of proteasome components in beta5t-deficient cTECs by western analysis and flow cytometry analysis. On the other hand, constitutive stress response, which was reported to be ignited by proteasome deficiency, was not observed in beta5t-deficient cTECs, indicating a highly specific impact of beta5t on proteasome subunit composition in cTECs, rather than a pervasive effect on cTEC functions (submitted to *Cell Reports*). Next, we isolated transcriptional regulators that showed significant difference in the expression between cTECs and mTECs in omics profiles, to identify the responsible molecules regulating the differentiation and development of cTECs and mTECs. We examined thymuses isolated from several kinds of deficient mice of molecules. Among them, we found that the systemic deficient mice of a molecule that belongs to homeobox transcription factor and is highly expressed in cTECs than mTECs exhibit thymus hypoplasia and reduced expression of functional cTEC-molecules. However, the expression of this transcription factor is ubiquitous. Therefore, to examine the impact of this

transcription factor in TEC specifically, we are currently generating conditional deficient mice. In addition to this homeobox transcription factor, we focused on Pithd1 that is highly detected in cTECs than mTECs. It has been reported that Pithd1 regulates the transcription of Runx1 resulting in the regulation of megakaryocyte differentiation in *in vitro*[4]. Furthermore, Pithd1 has a putative domain capable of interacting with proteasome. However, the functional significance of Pithd1 in *in vivo* is unknown. We first examined the expression of Pithd1 in the thymus and several other tissues. We confirmed that Pithd1 is highly expressed in cTECs than other thymic cells, including mTECs, and other tissues. Additionally, highly expression of Pithd1 was detectable also in testis. We next examined the proteasome interacting capability of Pithd1. Immunoprecipitation followed by immunoblotting analysis showed that Pithd1 is incapable of interacting with thymoproteasome in cTECs. On the contrary, Pithd1 was able to interact with proteasome expressed in testis. Then, we next generated Pithd1-deficient mice to examine the role of Pithd1 in *in vivo*. We found that the organization of cortical and medullary microenvironment was not disturbed by Pithd1 deficiency. We also found that the differentiation and development of cTECs as well as T cell development in the thymus was not impaired in Pithd1-deficient mice. These results indicate that Pithd1 is dispensable in the development and function of cTECs. On the other hand, we noticed that Pithd1-deficient male mice are infertile. Then, we carried out the detail analysis of sperm isolated from Pithd1-deficient mice. Pithd1-deficient sperm exhibited the abnormal morphology and impaired motility. Furthermore, *in vitro* fertilization assay revealed that Pithd1-deficient sperm are disable to fertilize even in the cumulus free condition. Finally, we carried out proteome analysis of sperm isolated from wild-type mice and Pithd1-deficient mice. We found that the amount of proteins known to be involved in the male fertility is decreased in sperm from Pithd1-deficient mice. Therefore, these results indicate that Pithd1 is indispensable for the male reproductive system (manuscript under preparation).

Discussion & Conclusion

The omics analysis we carried out in this study revealed previously unknown quantitative profiles of unbiased proteomes in freshly isolated cTECs and mTECs. In combination of transcriptomic analysis with proteomic analysis, we could isolate several molecules that are differently expressed between cTECs and mTECs and are related to the transcriptional regulation. Among them, we are currently studying the role of a molecule that belongs to homeobox transcription factor. In addition to this, we are also studying the role of molecule that functions as transcriptional co-activator. Our omics data from cTECs and mTECs offer a useful resource for further exploration of the biology of TECs and their subpopulation. In this study, we also examined the functional significance of Pithd1 that was highly detected in cTECs than mTECs in omics analysis. Although no abnormalities were detected in the thymus, we unexpectedly detected male infertility in Pithd1-deficient mice. Pithd1-deficent sperm exhibited morphological abnormality. Especially, the frequency of sperm having multi heads was significantly increased in Pithd1-deficient mice compared to control mice. Our results will contribute to elucidating the mechanism for acquisition of male fertilization capability, and the development of therapeutic tool for male infertility.

References

1. Murata S, Sasaki K, Kishimoto T, Niwa S, Hayashi H, Takahama Y, Tanaka K. Regulation of CD8+T cell development by thymus-specific proteasome. *Science* 16:1349-1353, 2007.
2. Ohigashi I, Zuklys S, Sakata M, Mayer CE, Zhanybekova S, Murata S, Tanaka K, Hollander GA, Takahama Y. Aire expressing thymic medullary epithelial cells originate from β5t-expressing progenitors. *PNAS*. 110:9885-9890, 2013.
3. Ohigashi I, Zuklys S, Sakata M, Mayer CE, Hamazaki Y, Minato N, Hollander GA, Takahama Y. Adult thymic medullary epithelium is maintained and regenerated by lineage-restricted cells rather than bipotent progenitors. *Cell Rep*. 13:1432-1443, 2015.
4. Lu B, Sun X, Chen Y, Jin Q, Liang Q, Liu S, Li Y, Zhou Y, Li W, Huang Z. Novel function of PITH domain-containing 1 as an activator of internal ribosomal entry site to enhance RUNX1 expression and promote megakaryocyte differentiation. *Cell. Mo. Life. Sci*. 72:821-832, 2015.

一般の皆様へ

免疫の中枢器官である胸腺を構成する皮質、および、髄質上皮細胞は、生体防御に必須なT細胞の産生を担います。本研究では、皮質 / 髄質上皮細胞の分化を制御するメカニズムの解明を目指しました。上皮細胞の分化制御メカニズムを解明することは、将来、免疫不全症や自己免疫疾患の根本的治療法開発につながると考えられます。また、本研究を進める中で、胸腺上皮細胞で発現する遺伝子が精巣でも発現しており、生殖能獲得に重要であるという、予想外の結果を得ました。男性不妊発症のメカニズム解明や、治療法開発につながることが期待されます。

The role of Heat shock protein 40 Member C1 in hepatic lipid metabolism

Atsuko Nakatsuka
atsuko-n@md.okayama-u.ac.jp
Okayama University Hospital.

Summary Abstract

Recently non-alcoholic fatty liver disease is increasing worldwide. However, mechanisms of progression from simple fatty liver to steatohepatitis (NASH) are not well explored. We focused on Dnajc1, which is one of 40 kDa heat shock proteins. In Dnajc1 null mice fed with high-fat high-sucrose diet, fatty liver was exacerbated with upregulation of fatty acid synthase and lipocalin 2 revealed by DNA microarray analysis. *In vitro* analysis, Dnajc1 activated AMPK, and inhibited JNK phosphorylation. GRP78/eIF4B and keratin were identified as Dnajc1 interactive molecules, respectively. Dnajc1 may be one of key molecules, that prevents fatty liver and a progression to NASH.

Key Words：Non-alcoholic fatty liver disease, Heat shock protein, Dnajc1,

Introduction

Heat shock protein (Hsp)s are known as molecular chaperones, which are involved in protein quality control, and categorized by their molecular weights. Hsps of 40 kDa (Hsp40s) is also known as DnaJ, and there are at least 50 homologs of HSP40s/DNAJ in human (1). We focused on Dnajc1, which we identified as 78 kDa glucose-regulated protein (GRP78)-interactive molecule on hepatocyte (2). However, roles of Dnajc1 in human pathophysiology and pathogenesis are not well investigated. In present study, we investigated beneficial effects and molecular mechanisms of Dnajc1 on non-alcoholic fatty liver diseases.

Results

1) Distribution of Dnajc1 protein in various organs of C57BL/6 mice.

We performed western blot analyses using multiple organ samples of C57BL/6 mice, and ubiquitous distribution of Dnajc1 was observed. Especially, Dnajc1 was heavily expressed in pancreas and visceral adipose tissues, and they were followed by stomach, liver and kidney. Dnajc1 was also detected in serum samples, suggesting that soluble form of Dnajc1 is secreted into blood.

2) Expression of Dnajc1 in cultured hepatocyte, HepG2 and H4-II-E-C3 cells.

We investigated the expression of Dnajc1 in cultured hepatocyte cell line, HepG2 and H4-II-E-C3 cells. In the presence of 100 nM insulin, 1μg/ml tunicamycin, 1 μM thapsigargin, and 500 μM palmitate, Dnajc1 protein increased. In immunofluorescence staining, insulin, tunicamycin, thapsigargin and palmitate increased intracellular punctate signals of Dnajc1 (Figure 1). Next, when H4-II-E-C3 cells were transfected with pcDNA3.1-Dnajc1 vectors, prominent intracellular vacuolar formations were observed (Figure 2), and Dnajc1 on vacuole was partially co-localized with a lysosomal membrane associated protein 2 (lamp2).

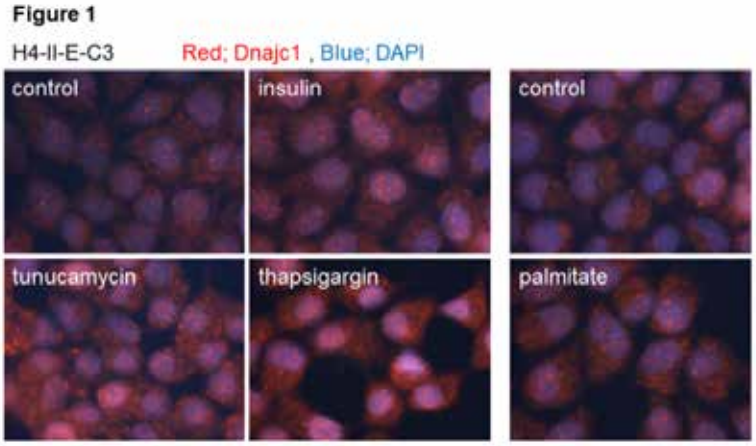

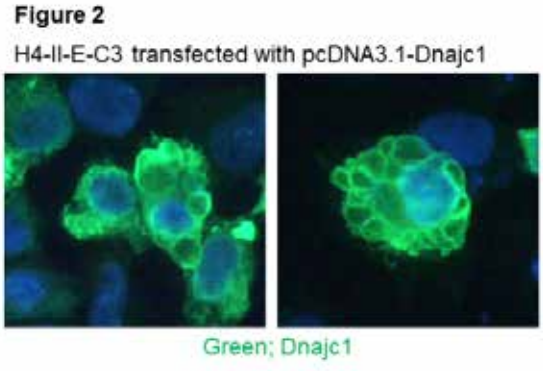

3) Fatty liver was exacerbated in Dnajc1-/- under high-fat high-sucrose (HFHS) diet.

Dnajc1 hepatocyte-specific null mice were generated by crossing floxed Dnajc1 mice with C57BL/6 transgenic mice expressing Cre recombinase under control of the albumin promoter. Dnajc1-/- and Djanc1+/+ mice were fed with HFHS diet or standard chow (STD), and at 25 weeks of age we obtained blood and liver samples. There was no difference of body weight gain and blood glucose levels between Dnajc1-/- and Dnajc1+/+. At 10 weeks of age, we performed intraperitoneal glucose tolerance test, and an area under the curve (AUC) of blood glucose in Dnajc1-/- was higher than Dnajc1+/+ under HFHS (40245±5952 vs 33313±2044 mg•hr/dL) with statistically significance, although there were no differences under STD. In insulin tolerance test, blood glucose levels were not altered between Dnajc1-/- and Dnajc1+/+. Food intake was also not altered between both groups. At 25 weeks of age, liver weight of Dnajc1-/- was heavier than Dnajc1+/+ under HFHS diet and fatty liver was histologically exacerbated in Dnajc1-/-.

In DNA microarray analysis using liver tissues, fatty acid synthase (FAS) was one of the top 5 upregulated genes in Dnajc1-/- compared with Dnajc1+/+. The expression of Lipocalin 2 (LCN2) also upregulated in Dnajc1-/-. Pathway analysis demonstrated that Dnajc1 was strongly associated with three pathways, *i.e.* metabolic pathway, pathway in cancer, and PI3-Akt pathway.

4) Dnajc1 enhance AMPK activation and inhibited phosphorylation of JNK.

We performed *in vitro* analysis using cultured hepatic cell line, H4-II-E3. Overexpression of Dnajc1 increased an expression of phosphorylated AMP-activated protein kinase (AMPK), and supressed phosphorylation of c-Jun N-terminal kinase (JNK).

5) Identification of Dnajc1 interactive molecules

We generated plasmid expressing p3xFLAG-Dnajc1 and cloned genes were transfected into HK2 cells. Soluble proteins were purified by anti-FLAG M2 affinity agarose gel and subjected to SDS-PAGE and Ag staining. Visible bands were excised and in-gel digested with trypsin and analyzed liquid chromatography-tandem mass spectrometry. As a result, several candidate molecules were identified as Dnajc1-interactive molecules; heat shock-related 70kDa protein 2 (HSP72), 78kDa glucose-regulated protein (GRP78), eukaryotic elongation initiation factor 4B (eIF4B), SCY1-like protein 2, importin-8, RL40, Ubiquitin-60S ribosomal protein L40, and keratin. We confirmed a binding of Dnajc1 to GRP78/eIF4B and keratin, respectively by immunoprecipitation and western blot analysis.

Discussion & Conclusion

Fatty liver and insulin resistance were exacerbated in Dnajc1-/- mice under HFHS diet. DNA microarray analysis showed that deficiency of Dnajc1 is associated with up-regulation of FAS and LCN2. These findings indicate that Dnajc1 protect against lipid accumulation and inflammation in liver. Now we are going to promote further investigations for insulin signaling, lipid metabolism, and inflammatory signaling.

Dnajc1 forms a complex with GRP78/eIF4B. It is known that eIF4B plays roles on mRNA cap-dependent translation initiation, and the decrease in eIF4B phosphorylation correlates with a decrease in cap-dependent translation (3). Kose S reported that Hsp70s are transported into nuclei during heat shock stress (4), therefore we speculate that Dnajc1/GRP78 complexes have roles in nulclei under metabolic or cellular stresses. Further investigations are required to confirm this hypothesis.

Dnajc1 also binds to keratin. Mallory-Denk bodies (MDBs) are cytoplasmic inclusions, found in various liver diseases. MDBs consist of intermediate filament proteins, keratins 8/18, ubiquitin, p62 and Hsps (5). Decrease of proteasome activity and/or impairment of autophagy are one of mechanisms that form MDBs, therefore we would like to investigate the relation of Dnajc1 and intracellular degradation systems, such as autophagy and ubiquitin-proteasome pathway. Other report demonstrated that keratin regulate FasR signaling through modulation of acin/ezrin interplay at lipid rafts in hepatocyte (6). Further investigation for a role of Dnajc1/keratin complex on Fas-induced apoptosis are needed.

References

(1) Kampinga HH, Hageman J, Vos MJ, et al., Guidelines for the nomenclasture of the human heat shock proteins. ***Cell Stress and Chaperons*** 14:105-111, 2009.

(2) Nakatsuka A, Wada J, Iseda I, et al., Vaspin is an adipokine ameliorating ER stress in obesity as a ligand for cell-surface GRP78/MTJ-1 complex. ***Diabetes***. 61(11):2823-2832, 2012.

(3) Dennis MD, Jefferson LS, Kimball SR. Role of p70S6K1-mediated phosphorylation of eI4B and PDCD4 proteins in the regulation of protein synthesis. ***J Biol. Chem*** 51:42890-42899, 2012.

(4) Kose S, Furuta M, Imamoto N. Hikeshi, a nuclear import carrier for Hsp70s, protects cells from heat shock-induced nuclear damage. ***Cell*** 149(3): 578-589, 2012.

(5) Hanada S, Harada M, Abe M, et al., Aging modulates susceptibility to mouse liver Mallory-Denk body formation. ***J Histochem Cytochem***. 60(6):475-483, 2012.

(6) Gilbert S, Loranger A, Lavoie JN, et. al., Cytoskeleton keratin regulation of FasR signaling through modulation of actin/ezrin interplay at lipid rafts in hepatocytes. ***Apoptosis***. 17(8):880-894, 2012.

一般の皆様へ

近年脂肪肝や脂肪肝炎が増加していますが、発症・進展のメカニズムについて未解明な部分も多くあります。細胞は生存・機能に必要な蛋白を合成しており、蛋白が正しい構造になるのを手助けする多種類の“シャペロン分子”が存在しています。近年、それぞれが、シャペロン機能とは無関係の、独自の「固有機能」を持つことが分かってきました。Dnajc1 はいまだ未解明な点が多い分子ですが、我々が以前の研究で、肝細胞の細胞質のみならず細胞表面にも存在し、糖脂質代謝に関係する可能性を見出したシャペロン分子の一つです。Dnajc1 は肝臓で糖代謝を改善させ、炎症を抑制する結果が得られました。さらに今後研究を進め、脂肪肝・脂肪肝炎の予防や治療に結び付けたいと考えています。

Novel strategy targeting neutrophils in the tumor microenvironment of colorectal cancer

Kenji Kawada
kkawada@kuhp.kyoto-u.ac.jp
Kyoto University, Department of Surgery,

Summary Abstract

SMAD4 is a key transcriptional factor of TGF-β signaling, and acts as a tumor suppressor in colorectal cancer (CRC). In the present study, we explored the immunological effect of SMAD4 on the tumor microenvironment.

We have shown that blockade of the CXCL1/8-CXCR2 axis and/or CCL15-CCR1 axis could be a novel therapeutic approach against SMAD4-negative CRC.

Key Words：colorectal cancer, SMAD4, CCR1, myeloid cells

Introduction

SMAD4 acts as a tumor suppressor in colorectal cancer (CRC), and loss of SMAD4 protein is associated with a poor prognosis. We previously reported that loss of SMAD4 in human CRC cells resulted in the up-regulation of CCL15, which caused the recruitment of $CCR1^{+}$-myeloid cells via the CCL15-CCR1 axis to facilitate tumor invasion and metastasis. In the present study, we explored the immunological effect of SMAD4 on the tumor microenvironment.

Results

1. CXCL1/8-CXCR2 axis

Given that myeloid cells express several types of chemokine receptors, we hypothesized that the recruitment of myeloid cells could be taking place in the tumor microenvironment via chemokine receptors other than CCR1.

Human CRC cell lines, SW837 and Caco2, express wild-type SMAD4. To identify the determinants responsible for neutrophil infiltration, we conducted a chemokine array containing a panel of chemokines using the *SMAD4*-knockdown cells. We found that loss of SMAD4 from human CRC cells (SW837 and Caco2) resulted in a significant increase of CXCL1 and CXCL8 expression, which was associated with the recruitment of neutrophils via CXCR2. In turn, when neutrophils were exposed to the supernatant of SMAD4-negative CRC cells (SW837), they produced a large amount of CXCL1 and CXCL8 *in vitro.*

In human clinical specimens, we found that neutrophil infiltration into the peritumoral stroma was more marked in SMAD4-negative CRC compared to that in SMAD4-positive CRC, and that both CXCL1 and CXCL8 were abundantly expressed in the tumor-infiltrating neutrophils. We further found that the neutrophils isolated from primary CRC expressed significantly higher levels of CXCL1 and CXCL8 than did those isolated from peripheral blood. Furthermore, we next characterized the tumor-infiltrating neutrophils using double immunofluorescence staining, and found that the majority of tumor-infiltrating neutrophils were $CXCR2^{+}$, and expressed MMP2 and

MMP9 in addition to ARG1 and IDO.

We measured the levels of CXCL1 and CXCL8 in serum samples from CRC patients (n = 125) and healthy donors (n = 11) by ELISA. Serum CXCL8 level was significantly higher in CRC patients that in controls (median, 13.7 vs. 2.9 pg/mL; $P < 0.01$), whereas the serum CXCL1 level was significantly lower in CRC patients (median, 8.8 vs 100.4 pg/mL; $P < 0.01$). We then investigated the serum CXCL8 level by the stage-based classification, and found it was significantly increased at Stage II/III and then decreased at Stage IV. To evaluate the clinical outcome, we analyzed the OS and RFS of the 125 CRC patients. Statistical analysis indicated that the CRC patients with high CXCL8 level exhibited a shorter overall survival and relapse-free survival compared to those with low CXCL8 level, although not a significant difference ($P = 0.07$ and 0.08, respectively). In particular, the Stage II/III cases with high CXCL8 level exhibited a significantly shorter OS compared to those with low CXCL8 level ($P = 0.04$). On the other hand, there was no association between the CXCL1 concentration and prognosis.

2. CCL15-CCR1 axis

Regarding the CCL15-CCR1 axis, we investigated the effect of CCR1 deletion on stromal and hematopoietic cells in mouse models. We used MC38 cells (for primary CRC model) and CMT93 cells (for liver metastasis model).

First, we injected tumor cells into the syngeneic C57BL/6 mice, and found that tumor development was strongly impaired into the CCR1-knockout mice compared to control mice in MC38 and CMT93 cells.

Next, to delineate the contribution of CCR1 on myeloid cells compared to non-hematopoietic cells, we performed bone marrow (BM) chimera experiments in which sublethally irradiated mice were reconstituted with CCR1-deficient BM. After tumor cell inoculation, CCR1-/- recipient mice showed significantly decreased tumor burden in MC38 (primary CRC model) and CMT93 cells (liver metastasis model).

Finally, we have investigated the effect of anti-CCR1 antibody in mouse moldels. We developed a new anti-CCR1 antibody, and so we have tested the effect of this antibody *in vivo.*

Discussion & Conclusion

Regarding the project of CXCL1/8-CXCR2 axis, our data suggest that blocking the CXCL1/8-CXCR2 axis may provide the possibility of a novel therapeutic strategy for SMAD4-negative CRC. CXCR2 and its ligands are responsible for recruiting neutrophils under physiological conditions and have been implicated in tumor-associated neutrophil mobilization. Notably, pharmacological inhibitors of CXCR1/2 are already used in clinical trials of inflammatory diseases (e.g. rheumatoid arthritis, asthma, and chronic obstructive pulmonary disease) as well as certain cancers (e.g. melanoma and breast cancer)

Regarding the project of CCL15-CCR1 axis, our data indicated that CCR1 deletion on hematopoietic cells could suppress CRC progression in mouse models. CCR1 antagonists could be a promising therapeutic strategy to prevent CRC.

References

•Ogawa R, Yamamoto T, Hirai H, Hanada K, Kiyasu Y, Nishikawa G, Mizuno R, Inamoto S, Itatani Y, Sakai Y, Kawada K.
“Loss of SMAD4 promotes colorectal cancer progression by recruiting tumor-associated neutrophils via CXCL1/8-CXCR2 axis” Clin Cancer Res. 2019 Jan 31. doi: 10.1158/1078-0432.CCR-18-3684. [Epub ahead of print]

一般の皆様へ

大腸癌に対する新規治療法として、腫瘍微小環境にある宿主因子である骨髄球、とくに好中球に着目して研究を進めています。マウスモデルや臨床検体を用いて検討してきた結果、ケモカイン受容体である CCR1 と CXCR2 がとくに重要なターゲットになり得ることを明らかにすることができました。臨床の現場で役立つところまではもう少し時間がかかるとは思いますが、さらに研究を進めていけたらと考えています。

Evolution of sex determination systems

Yusuke Takehana
y_takehana@nagahama-i-bio.ac.jp
Nagahama Institute of Bio-Science and Technology

Summary Abstract

To understand the molecular mechanism underling the XY-ZW transitions, we analyzed sex chromosomes and sex-determining genes of medaka species. We found that duplicated copies of *Dmrt1* at the Y chromosomes were required for male determination in the XY species, *Oryzias haugiangensis*. Although no sex-determining gene was isolated in the ZW species, *O. hubbsi* or *O. javanicus, Gsdf* was not a conserved downstream component of male determination pathway in *O. hubbsi.* These results suggest that sex-determining genes have more diverse downstream targets between XY and ZW systems than previously thought.
Key Words：Sex-determining genes / Sex chromosome / Medaka fishes

Introduction

Sex chromosomes harbor a primary sex-determining signal that triggers sexual development of the organism. However, independent evolution of sex chromosomes is widespread in non-mammalian vertebrates, suggesting that sex determination mechanisms are regulated by different genes and have evolved rapidly. Medaka fishes in the genus *Oryzias* have different sex chromosomes with different systems (XY and ZW), providing ideal condition for investigating the mechanisms that lead to the rapid turnover of sex chromosomes. In this study, we analyzed sex determination genes and pathways in both XY- and ZW-species to understand the molecular mechanism underling the XY-ZW transitions.

Results

In *Oryzias haugiangensis* having XY system, we found *Dmrt1* gene at its sex-determining locus on Chr 10. Fluorescence *in situ* hybridization analysis showed that a BAC clone containing *Dmrt1* gave a strong hybridization signal only on the Y chromosome, but not on the X chromosome. In addition, weak signals were obtained at the subtelomeric region of a chromosome pair that is equivalent to Chr 9 (autosome), suggesting multiple duplicated copies of *Dmrt1* only on the Y chromosome. Quantitative-PCR assay indicated approximately 10 copies of *Dmrt1* genes on the Y chromosome, confirming its multiple array. Furthermore, *Dmrt1* shows higher expression exclusively in XY individuals at hatching day (the sex-determining period). Then we knockout the *Dmrt1* using CRIPSR/Cas system to determine its sex determining function. XY individuals having multiple mutations on Y chromosomal *Dmrt1* developed as female, suggesting that *Dmrt1*Y was required for male development.

In *O. hubbsi* and *O. javaniucs*, both species have ZW system but their sex chromosomes are not homologous (Chr 5 and Chr 16, respectively). Based on synteny analysis, we found several candidate genes on their sex chromosomes, and knocked out these genes using CRIPSR/Cas system. However, no sex reversal phenotype was observed in any genes, suggesting unknown genes at their sex-

determining loci. Then we sequenced whole genome of *O. javanicus* to obtain a reference genome sequence in the javanicus species group. Complementary sequencing approaches including long-read technology and data integration with a genetic map allowed the final assembly of 908 Mbp of the *O. javanicus* genome. Further analyses estimate that the *O. javanicus* genome contains 33% of repeat sequences and has a heterozygosity of 0.96%. The achieved draft assembly contains 525 scaffolds with a total length of 809.7 Mbp, a N50 of 6.3 Mbp and a L50 of 37 scaffolds. We identified 21454 expressed transcripts for a total transcriptome size of 57,146,583 bps. To detect sex chromosome-specific region and isolate candidate genes for sex determination, we are now sequencing haploid individuals having either Z or W chromosome in both species.

In *Oryzias, Gsdf* is considered to be a key component of the male determination pathway, because *Dmy* and $Sox3^{Y}$ have evolved as the master sex-determining gene by activating the downstream *Gsdf* in *O. latipes* and *O. dancena* respectively. In addition, *Gsdf* itself has evolved as male determining gene in *O. luzonensis*. These findings suggests that *Gsdf* is the conserved downstream components and *Gsdf* itself or its potential transcriptional regulators might have been generated a novel sex determination pathway. In fact, we obtained sex reversal XY females in homozygous mutants of *Gsdf* in the XY species, *O. dancena*, which was a close relative of *O. hubbsi*. On the other hand, we found that *Gsdf* is not required for male determination in *O. hubbsi*, having a ZW system. In the homozygous mutants of *Gsdf*, ZW fish developed as females having ovary and ZZ as males having testis although they showed excessive proliferation of germ cells, demonstrating that *Gsdf* is not required for male determination in this ZW species. This *Gsdf*–independent male determination system suggests other contributors to generate novel sex determination pathway in ZW system.

Discussion & Conclusion

Our data suggest that duplicated copies of *Dmrt1* on the Y chromosome is the sex-determining gene of the XY species, *O. haugiangensis*. Similar situation is also observed in *O. latipes* because its sex-determining gene, *Dmy* is the Y chromosome-specific duplicated copy of *Dmrt1*. These findings suggest that duplications and subsequent functional divergences of *Dmrt1* have contributed to generate new sex-determining genes independently in *O. latipes* and *O. haugiangensis*.

As for their sex determination pathway, we found that *Gsdf* was not a conserved downstream component of male determination pathway at least in the ZW species, *O. hubbsi*. This indicates that downstream target of its sex-determining gene was different from that of other XY species. These results suggest that sex-determining genes have more diverse downstream targets between XY and ZW systems than previously thought.

一般の皆様へ

ほとんどすべての動物にオス・メスがあるのと対照的に、オス・メスを決定する仕組みは動物種によってさまざまです。しかし、この性決定の仕組みがどのように多様化してきたのかは、ほとんどわかっていません。今回の研究により、メダカ属という近縁なグループ内で、下流遺伝子の重複転座によって異なる性染色体が独立に進化してきたことや、XY 型と ZW 型で性決定遺伝子の作用点が異なることを示すことができました。これらの成果は、性決定の仕組みが（従来考えられてきたよりも）さらに多様である可能性を示唆しています。

Design principle for specific chemical probes toward 3D neuropathology

Kazuki Tainaka
kztainaka@bri.niigata-u.ac.jp
Brain Research Institute, Niigata University

Summary Abstract

Current biopsy and histology have long depended on sectioned 2D images with various chemical staining methods and specific immunohistochemistry. Facile 3D visualization of human brain tissue with high resolution would provide a novel concept of the neuropathological diagnosis and contribute our understanding of pathological mechanisms based on comprehensive and quantitative analysis of individual biomarker. In this project, we aimed at establishing a novel 3D neuropathology by developing a highly efficient clearing protocol for human brain tissue and combining with specific chemical probes to visualize specific targets.
Key Words：Tissue clearing, 3D imaging, Chemical probes, 3D neuropathology

Introduction

Comprehensive analysis of pathological molecules (e.g. Senile plaques, pTau, α-synuclein) in human brain tissue would accelerate our understanding of molecular bases in neurodegenerative diseases. Three-dimensional (3D) imaging based on tissue clearing technique that are compatible with various fluorescent labeling techniques are promising approaches. Recently, we have developed a whole-brain/body clearing and imaging method, termed CUBIC (Clear, Unobstructed Brain/Body Imaging Cocktails and Computational analysis)[1,2]. However, to establish tissue-clearing based 3D neuropathology, we have to 1) improve clearing performance for human brain tissues and to 2) discover chemical probes compatible with tissue clearing protocols.

Results

In this study, we applied a strategy for designing hydrophilic chemical cocktails optimized for delipidation and refractive index (RI) matching step. To achieve the scalable clearing of human brain tissue samples, we considered a high-throughput chemical screening system for delipidation and RI matching.

In delipidation, the lipid solubility of a chemical is roughly and inversely correlated with the turbidity of a fixed brain suspension treated with the chemical1. Thus, we obtained lipid solubility scores from the OD600 of a mixture of brain suspension and each chemical solution. To determine the effective chemical parameters for delipidation, we conducted comprehensive chemical profiling by using a multivariate linear regression model. Our model revealed logP (octanol/water partition-coefficient) to be the most influential property. Actually, the LS score of less polar amines was linearly correlated with their logP. Therefore, water-soluble, relatively hydrophobic, and uncharged amine derivatives had the potential for high lipid solubility. Next, we measured the residual phospholipid and cholesterol contents of mouse brains treated with the chemicals, and evaluated the

relative transmittance of these brains after RI matching. The delipidation efficiency, especially for the phospholipid content, was correlated with the final tissue transparency, indicating that delipidation is essential for thorough tissue clearing. Importantly, the logP value of these chemicals could predict the final transparency of the chemically treated brain.

To clarify whether the RI value of the medium itself is important for the final transparency or whether specific chemical groups are important for RI homogenization, we used a non-biased approach to determine the best RI-matched chemicals. To develop an alternative high-RI medium based on hydrophilic chemicals, we selected candidate chemicals that had high water solubility and a high RI value per unit weight, because the RI value of aqueous medium increases according to the solute concentration. Chemical profiling of the RI values of 10% chemical solutions with an Abbe refractometer revealed that aromatic groups exhibited higher RI values among the chemical groups. We chose 21 extremely water-soluble RI-matching candidates, whose RIs ranged from 1.47 to 1.52. To examine the clearing performance of these chemicals qualitatively, the OD600 of small pieces of chemically treated mouse lung was measured. The RI values of the mounting medium showed no correlation with the tissue transparency, suggesting that the clearing performance does not depend solely on the RI value of the medium but also reflects some chemical properties of the constituent. We further applied the multivariate linear regression model to this result. Interestingly, the amide group showed a significantly higher clearing performance than the other chemical groups.

Through the combinatorial evaluation by using biological tissues, we identified effective delipidation cocktail composed of *N*-butyldiethanolamine and Triton X-100 (CUBIC-L) and RI matching cocktail composed of nicotinamide and antipyrine (CUBIC-R). Our new CUBIC protocol combined with CUBIC-L and CUBIC-R enabled sufficient clearing of human brain tissue including white matter3. However, we still had to 1) overcome optical issues in human brain tissues including the resulting brownish color of cleared sample and relatively strong autofluorescence from lipofuscin and other pigments, and to 2) discover chemical probes compatible with tissue clearing protocols. By further chemical screening of a series of oxidants and reductants for human brain tissues, we developed several bleach-CUBIC protocols enabling efficient anti-browning and photobleaching of autofluorescence in human brain tissues. Furthermore, we also screened over 200 chemical probes visualizing specific targets by using bleached brain samples. Finally, we achieved various kinds of specific chemical staining protocols including neurons, fibers, vascular structures, and senile plaques. Cleared brain samples by our protocol showed preserved subcellular microstructures, and most of the endogenous protein was retained after CUBIC clearing. In addition, our protocol also largely retained the antigenicity of the proteins.

Discussion & Conclusion

In this project, we described a strategy for developing hydrophilic chemical cocktails for tissue delipidation, and RI matching based on comprehensive chemical profiling. The chemical profiling revealed important chemical factors: salt-free amine with high logP for delipidation and aromatic amide for RI matching. Amine derivatives with high logP values are expected to be more cell-permeable and more miscible with hydrophobic lipids. Since highly delipidated tissues are regarded as protein-based biomaterials, it is plausible that hydrophilic aromatic amides contributed to RI homogenization due to their efficient solvation of protein backbone amides. The strategic integration of optimal chemical cocktails provided an effective clearing protocol for human brain tissues. This strategy represents a future paradigm for the rational design of hydrophilic clearing cocktails that can be used for large tissues.

By combining of bleach step, we finally enabled multicolor imaging of brain tissue samples. Comprehensive dye screening provided a series of specific chemical probes for neurons, fibers, vascular structures, and senile plaques. Our clearing and staining protocol would be expected to establish future 3D neuropathology.

References

1. Susaki EA, Tainaka K, Perrin D, Kishino F, Tawara T, Watanabe TM, Yokoyama C, Onoe H, Eguchi M, Yamaguchi S, Abe T, Kiyonari H, Shimizu Y, Miyawaki A, Yokota H, Ueda HR: Whole-brain imaging with single-cell resolution using chemical cocktails and computational analysis. Cell, 2014,157(3):726-739.
2. Tainaka K, Kubota SI, Suyama TQ, Susaki EA, Perrin D, Ukai-Tadenuma M, Ukai H, Ueda HR: Whole-body imaging with single-cell resolution by tissue decolorization. Cell, 2014, 159(4):911-924.
3. Tainaka K, Murakami TC, Susaki EA, Shimizu C, Saito R, Takahashi K, Hayashi-Takagi A, Sekiya H, Arima Y, Nojima S, Ikemura M, Ushiku T, Shimizu Y, Murakami M, Tanaka KF, Iino M, Kasai H, Sasaoka T, Kobayashi K, Miyazono K, Morii E, Isa T, Fukayama M, Kakita A, Ueda HR: Chemical Landscape for Tissue Clearing Based on Hydrophilic Reagents. Cell Rep., 2018, 24(8):2196-2210.e9.

一般の皆様へ

現在の神経病理学では、薄切標本に基づく２次元平面の病理学的解析が基盤となっていますが、平面の病理学的解析だけでは対処困難な多くの課題があります。私たちは、この課題を解決するために「立体的な脳組織を立体のままもれなく観察すること」を実現する、組織透明化技術に基づく３次元イメージング CUBIC を開発しました。今回の助成研究では、ヒト脳組織の高度な透明化に取り組むと共に、透明化手法に適用可能な種々の染色手法を確立しました。本手法を用いて、３次元画像に基づく病理診断技術の実現を目指します。

Molecular basis of osmoregulatory ionocytes

Hiroshi Miyanishi
miyanishi@cc.miyazaki-u.ac.jp
University of Miyazaki

Summary Abstract

The differentiation mechanisms of osmoregulatory ionocyte in gills are not fully understood. We focused on transcription factor foxi3 and concluded that foxi3 is necessary for differentiation of all-types of ionocytes in medaka. To identify novel target involved in ionocyte differentiation, we conducted comparative transcriptome analysis in specific FW- and SW-type ionoctes. According to the transcriptome analysis, we identified at least 20 genes involved in functional differentiation between FW- and SW-type ionocytes.

Key Words：Environmental adaptation, Osmoregulation, ionocyte, medaka,

Introduction

Teleost fishes maintain their body fluid osmolality at approximately one-third that of seawater regardless of whether they inhabit freshwater (FW) or seawater (SW). Then, regulation of Na+ and Cl- is of primary importance in adaptation of teleost fish to aquatic environments. Gill ionocytes (also referred to as mitochondrion-rich cells or chloride cells) are in maintaining the body fluid homeostasis, absorbing and excreting Na+ and Cl- in FW and SW, respectively. Therefore, ionocytes assume an important role for environmental adaptation in fish. However, the mechanisms of ionocyte differentiation and functional plasticity are largely unknown.

Results

In zebrafish, forkhead box I (foxi)3 is an important transcriptional factor involved in differentiation of FW-type ionocytes (1). However, zebrafish is stenohaline FW fish. Therefore, in euryhaline teleosts, little is unknown about the differentiation factor inducing functional expression to SW-type ionocyte. To clarify the localization of each medaka FOXI3 in all types of ionocytes, immunohistochecal analysis was applied in FW- and SW-acclimated medaka gills. FOXI3 localized in nuclei of all types ionocytes (Fig. 1). For functional analysis, we first performed foxi3 gene knockdown. Then approximately 90% embryos injected antisense oligo were died within 2-day post fertilization (dpf). In response to this result, foxi3 mRNA was injected in one-cell stage embryos in FW and SW medium. The number of ionocytes were significantly increased by FOXI3 mRNA over-expression (Fig. 2). For loss-of function analysis, we established in vivo conditional gene knockdown in developing embryos. Almost embryos survived in FW and SW by in vivo conditional

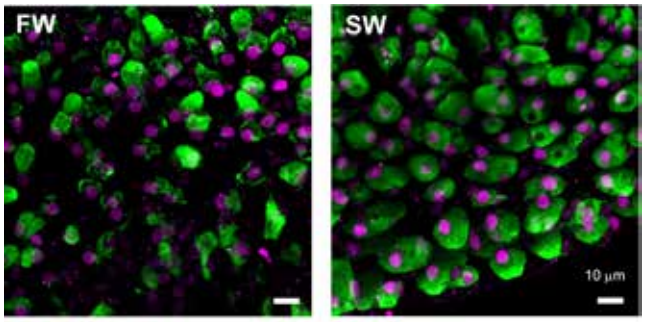

Fig.1 Immunohistochemical staining of Na/K-ATPase (Green) and FOXI3 (magenda) in FW and SW acclimated medaka gill.

gene knockdown of foxi3 from 2 dpf (ionocytes expressing stage). Then number of ionocytes significantly reduced by in vivo conditional gene knockdown of foxi3 from 2 dpf to 4 dpf. The body fluid osmolality of SW acclimated embryo was significantly increased by foxi3 knockdown although there were no significant differences between control group and knockdowned group in that of FW one. These results show that the transcription factor foxi3 is necessary for differentiation of all types ionocytes.

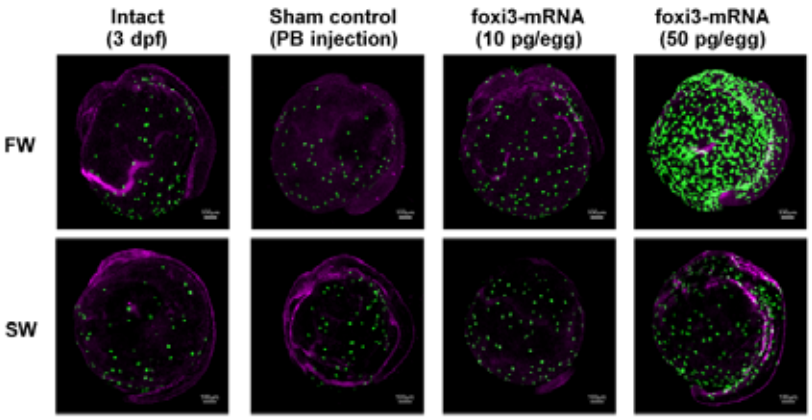

Fig. 2 Foxi3 gain-of-function in differentiation of ionocytes (green).

Foxi family consist foxi1, foxi2, foxi3 in vertebrates. In medaka, foxi1, 2 and 3 also were identified with whole genome data and PCR cloning. In medaka foxi family, only foxi3 was specifically expressed in gill. According to phylogenetic analysis of foxi family, teleost foxi3 genes were clustered with mammalian foxi1 genes. Therefore, it is highly possible that teleosts foxi3 was homologue of mammalian foxi1 involved in ion regulation of inner ear.

To identify novel target involved in ionocyte differentiation, we conducted transcriptome analysis in FW- and SW-type ionocte. We first established live tissue staining with mitobright for detection ionocytes under fluorescent observation in non-fixed frozen gill section. Thereafter, each FW- and SW-type ionocyte was collected using laser capture microdissection. The collected samples were analyzed by single cell RNA-seq. In total average, 51,029,046 reads and 20547 contigs were sequenced. According to comparative transcriptome analysis, the expression of 350 genes in SW-type ionocytes were more than 8 folds higher than in FW-type ionocytes. Meanwhile, the expression of 1357 genes in FW-type ionocytes were more than 8 folds higher than in SW-type ionocytes. In the 350 genes in SW-type ionocytes, the expression of at least 20 genes in ionocytes were significantly higher than control SW acclimated pavement cells in gills.

Discussion & Conclusion

We applied euryhaline medaka, *Oryzias latipes*, as model for studying mechanisms of inocyte differentiation. In this study, we concluded that the transcription factor foxi3 (mammalian foxi1 homologue) is necessary for differentiation of all types ionocytes in medaka. To identify novel target involved in ionocyte differentiation, we conducted comparative transcriptome analysis in specific FW- and SW-type ionoctes. According to the transcriptome analysis, we identified at least 20 genes involved in functional differentiation between FW- and SW-type ionocytes. Thus, we identified new target genes in this study. in addition, we established the molecular basis of osmoregulatory ionocytes for clarifying the mechanism of functional differentiation between FW- and SW-type ionocytes in the future.

References

[1] Guh YJ and Hwang PP (2017) Insights into molecular and cellular mechanisms of hormonal actions on fish ion regulation derived from the zebrafish model. *Gen Comp Endocrinol*, 251: 12-20.

一般の皆様へ

淡水と海水の両方で生きられる魚は、異なる塩分環境に適応するため、鰓に存在する塩類細胞の機能を、環境に合わせてイオンの取り込む（淡水中）、または排出（海水中）するように切り替えます。しかし、塩類細胞の分化および機能的可塑性に関する機構は分かっていません。まず我々は、転写因子 FOXI1 が、全てのイオン取り込み型および排出型の塩類細胞の分化に必須であることを証明しました。FOXI1 のさらに下流のシグナリングを明らかにするために、イオン取り込み型および排出型の塩類細胞特有の遺伝子プロファイルを明らかにしました。さらなる解析をとおして、なぜ魚が川や海で生きられるか？を明らかにするとともに、FOXI1 の関与が示唆されるヒトの難治性難聴の発症機序の基礎知見に繋げていきます。

Clarification of molecular mechanisms underlying the maintenance of satellite cell stemness and its therapeutic application for Muscular Dystrophy

Shinichiro Hayashi
shinhayashi@ncnp.go.jp
Department of Neuromuscular Research, National Institute of Neuroscience,
National Center of Neurology and Psychiatry

Summary Abstract

Muscle stem cells (MuSCs) cannot maintain their stemness in vitro. In this study, we focused on the mechanisms of maintenance of MuSC stemness regulated by a transcription factor Klf5. Klf5 knockout MuSCs showed high stemness properties in differentiation medium. By the retinoic acid treatment, Klf5 expression in MuSCs was decreased and MuSCs maintained their stemness in long-term culture. In addition, the efficacy of MuSC transplantation was significantly improved.
Key Words：Muscle stem cells, muscle differentiation, retinoic acid

Introduction

Skeletal muscle has a robust regenerative capacity, and the cell responsible for muscle regeneration is the Muscle stem cells (MuSCs, satellite cell). MuSC transplantation after in vitro expansion would be beneficial for the treatment of any muscle disease, particularly in the replacement of genetically defective muscle fibers such as those lacking dystrophin in patients with Duchenne muscular dystrophy (DMD). However, MuSCs rapidly lose their regenerative potential in culture. Therefore, in this research, we attempted to understand the molecular mechanisms underlying the maintenance of MuSC stemness.

Results

We have previously shown that the zinc finger transcription factor Klf5 is expressed temporarily during muscle regeneration and differentiation, and promotes muscle differentiation in cooperation with MyoD1[1]. These findings led us to analyze the role of Klf5 in MuSCs in the present study. First, we crossed $Pax3^{Cre/+}$ mice with $Klf5^{flox/flox}$ mice to generate muscle progenitor cell specific Klf5 knockout mice (Klf5cKO). Then we isolated MuSCs from Klf5cKO and control ($Klf5^{flox/flox}$) mice by fluorescence-activated cell sorting (FACS). Three days after induction of differentiation, although FACS sorted control MuSCs fused to form multinucleated myotubes, 35% of Klf5cKO cells failed to differentiate and maintained expression of Pax7, a stem cell marker of MuSCs. To further elucidate the functions of Klf5 in MuSCs, we analyzed transcriptome and epigenome in control and Klf5cKO MuSCs by RNA-seq and ChIP-seq. As we expected, gene ontology analysis revealed the genes whose expression was significantly reduced by loss of Klf5 were involved in the muscle structure development, myogenesis and muscle cell development. On the other hand, the genes associated with extracellular matrix organization and epithelial mesenchymal transition were upregulated in Klf5cKO MuSCs. Based on these findings, we hypothesized that when the expression of Klf5 is inhibited, MuSCs maintains their stemness.

Previously, it has been reported that retinoic receptor agonist Am80 inhibits Klf5 expression and transcriptional activity in smooth muscle cells[2]. To determine whether retinoic receptor agonists had an impact on Klf5 expression in MuSCs, different concentrations of Am80 or all-trans retinoic acid (atRA) were added to the culture medium. Consistent with the previous report, Klf5 expression was significantly decreased in MuSCs by retinoic receptor agonists. Immunocytochemistry also revealed that the proportion of Pax7 positive MuSCs was significantly increased by retinoid treatment. More than 80% of MuSCs expressed Pax7 even after 20 passages. On the contrary, the number of Myogenin positive differentiating myocytes was decreased by the treatment. It is known that atRA acts through binding to the RAR and RXR receptors, and each of which has three isoforms α, β and γ. To determine the role of these two receptor classes in atRA effect on MuSC stemness, we treated MuSCs with RAR agonists and RXR agonists. Treatment with RAR agonists, but not RXR agonists, inhibited muscle differentiation. We further investigated the effect of RARα, RARβ, and RARγ depletion on MuSC stemness by siRNA-mediated knock-down. We found that siRARα, but not siRARβ or siRARγ induced muscle differentiation when we treated atRA. These results indicate that atRA promotes MuSC stemness and inhibits differentiation through RARα.

We next investigated whether MuSCs expanded by atRA treatment could contribute muscle regeneration after transplantation. Human MuSCs were cultured with or without atRA and transplanted by intramuscular injection into the TA muscle of immuno-deficient mdx mice. Twenty-four hours before transplantation, TA muscles of recipient mice were injected with cardiotoxin to induce muscle damage. One month after transplantation, we investigated the contribution of transplanted cells to the regeneration of muscle tissue by detection of dystrophin+ fibers. Transplantation of MuSCs cultured with atRA produced significantly more dystrophin+ fibers than those cultures without atRA treatment. These data suggest atRA treatment enhances ability to contribute to muscle regeneration.

Discussion & Conclusion

Therapeutic approaches to both repair myofibers and repopulate the MuSC pool are required for DMD patients. MuSCs have great potentials in cell-based therapies to treat muscle diseases. However, conventional culturing condition cannot be utilized because MuSCs differentiate and quickly lost their abilities to regenerate muscles in vivo. In this study, we found that MuSCs from Klf5cKO showed highly resistance to differentiation. In addition, we found that atRA treatment inhibits MuSC differentiation and MuSC stemness was maintained through RARα. Transplantation of MuSCs treated with atRA efficiently contributed to the repair of muscle regeneration. Although atRA inhibits Klf5 expression in MuSCs, the relationship between Klf5 and retinoic acid is still unclear. Further studies are ongoing. In conclusion, we provide the evidences for an important role of the retinoic acid signaling in the regulation of maintenance of the stem cell state of MuSCs.

References

1. Hayashi S, Manabe I, Suzuki Y, Relaix F, Oishi Y. Klf5 regulates muscle differentiation by directly targeting muscle-specific genes in cooperation with MyoD in mice. Elife. 2016;5. pii: e17462.

2. Fujiu K, Manabe I, Ishihara A, Oishi Y, Iwata H, Nishimura G, Shindo T, Maemura K, Kagechika H, Shudo K, Nagai R. Synthetic Retinoid Am80 Suppresses Smooth Muscle Phenotypic Modulation and In-Stent Neointima Formation by Inhibiting KLF5. Circ Res. 2005 ;97(11):1132-41.

一般の皆様へ

遺伝性の筋疾患である筋ジストロフィーの根本的な治療法は未だ確立されていません。筋幹細胞を移植する方法が根治療法の一つとして期待されていますが、生体外で筋幹細胞の未分化性を保持したまま培養することが難しく、筋幹細胞の未分化性維持機構の解明が課題となっています。本研究では筋幹細胞の未分化性をレチノイン酸受容体アゴニストによって維持できること、また、そのシグナルは RAR α を介していることを明らかにしました。本研究をさらに進め、難治性筋疾患治療法開発に役立てたいと考えています。

III.

Reports from the Recipients of Grants for International Meetings

Report on Research Meeting

1. Name of Research Meeting / Conference
   Symposium on Molecular Chirality 2018

2. Representative
   Masami Sakamoto in Chiba University

3. Opening period and Place
   May 12 – 13, 2018
   Keyaki-Kaikan, Nishi-Chiba Campus, Chiba University

4. Number of participants / Number of participating countries and areas
   200 participants / 6 countries

5. Total cost
   ¥ 3,160,000

6. Main use of subsidy
   Venue setup cost and travel fee

7. Result and Impression

   We had good weather during the symposium, and about 200 people participated from six countries joined this meeting. A French Professor Coquerel of University of Rouen Normandie, the famous chemist on crystal chirality, had a lecture for dynamic crystallization of pharmaceutical materials leading to total optical resolution. The US Professor Sivaguru of Bowling Green State University introduced their latest results on the photochemical asymmetric reactions. Six Japanese invited speakers, Professor Tomooka of Kyushu University, Professor Suginome of Kyoto University, Professor Fujiki of Nara Institute of Science and Technology, Professor Nagasawa of Tokyo University of Agriculture and Technology, Professor Omatsu of Chiba University, and Professor Hayashi of Tohoku University, had special lectures for the latest research results on asymmetric synthesis, chiral supramolecules, CD spectroscopy, chiral laser science technology, and total synthesis of natural products. Furthermore, we had 16 other oral presentations and 65 poster presentations. We could provide a special forum for international information exchange and discussion on all fields related to "Molecular Chirality", such as “pharmacology, toxicity, pharmacokinetics of chiral compounds", "analysis and separation of chiral materials", "chiral detection", "optical resolution", "asymmetric synthesis", "chiral functional materials", "origin of chirality on Earth", "chiral compounds”, "Industrial production of industrial production". We hope that this symposium will contribute to the innovative development of research on chiral molecular chemistry.

8. Additional description

   We would like to express my gratitude for your support from the NOVARTIS Foundation (Japan) for the Promotion of Science.

Report on Research Meeting

1. Name of Research Meeting / Conference
   The 2nd research conference for the Research Society for Cancer 3-D culture

2. Representative
   Koji Okamoto, MD, PhD., Chief
   National Cancer Center Research Institute, Division of Cancer Differentiation

3. Opening period and Place
   2018, November 27, National Cancer Center Research Institute (Tokyo)

4. Number of participants / Number of participating countries and areas
   199 people (total)
   Japan (198), USA (1)

5. Total cost
   ¥ 1,688,000

6. Main use of subsidy
   Travel expenses for the foreign invited speaker, printing costs for poster and programs

7. Result and Impression
   The meeting was quite succeful in many aspects. There were many audiences with excellent talks and discussion. I would like to thank the Novartis foundation for invaluable supports.

8. Additional description

Report on Research Meeting

1. Name of Research Meeting / Conference
   International Consortium on Hallucination Research and Related Symptoms Kyoto SatelliteMeeting (ICHR 2018 Kyoto)

2. Representative
   Jun Miyata (Kyoto University)

3. Opening period and Place
   18-19 October, 2018 at Clock Tower Centennial Hall, Kyoto University

4. Number of participants / Number of participating countries and areas
   Participants: 71
   Countries/areas: 15

5. Total cost
   6,442,469JPY

6. Main use of subsidy
   Transfer expenses and accommodation cost for invited speakers

7. Result and Impression

   We had two keynote lectures, 3 symposia, 1 oral session and two poster sessions in the meeting.

   In the first keynote lecture on 18th, Prof. Renaud Jardri, Lille University, summarized current status of neuroimaging studies of hallucination, as well as latest results from his laboratory. He also introduced his latest work on circular inference model of psychotic symptoms including hallucination.

   In the second keynote lecture on 19, Prof. Pascal Belin, Institut de Neurosciences de la Timone, first talked about his monumental discovery of the auditory voice area. He then talked about his continuous work on human / animal voice perception.

   In the symposium 1 "Neurophysiology" on 18th, Dr. Yoji Hirano, Kyushu University, introduced his research on hallucination using EEG. Dr. Michio Koeda, the vice-president of this meeting from Nippon Medical School, talked about his research on hallucination using functional magnetic resonance imaging. Prof. Thomas Whitford, University of New South Wales, introduced his electrophysiological research on the origin of hallucination focusing on inner speech. Prof. Daniel Mathalon, University of California San Francisco, talked about relationship between corollary discharge and psychotic symptoms including delusion and hallucination.

   In the symposium 2 "Hallucinations and delusions" on 19th, Prof. Todd Woodward introduced his series of research on the commonality / segregation of neural basis of delusions and hallucinations. Dr. Jun Miyata, the president of this meeting from Kyoto University, talked about the connectivity analysis of delusion and salience. Dr. Keisuke Takahata, National Institute of Radiological Sciences, talked about tau neuropathology of late life psychosis, using positron

emission tomography. Prof. Philip Corlett, Yale University, introduced his computational model of hallucination.

In the symposium 3 "Recovery and treatment of approaches" on 19th, Prof. Yong-Sik Kim, Dongguk Univeristy, addressed the pharmacological treatment of hallucinations. Mr. Wakio Sato, Hearing Voices Network Japan, talked about first-person experience of hallucination. Prof. Emmanuelle Peters, King's College London, talked about psychological treatment of hallucination, specifically cognitive behavior therapy. Prof. Flavie Waters, The University of Western Australia, demonstrated the relationship between hallucination and sleep.

In the oral session on 18th, we had 9 presentations. The topics covered broad area from cultural research to biological research.

In the poster sessions on 18th and 19th, we had 21 posters mainly by young researchers. We had exciting discussions here and there.

In summary, this was the first meeting of ICHR in Japan, and top researchers from every corner of the world gathered together, and had a fruitful discussion. These experience would result in international collaborative research in the near future.

8. Additional description

We deeply thank for the support by Novartis Foundation Japan for the Promotion of Science.

Report on Research Meeting

Dec. 21, 2018

1. Name of Research Meeting / Conference
   International Tuberous Sclerosis Complex Research Conference 2018

2. Representative
   Okio Hino, M.D., Ph.D. (Professor, Juntendo University Faculty of Medicine)

3. Opening period and Place
   Sept. 13 – 15, 2018
   JR Tokyo General Hospital and Hotel Sunroute Plaza Shinjuku, Tokyo

4. Number of participants / Number of participating countries and areas
   200 participants / 17 countries and areas
   Australia, Belgium, China, Germany, Hong Kong, Israel, Italy, Japan, Netherlands, Poland, Portugal, South Africa, Spain, Sweden, Switzerland, UK, USA,

5. Total cost
   10,433,919 yen

6. Main use of subsidy
   Traveling expenses for invited speakers (including a committee member)

7. Result and Impression

   The conference was held in mid-September in Tokyo, for the first time in Japan. The theme was “New Horizons in TSC: Mechanisms, preventive and novel therapies, and improving quality of life”. From many countries and arias, 200 participants in total got together. Among them, there were over 70 family members of tuberous sclerosis complex (TSC) patients.

   In 10 oral sessions, 39 presentations including 25 invited ones by famous or up-and-coming researchers and medical were given. Also, in the poster session, 36 presentations were done by young and energetic researchers. Various topics from basic sciences as well as clinical trials were taken up in those oral and poster sessions. An active discussion was seen in each session and sometimes made program behind schedule. One of the important topics was TAND (TSC-associated neuropsychiatric disorders) and the establishment of its checklist. The Japanese version of TAND checklist had been completed and was introduced in this conference. It will become a useful tool to develop the examination and treatment of TSC in Japan.

   During each break, participants promoted exchanges and friendship. Luncheon seminars were held and foreign participants enjoyed Japanese-style lunch. There was a reception on the first day when the ceremony for the travel awards was performed. Four young scientists won the award and were encouraged. During the poster session, food and drink were served and discussion was done with a good atmosphere.

   On the afternoon of the last day, a special session, planed by Japanese patient’s families, was

held in a panel discussion style on three clinical topics (seizure, TAND, and lung/kidney). It aimed to promote exchange between medical doctors and the families and to introduce state-of-the-art knowledge on medical activities for TSC to the families. The families gave many questions and comments on them to which medical specialists answered and discussed with all participants. Issues to be considered in the future were understood in common.

This conference as a whole was meaningful to develop ideal examinations and therapies for TSC with a global cooperation. We appreciate the NOVARTIS Foundation for the Promotion of Science for supporting this conference.

8. Additional description

Report on Research Meeting

1. Name of Research Meeting / Conference
   Workshop on Frontiers in Phosphatase Research and Drug Discovery (ICPP13)

2. Representative
   Takeshi Tsubata

3. Opening period and Place
   October 23rd ~ October 25th, 2018　　Tokyo Medical and Dental University

4. Number of participants / Number of participating countries and areas
   100/ Japan, Germany, United States, Canada, Taiwan, Belgium

5. Total cost
   3,246,167 Yen

6. Main use of subsidy
   Travel expenses for the invited speakers

7. Result and Impression

   Protein phosphatase involves in extremely important various enzymatic phenomenon as intracellular signaling, membranous transport and cellular cycle inhibitor. From recent new tool and basic technology development, it is now established that phosphatases are tightly regulated and that they show a degree of substrate specificity similar to that of kinases. It has been indicated that various phosphatases are important target factors for the new treatment method for nerve, immune, and metabolic disorder by specifically inhibiting cell growth and its differentiation as well as metabolism, nerve function, and immune function.

   The conference, “Workshop on Frontiers in Phosphatase Research and Drug Discovery” has been held between October 22nd to 25th, 2018 at Suzuki Memorial hall of Tokyo Medical and dental university. The presentations and discussions have been held in regards to the role of protein phosphatase in terms of life phenomenon and drug discovery targeting protein phosphatase. There was approximately 100 participants for this conference.

   Protein phosphatase is distinguished in two different ways, serine/threonine phosphatase and tyrosine phosphatase (PTP). There is also phosphatidylinositol phosphatase as a related molecule. In this conference, professor Brautigan, the leading researcher of serine/threonine phosphatase from United States has participated as well as professor Bollen (Belgium) and Professor Neel (United States) who is the leading researchers of PTP. Professor Tonks (United States) and 14 international invited speakers (2 female researchers), and 13 Japanese invited speakers (2 female researchers) lectured the presentations during the conference. The main themes of the presentations were the mechanisms and roles of holoenzymes made out of catalytic and inhibitory subunit of serine/threonine phosphatase, atypical structures and mechanism of phosphatase, and functional mechanisms of phosphatase in terms of nerve function, cardiogenic disorders, and immunology and inflammation. Among others, various kinds of phosphatase are associated with carcinogenic mechanisms. There were many presentations in regards to the mechanisms and

role of phosphatidylinositol phosphatase in association with PRL family molecules inhibiting or developing the carcinogenic mechanisms as well as protein phosphatase inhibiting carcinogenic mechanisms.

It is a fact that the development of phosphatase inhibitor has been delay compared to phosphatase. It was because development of targeting active center of compound in phosphatase (PTP) is impossible compared to kinase inhibitor. However, it has been reported that the promising result has been obtained for the development of phosphatase inhibitor targeting compound outside of active center. There were also the intriguing presentations lecturing cancer treatment with the molecule by inhibiting allosteric binding site to inactive SHP-2 and the development of immunotherapy inhibiting PTP1B and TC-PTP by binding to the molecular pocket close to active center of compound.

There were total of 33 young researchers for the poster presentations (3 participants from foreign counties). During the poster presentation, the opportunities of many active discussions were held among the young researchers, presenters and invited speakers. Among the poster presenters, 8 cases have been picked for short talk presentations which was the excellent opportunities for the young researchers to present their research achievements to the internationally known experts. Many participants including the invited speakers and young researchers participated the reception dinner which provided all participants for international networking among phosphatase research field.

8. Additional description
None

32nd Grant Report (FY2018)

The foundation has been conducting public interest activities such as research grant, meeting grant and international exchange programs since its establishment on Sep. 4, 1987 in Japan under authorization of the Ministry of Education, Science, Sports and Culture, followed by a transition to a public interest incorporated foundation on Apr. 1, 2012. The grants conducted in FY 2018 are as follows.

32nd Novartis Research Grant:	37Researchers (JPY 1 mil.),	Subtotal JPY37.0 mil.
Research Meeting Grant:	5 Meetings (JPY 0.4 mil.),	Subtotal JPY 2.0 mil.
		Total JPY39.0 mil.

32nd Novartis Research Grant (FY2018)

The Grant is to aim supporting creative research in Japan in the field of Bio, life science and relevant chemistry.

#	Name	Institution	Title	Research Project
1	Tanaka Tomoaki	Chiba University, Graduate School Medicine,)	Professor	Fundamental study for GATA3 transcriptional complex and new insight into functional role of type2 innate lymphoid cells to control life-style related disease
2	Gotoh Eiji	Faculty of Agriculture, Kyushu University	Assistant Professor	Chloroplast movement optimizes plant growth through novel signal transduction
3	Arai Yasuyuki	Department of Hematology, Kyoto University Hospital,	Senior Clinical Staff	Machine learning- and next generation sequencing-oriented correlation analysis between gut microbiota and the risk of graft-versus-host disease
4	Iijima Norifumi	National Institutes of Biomedical Innovation, Health and Nutriti,	Sub-project leader	Importance of tissue-resident memory Tcells in mucosal tissue
5	Watanabe Yusuke	Molecular Phys lab, National Cerebral and Cardiovascular Center,	Laboratory chief	Analysis of cell lineage and transcriptional regulation during ventricular development of heart
6	Muguruma Keiko	Dept. of iPS Cell Applied Medicine, Kansai Medical University,	Professor	Construction of human complex brain organoids for analysis of brain development and neurological diseases
7	Shibutani Shusaku	Lab. of Vet. Hygiene, Joint Faculty of Vet. Med., Yamaguchi Univ,	Assistant Professor	A Novel Regulatory Mechanism of the Metabolic Signaling Complex mTORC1
8	Takeuchi Jun	MRI, Tokyo Medical and Dental University,	Associate Professor	Generation of functional-atrialventricular heart organdies in vitro
9	Sakakura Akira	Grad. Sch. of Natural Science and Technology, Okayama Universtiy,	Professor	Development of Catalytic Asymmetric Cycloaddition Reaction of alpha-Keto Esters for the Innovative Synthesis of Tetrahydrofuran Compounds
10	Suganami Takayoshi	Dept. of Molecular Medicine and Metabolism, Nagoya University,	Professor	Pathophysiologic role of a novel microenvironment that prolongs tissue damage in acute kidney injury

#	Name	Institution	Title	Research Project
11	Okuno Hiroyuki	Dept of Biochem and Mol Biol, Grad Sch of Med, Kagoshima Univ,	Professor	Role of a novel activity-dependent gene encoding a lipid modification enzyme on neuronal and cognitive function
12	Ukaji Yutaka	Dept. of Chemistry, Inst. of Sci. and Eng., Kanazawa University,	Professor	Synthesis of Phytochrome-type Chromophores Based on Oxidative Functionalization toward Investigation of their Functions
13	Yachie Nozomu	Yachie laboratory, RCAST, The University of Tokyo,	Associate Professor	Development of new base editor systems
14	Kitagishi Hiroaki	Faculty of Science and Engineering, Doshisha University,	Associate Professor	Study on the circadian rhythm system regulated by intracellular carbon monoxide
15	Haraguchi Shogo	Department of Biochemistry, Showa University School of Medicine,	Assistant Professor	Age-related endocrine disruption of skin leads to senescent alopecia
16	Iijima Takatoshi	Tokai University Institute of Innovative Science and Technology,	Associate professor	The RNA-based mechanism underlying pathophysiology in the neurological diseases
17	Nakatogawa Hitoshi	Sch. of Life Sci. and Tech., Tokyo Institute of Technology,	Associate Professor	Elucidation of the molecular basis and physiological significance of autophagic degradation of the nuclear pore complex
18	Abe Takayuki	Kobe University Graduate School of Medicine,	Associate Professor	Comprehensive understanding of intracellular innate immune response in chronic hepatitis B reactivation
19	Ishimizu Takeshi	Dept. of Biotechnol., Col. of Life Sci., Ritsumeikan Univ.,	Associate Professor	Identification of glycosyltransferases involved in biosynthesis of pectin in plant cell wall
20	Kai Toshie	Graduate School of Frontier Biosciences, Osaka University,	Professor	RNA base modification and RNA processing regulate the maintenance and development of germline stem cells
21	Fukuhara Shigetomo	Inst. of Adv. Med. Sci., Nippon Medical School,	Professor	Unveiling a novel regulatory mechanism of angiogenesis by intraluminal pressure
22	Tomita Kengo	Dept. of Internal Medicine, National Defense Medical College,	Associate Professor	Development of new treatment for obesity-related liver cancer, focusing on a Wnt ligand, ACLP, secreted by hepatic stellate cells
23	KizakaKondo Shinae	Tokyo Institute of Technology,	Professor	Construction of ultra-sensitive bioluminescence imaging Tg mice
24	Yakushiji Nayuta	Ikawa Laboratory, Tokyo University of Science,	Assistant Professor	Novel long-range regulatory mechanisms controlling B-cell lineage program
25	Miyoshi Keita	Div. of Invertebrate Genetics, National Institute of Genetics,	Assistant professor	Molecular mechanisms of extracellular vesicle formations of endogenous retroviruses
26	Naramto Satoshi	Lab.of Plant Dev.Biol., Grad. Sch.Life Sci., Tohoku university,	Assistant Professor	Molecular mechanisms of axis formation in plants: Organization, function and spatiotemporal dynamics of PIN clusters that regulate polar localization of auxin efflux carrier PIN proteins
27	Hashimotodani Yuki	Organization for Research Initiatives and Development,	Associate Professor	Physiological roles and molecular mechanisms underlying the synaptic plasticity in the dentate gyrus
28	Nishikii Hidekazu	Department of Hematology, University of Tsukuba,	Associate Professor	Genomic analysis of human hematopoietic stem cell niche in myelodysplastic syndrome.

#	Name	Institution	Title	Research Project
29	SegiNishida Eri	Segi lab, Dept. of Biol. Sci. and Tech., Tokyo University of Sci,	Associate professor	The role of desmoplakin in the antidepressant-like effects in the hippocampus
30	KimuraYoshida Chiharu	Dept. Mol Embry, Res. Inst. Osaka WCH,	Chief Scientist	Functional analysis of the GRHL3 factor in epithelial fusion.
31	Suzuki Yoshiro	Div. Cell Signaling, Nat. Inst. Physiol. Sci.,	Assistant Professor	Identification and molecular mechanism of novel calcium transport disease ;possible therapeutic target for bone mineralization defects
32	Akimitsu Nobuyoshi	Isotope Science Center, the University of Tokyo,	Professor	Nuclear noncoding RNA degradation regulates innate immune response
33	Tagawa Yoshiaki	Dept. Physiology, Faculty of Medicine, Kagoshima University,	Professor	Projection-specific circuit formation in the developing cerebral cortex
34	Komura Kazumasa	Department of Urology,Osaka Medical College,	Assistant Professor	Uncovering the Biomarker for Treatment with ATR Inhibitor in Solid Tumor
35	Demizu Yosuke	Division of Organic Chemistry, NIHS,	Head	Peptide foldamers in drug discovery
36	Maruyama Reo	Project for Cancer Epigenomics, Cancer Institute, JFCR,	Project Leader	Evaluation of Intra-tumor epigenetic heterogeneity of breast cancer
37	Taniguchi Koji	Department of Microbiology and Immunology, Keio University Schoo,	Associate Professor	Research on metabolic reprogramming induced by cancer development and inflammation

FY2018 Research Meeting Grant

(JPY 400 thousand x5 = 2.0 million)

#	Meeting	Date (Place)	Institution / Title	Name
1	Symposium on Molecular Chirality 2018	2018.05.11-12 (Chiba)	Chiba University / Professor	Sakamoto Masami
2	The 2nd research conference for the Research Society for Cancer 3-D culture	2018.12.3 (Tokyo)	National Cancer Center Research Institute / Chief	Okamoto Koji
3	International Consortium on Hallucination Research Satellite Meeting 2018 Kyoto	2018.11.29-30 (Kyoto)	Department of Psychiatry, Kyoto University / Senior Lecturer	Miyata Jun
4	International Tuberous Sclerosis Complex Research Conference 2018	2018.9.13-15 (Tokyo)	Juntendo University / Professor	Hino Okio
5	International Conference on Protein Phosphatase Workshop on Frontiers in Phosphatase Research and Drug Discovery	2018.10 (Tokyo)	Tokyo Medical and Dental University Medical Research Insti / professor	Tsubata Takeshi

第32期（2018年度）助成事業報告

当財団は、文部大臣の認可を得て1987年9月4日に設立されて以来、研究助成を中心とした公益事業を行って来ました。2012年4月1日には、制度改革に伴い、公益財団法人へ移行しております。2018年度は、下記の総額3,900万円の助成事業を実施しました。

第32回ノバルティス研究奨励金	37件（1件100万円）	3,700万円
研究集会助成	5件（1件 40万円）	200万円
	総額	3,900万円

第32回ノバルティス研究奨励金（2018年度）

この事業は、生物・生命科学および関連する化学の領域において、我が国で行われる創造的な研究の助成を目的としています。

（受付順、敬称略、所属職位は申請時、贈呈額：1件 100万円）

No.	氏　名	所　属	職　位	研究課題
1	田中　知明	千葉大学大学院医学研究院	教授	GATA3 転写複合体解析を基盤とした生活習慣病における 2 型 ILC 2 細胞の新たな機能的役割
2	後藤　栄治	九州大学 大学院農学研究院	助教	植物の生長を司る葉緑体局在変化の新たな制御機構の解明
3	新井　康之	京都大学医学部附属病院 血液内科	医員	機械学習と次世代シーケンス技術を用いた、同種造血幹細胞移植後の腸内細菌叢と、腸管 GVHD 発症リスクとの関連解析
4	飯島　則文	医薬基盤・健康・ 栄養研究所	サブプロジェクトリーダー	粘膜組織における組織局在型メモリー T 細胞の重要性
5	渡邉　裕介	国立研究開発法人、 国立循環器病研究センター、 分子生理部	室長	胎生期心室筋形成における転写制御機構と細胞系譜の解析
6	六車　恵子	関西医科大学　医学部 iPS・幹細胞応用医学講座	教授	複雑系脳オルガノイドによるヒト脳発生の解明と中枢神経疾患への応用
7	渋谷　周作	山口大学共同獣医学部獣医 衛生学分野	テニュアトラック助教	代謝シグナル複合体 mTORC1 の新規制御メカニズムの研究
8	竹内　　純	東京医科歯科大学	准教授	心筋タイプ別誘導法を用いた in vitro 機能性心臓組織の構築
9	坂倉　　彰	岡山大学大学院自然科学 研究科応用化学専攻	教授	テトラヒドロフラン環の構築法を革新するα - ケトエステルの不斉環化付加反応の開発
10	菅波　孝祥	名古屋大学環境医学研究所 分子代謝医学分野	教授	急性腎障害において炎症の遷延化をもたらす新規微小環境の病態生理的意義の解明
11	奥野　浩行	鹿児島大学大学院 医歯学総合研究科生化学・ 分子生物学	教授	神経活動依存的発現を示す新しい脂質修飾酵素による神経・認知機能調節機構
12	宇梶　裕	金沢大学理工研究域 物質化学系	教授	酸化的官能基化を基盤とするフィトクロム型発色団の合成と機能解明

No.	氏　名	所　属	職　位	研究課題
13	谷内江　望	東京大学先端科学技術 研究センター谷内江研究室	准教授	新規塩基編集ツールの開発
14	北岸　宏亮	同志社大学理工学部 機能分子・生命化学科	准教授	細胞内一酸化炭素によって調節される サーカディアンリズム機構の解明
15	原口　省吾	昭和大学医学部生化学講座	助教	加齢に伴う皮膚内分泌環境恒常性維持機 構の破綻により生じる老人性脱毛症の分 子機構解明
16	飯島　崇利	東海大学創造科学技術 研究機構医学部門	准教授	RNA 情報発現系の破綻による脳神経疾患 の分子病態解明
17	中戸川　仁	東京工業大学 生命理工学院	准教授	オートファジーによる核膜孔複合体の分 解の分子基盤と生理的意義の解明
18	阿部　隆之	神戸大学大学院 医学研究科 感染制御学分野	准教授	B 型肝炎ウイルスの再活性化・再燃に伴 う細胞内自然免疫応答の包括的理解
19	石水　　毅	立命館大学生命科学部 生物工学科 バイオエネルギー研究室	准教授	植物細胞壁ペクチンの生合成に関わる糖 転移酵素の同定
20	甲斐　歳恵	大阪大学大学院生命機能 研究科生殖生物学研究室	教授	生殖幹細胞の維持と分化を制御する RNA 修飾とプロセシングの解明
21	福原　茂朋	日本医科大学 先端医学 研究所 分子細胞構造学分野	教授	血管内腔圧による血管新生の新たな制御 機構の解明
22	冨田　謙吾	防衛医科大学校 消化器内科学教室	准教授	肝星細胞分泌 Wnt リガンド ACLP に着 目した、肥満関連肝がんの新たな治療法 の開発
23	近藤　科江	東京工業大学	教授	超高感度発光イメージング Tg マウスの 構築
24	藥師寺那由他	東京理科大学生命医科学 研究所免疫生物学研究部門 伊川研究室	助教	オープンクロマチン領域解析による B 細 胞特異的エンハンサーの同定とその制御 機構の解明
25	三好　啓太	国立遺伝学研究所 系統生物研究センター 無脊椎動物遺伝研究室	助教	内在性レトロウイルスによる細胞外粒子 形成の分子機構の解明
26	楢本　悟史	東北大学大学院生命科学 研究科植物発生分野	助教	植物の体軸形成の分子基盤の解明：オー キシン排出担体 PIN の局在を制御する PIN クラスターの構造とその機能
27	橋本谷祐輝	同志社大学 研究開発推進機構	准教授	海馬歯状回の局所回路におけるシナプス 可塑性のメカニズムと生理的役割
28	錦井　秀和	筑波大学医学医療系血液内科	准教授	骨髄異形成症候群患者における造血幹細 胞ニッチの遺伝子発現解析
29	瀬木ー西田 恵里	東京理科大学　基礎工学部 生物工学科　瀬木研究室	准教授	接着制御因子デスモプラキンによる新規 うつ治療シグナルの解明
30	木村ー吉田 千春	大阪母子医療センター 研究所　病因病態部門	主任 研究員	上皮癒合に着目した GRHL3 因子の機能 解析
31	鈴木　喜郎	岩手医科大学医学部 生理学講座統合生理学分野	准教授	カルシウム輸送障害による新規骨石灰化 不全症の同定と病態メカニズム解明
32	秋光　信佳	東京大学アイソトープ 総合センター	教授	核内ノンコーディング RNA の分解制御 による自然免疫応答のコントロールに関 する研究
33	田川　義晃	鹿児島大学医学部医学科 神経筋生理学分野	教授	長距離・局所をつなぐ投射特異的な大脳 回路構築のメカニズム解明
34	小村　和正	大阪医科大学 泌尿生殖・発達医学講座 泌尿器科学教室	助教	固形腫瘍における ATR 阻害薬の治療効 果予測バイオマーカーの同定
35	出水　庸介	国立医薬品食品衛生研究所 有機化学部	部長	ペプチドフォルダマー創薬研究

No.	氏　名	所　属	職　位	研究課題
36	丸山　玲緒	公益財団法人がん研究会 がん研究所 がんエピゲノムプロジェクト	プロジェクトリーダー	乳癌における腫瘍内エピゲノム不均一性の解明
37	谷口　浩二	慶應義塾大学医学部 微生物学・免疫学教室	特任 准教授	がん進展と炎症による代謝リプログラミング機構の研究

2018年度研究集会助成

この事業は、生物・生命科学および関連する化学の領域において、我が国で開催される国際色豊かな研究集会の助成を目的としています。2018年度は5件の助成を行いました。

（受付順、敬称略、所属・職位は申請時、贈呈額：１件40万円）

No.	研究集会名	開催日 （開催地）	所属・職位	氏　名
1	シンポジウム モレキュラー・キラリティー 2018	2018.05.11-12 （千葉）	千葉大学／教授	坂本　昌巳
2	第二回がん三次元培養研究会	2018.12.3 （東京）	国立がん研究センター 研究所／分野長	岡本　康司
3	国際幻聴研究コンソーシアム2018 京都	2018.11.29-30 （京都）	京都大学大学院医学研究科 脳病態生理学講座 精神医学教室／講師	宮田　　淳
4	国際結節性硬化症リサーチカンファレンス2018	2018.9.13-15 （東京）	順天堂大学／教授	樋野　興夫
5	国際プロテインホスファターゼ研究集会 プロテインホスファターゼと関連分子についての新たな研究ツールの開発と創薬への展開	2018.10.23-25 （東京）	東京医科歯科大学／教授	鍔田　武志

32nd Financial Report

Balance Sheet

As of March 31, 2019

(Unit：JP Yen)

Account	Amount
I Assets	
1. Current Assets	
Current Assets Total	16,270,588
2. Fixed Assets	
(1) Basic Fund	
Basic Fund Total	1,100,000,000
(2) Specific Assets	
Specific Assets Total	634,194
(3) Other Long - term Assets	
Other Long - term Assets Total	79,992,746
Fixed Assets Total	1,180,626,940
Assets Total	1,196,897,528
II Liabilities	
1. Current Liabilities	
Current Liabilities Total	37,148,627
Liabilities Total	37,148,627
III Equity(Net Assets)	
1. Designated Net Assets	
Designated Net Assets Total	1,000,634,194
(Amount Appropriating to basic Fund)	(1,000,000,000)
(Amount Appropriating to specific assets)	(634,194)
2. General Net Assets	159,114,707
(Amount Appropriating to)	100,000,000
Equity Total(Net Assets)	1,159,748,901
Liabilities & Equity Total	1,196,897,528

Statement of Net Assets

From April 1, 2018 to March 31, 2019

(Unit：JP Yen)

Account	Amount
I General Net Assets Changes	
1. Ordinary income & Expenditure	
(1) Ordinary income	
Interest from basic fund	13,556,807
Donation	53,000,000
Other Income	562,056
Ordinary Income Total	67,118,863
(2) Ordinaty Expenditure	
Project Expense	49,368,532
Grant Expense	39,000,000
Novartis Research Grant	37,000,000
Research Meeting Grant	2,000,000
Administrative Expense	6,220,958
Ordinary Expenditure Total	55,589,490
Ordinary Balance without Appraisal Profit or Loss	11,529,373
2. Nonrecurring Profit & Loss	
Nonrecurring Balance of Current Period	
General Net Assets Ending Balance	159,114,707
II Designated Net Assets Changes	
Designated Net Assets Change	0 1,000,634,194
Designated Net Assets Ending Balance	1,159,748,901
III Net Assets Balance Ending Balance	

第32期（2018年度）財務報告

貸借対照表

2019年3月31日現在

（単位：円）

科　　目	金　額
Ⅰ資産の部	
1．流動資産	
流動資産合計	16,270,588
2．固定資産	
(1)　基本財産	
基本財産合計	1,100,000,000
(2)　特定資産	
特定資産合計	634,194
(3)　その他固定資産	
その他固定資産合計	79,992,746
固定資産合計	1,180,626,940
資産合計	1,196,897,528
Ⅱ負債の部	
1．流動負債	
流動負債合計	37,148,627
負債合計	37,148,627
Ⅲ正味財産の部	
1．指定正味財産	
指定正味財産合計	1,000,634,194
（うち基本財産への充当額）	(1,000,000,000)
（うち特定資産への充当額）	(634,194)
2．一般正味財産	159,114,707
（うち基本財産への充当額）	100,000,000
正味財産合計	1,159,748,901
負債及び正味財産合計	1,196,897,528

正味財産増減計算書

2018年4月1日から2019年3月31日まで

（単位：円）

科　　目	金　額
Ⅰ一般正味財産増減の部	
1．経常増減の部	
(1)　経常収益	
基本財産運用益	13,556,807
受取寄付金	53,000,000
雑収益	562,056
経常収益　計	67,118,863
(2)　経常費用	
事業費	49,368,532
支払助成金	39,000,000
ノバルティス研究奨励金	37,000,000
研究集会助成金	2,000,000
管理費	6,220,958
経常費用　計	55,589,490
当期経常増減額	11,529,373
2．経常外増減の部	
当期形状外増減額	
一般正味財産期末残高	159,114,707
Ⅱ指定正味財産増減の部	
当期指定正味財産増減額	0
指定正味財産期末残高	1,000,634,194
Ⅲ正味財産期末残高	1,159,748,901

List of Board Members

[Board of Trustees] 5 trustees, 2 auditors As of Oct 1, 2019

Post	Name	Title
Chairman	Akimichi KANEKO	Professor, Keio University
Trustee	Shigetaka ASANO	Visiting Professor, MD, School of Medicine, Kobe University; Emeritus Professor, University of Tokyo
	Masao ENDOH	Emeritus Professor, MD, Yamagata University
	Kuniaki TAKATA	President, Gunma Prefectural College of Health Sciences President, Gunma Prefectural Public University Corporation
	Masao TORII	President, Novartis Holding Japan K.K.
Auditor	Tokuzo NAKAJIMA	Certified Public Accountant
	Masanori FUSE	Financial Advisor, Finance & Administration Div., Novartis Pharma K.K.

[Board of Councilors] 10 councilors As of Oct 1, 2019

Post	Name	Title
Chairman	Tsuneyoshi KUROIWA	Member of the Japan Academy; Emeritus Professor, University of Tokyo
Councilor	Norio AKAIKE	Head, Kumamoto Kinoh Hospital Clinical Research Center Visiting Professor, Kumamoto University, Graduate School of Medicine and Pharmaceutical Research Emeritus Professor, Kyushu University
	Hiroyuki KAWASHIMA	Former Professor, Graduate School of Medical & Dental Sciences, Niigata University
	Masakatsu SHIBASAKI	Director, Microbial Chemistry Research Center, Microbial Chemistry Research Foundation
	Akihiko NAKANO	Deputy Director, Photonics Engineering Research Center & Team Leader, Live Cell Super-Resolution Imaging Research, RIKEN
	Tadanori MAYUMI	Emeritus Professor, Osaka University
	Miwako MORI	Emeritus Professor, Hokkaido University
	Toyoshi FUJIMOTO	Specially appointed Professor, MD, Research Institute for Diseases of Old Age, School of Medicine, Juntendo University Emeritus Professor, Nagoya University
	Masamitsu IINO	Specially appointed Professor, MD, Nihon University Emeritus Professor, University of Tokyo
	Tohru HIROSE	Director, Division Head Japan Development, Novartis Pharma K.K.

[Grantee Selection Committee] 20 members As of Oct 1, 2019

Post	Name	Title
Chairman	Masafumi YANO	Professor, MD, School of Medicine, Yamaguchi University
Member	Jun YAMASHITA	Professor, MD, Center for iPS Cell Research and Application, Kyoto University
	Motoko YANAGITA	Professor, MD, Graduate School of Medicine, Kyoto University
	Hirokazu ARIMOTO	Professor, MD, Graduate School of Life Sciences, Tohoku University
	Hiroyuki TAKEDA	Professor, Graduate School of Science, University of Tokyo
	Eiji HARA	Professor, Research Institute for Microbial Diseases, Osaka University
	Makoto HAYASHI	Team Leader, Plant Symbiosis Reseach Team, RIKEN Center for Sustainable Resource Science
	Hirokazu HIRAI	Professor, MD, Head of Department of Neurophysiology and Neural Repair, Gunma University
	Kouichi FUKASE	Professor, Graduate School of Science, Osaka University
	Michisuke YUZAKI	Professor, School of Medicine, Keio University
	Akihiko YOSHIMURA	Professor, Department of Microbiology and Immunology,
	Hiroshi ITO	Graduate School of Medicine, Keio University
	Takashi OHSHIMA	Professor, Department of Graduate School of Medicine, Keio University
	Yoko HAMAZAKI	Professor, Drug Discovery and Development Center, Graduate School of Pharmaceutical Sciences affiliated Company-Academia-Government collaboration, Kyushu University
	Toshiaki OHTEKI	Professor, Graduate School of Medicine, Kyoto University
	Yasuyoshi SAKAI	Professor, Medical Research Institute Tokyo Medical and Dental University
	Taisuke TOMITA	Professor, Division of Applied Life Sciences, Graduate School of Agriculture, Kyoto University
	Fumiko TOYOSHIMA	Professor, Graduate School of Pharmaceutical Sciences, The University of Tokyo
	Tohru MINAMINO	Professor, Institute for Frontier and Medical Sciences, Kyoto University
	Yasuhiro YAMADA	Professor, Niigata University Graduate School of Medical and Dental Sciences

公益財団法人ノバルティス科学振興財団

役 員 名 簿

2019年10月1日現在（順不同、敬称略）

職　名	氏　名	現　　職	就任年月日	常勤・非常勤
代表理事	金子　章道	慶應義塾大学名誉教授	2018年6月25日	非常勤
理 事	浅野　茂隆	神戸大学大学院医学系研究科客員教授 東京大学名誉教授	2018年6月25日	非常勤
	遠藤　政夫	山形大学名誉教授	2018年6月25日	非常勤
	高田　邦昭	群馬県立県民健康科学大学学長 群馬県公立大学法人理事長	2018年6月25日	非常勤
	鳥居　正男	ノバルティスホールディングジャパン（株） 代表取締役社長	2018年6月25日	非常勤
監 事	中嶋　徳三	中嶋徳三公認会計士事務所 公認会計士	2016年6月10日	非常勤
	布施　正則	ノバルティスファーマ（株）企画管理本部 ファイナンシャルアドバイザー	2016年6月10日	非常勤

評 議 員 名 簿

2019年10月1日現在（順不同、敬称略）

職　名	氏　名	現　　職	就任年月日	常勤・非常勤
評議員長	黒岩　常祥	日本学士院会員 東京大学名誉教授	2016年6月10日	非常勤
評 議 員	赤池　紀扶	医療法人社団寿量会熊本機能病院 臨床研究センター所長、学術顧問 熊本大学大学院医学薬学研究部客員教授 九州大学名誉教授	2016年6月10日	非常勤
	川島　博行	元新潟大学大学院医歯学総合研究科教授	2016年6月10日	非常勤
	柴崎　正勝	公益財団法人微生物化学研究会 微生物化学研究所長	2016年6月10日	非常勤
	中野　明彦	理化学研究所 光量子工学研究センター 副センター長	2016年6月10日	非常勤
	眞弓　忠範	大阪大学名誉教授	2016年6月10日	非常勤
	森　　美和	北海道医療大学客員教授 北海道大学名誉教授	2016年6月10日	非常勤
	藤本　豊士	順天堂大学大学院医学研究科特任教授 名古屋大学名誉教授	2016年6月10日	非常勤
	飯野　正光	日本大学医学部特任教授 東京大学名誉教授	2016年6月10日	非常勤
	廣瀬　　徹	ノバルティスファーマ（株）取締役開発本部長	2016年6月10日	非常勤

選 考 委 員 名 簿

2019 年 10 月 1 日現在 (順不同、敬称略)

職　名	氏　名	現　　職	就任年月日	常勤・非常勤
選考委員長	矢野　雅文	山口大学大学院医学系研究科教授	2016年6月10日	非常勤
選考委員	山下　　潤	京都大学 iPS 細胞研究所教授	2016年6月10日	非常勤
	柳田　素子	京都大学大学院医学研究科教授	2016年6月10日	非常勤
	有本　博一	東北大学大学院生命科学研究科教授	2016年6月10日	非常勤
	武田　洋幸	東京大学大学院理学系研究科教授	2017年6月19日	非常勤
	原　　英二	大阪大学微生物病研究所教授	2017年6月19日	非常勤
	林　　誠	理化学研究所環境資源科学研究センター チームリーダー	2017年6月19日	非常勤
	平井　宏和	群馬大学大学院医学系研究科教授	2017年6月19日	非常勤
	深瀬　浩一	大阪大学大学院理学研究科教授	2017年6月19日	非常勤
	柚﨑　通介	慶應義塾大学医学部教授	2017年6月19日	非常勤
	吉村　昭彦	慶應義塾大学医学部教授	2017年6月19日	非常勤
	伊藤　　裕	慶應義塾大学医学部教授	2018年6月25日	非常勤
	大嶋　孝志	九州大学大学院薬学研究院教授	2018年6月25日	非常勤
	濵﨑　洋子	京都大学大学院医学研究科教授	2018年6月25日	非常勤
	樗木　俊聡	東京医科歯科大学難治疾患研究所教授	2019年6月10日	非常勤
	阪井　康能	京都大学大学院農学研究科教授	2019年6月10日	非常勤
	富田　泰輔	東京大学大学院薬学系研究科教授	2019年6月10日	非常勤
	豊島　文子	京都大学ウィルス・再生医科学研究所教授	2019年6月10日	非常勤
	南野　　徹	新潟大学大学院医歯学総合研究科教授	2019年6月10日	非常勤
	山田　泰広	東京大学医科学研究所教授	2019年6月10日	非常勤

事 務 局 便 り

ご寄附のお願い

当財団は、自然科学における創造的な研究の奨励等を行うことにより、学術の振興を図り、国民の健康と福祉の向上に寄与することを目的に公益事業を行っております。

当財団の事業は、基本財産の運用益並びに寄付金によって賄われており、財団では趣旨にご賛同いただける皆様からのご寄付を募っております。

当財団へのご寄付には、下記の税法上の優遇措置が適用されます。

優遇措置の概略

個人：年間寄付金の合計額もしくは年間所得の40％相当額のいずれか低い方から2千円を引いた金額が、所得税の寄付金控除額となります。

法人：支出した寄附金は、通常一般の寄附金の損金算入限度額とは別枠で、下記の範囲内で損金の算入できます。

（資本金等の額×当期の月数/12×0.375%＋所得の金額×6.25%）÷2

ご寄附は、随時受付けております。詳しくは、財団事務局までお問合せ下さい。

（電話：03-6899-2100、E-メール：foundation.japan@novartis.com）

事務局より

本年度もお陰様で、財団年報を発行できることとなりました。これも偏に、助成を受けられた皆様および財団関係者の皆様のお力添えの賜物と心より感謝申し上げます。

1987年9月の財団設立以来、助成件数は総数で1,764件、総額20億円を超えるものとなりました。

当財団は、自然科学の創造的研究への助成によって、日本の学術発展に寄与することを目指しております。

助成を受けられた研究成果がすぐに応用につながらなくとも、将来、新分野につながることを夢見て、この事業を継続して参ります。

引き続きご指導、ご支援の程よろしくお願い申し上げます。

2019年10月吉日

事務局長　原　　建記

公益財団法人 ノバルティス科学振興財団
〒105-6333 東京都港区虎ノ門1-23-1
虎ノ門ヒルズ森タワー
TEL：03-6899-2100　FAX：03-6899-2101
E-メール：foundation.japan@novartis.com
ホームページ：http://japanfoundation.novartis.org/